



University of
Stavanger

Faculty of Science and Technology

MASTER'S THESIS

Study program/ Specialization: Petroleum Engineering/ Reservoir	Spring semester, 2017. Open
Writer: Katrine Fredagsvik (Writer's signature)
Faculty supervisor: Dr. Mahmoud Khalifeh	
Thesis title: Formation as Barrier for Plug and Abandonment of Wells	
Credits (ECTS): 30	
Key words: Formation, barrier, creep, shale, clay, P&A	Pages:113..... + enclosure: Stavanger, 15.06.2017.

Formation as Barrier for Plug and Abandonment of Wells

Master thesis by Katrine Fredagsvik

University of Stavanger

Department of Petroleum Technology

June 2017



University of
Stavanger

Abstract

To permanently plug and abandon (P&A) of drilled wells, permanent barrier(s) should be established. Cement is the primer material used for zonal isolation and permanent P&A as barrier material. However, it is recognized that cement may not be a suitable material. Other barrier materials are being developed and tested. The high costs of establishing barriers and durability of materials persuaded engineers to check the usability of naturally established barriers, such as creeping formations.

The concept of formation as barrier (FAB) is to use earth itself as barrier material. It is desirable to exploit the displaced formation surrounding casing considering it is cost efficient, saves time and makes operation performance carried out in a safe manner. Bonded and impermeable in-situ formation (e.g. shale, salt) is known to have sufficient formation integrity and is accepted as an annulus well barrier element.

The present work reviews the fundamental concept of FAB, creep process, the properties of creeping formation(s), impacts causing creep, self-healing and self-sealing capability of formations, and description of empirical and rheological models and methods that need to be utilized to find creeping formations.

Due to the large deformations needed to establish a barrier through creep process, it appears that best candidates are shales with a low threshold for plastic flow and a high ability to sustain large plastic deformations. The findings show the mechanisms that may cause the gap closure process.

Acknowledgements

The work presented in this master thesis has been carried out at the University of Stavanger, department of Petroleum engineering where I am a student. The department has provided me with the necessary working conditions.

I wish to express my sincere thanks to my supervisor, Dr. Mahmoud Khalifeh, for his continuous support and great guidance during this semester.

I would like to thank Prof. Arild Saasen - UiS, Truls Carlsen - Statoil, Prof. Erling Fjær - SINTEF, Lars Hovda - ConocoPhillips and Prof. Rune M. Holt - NTNU for their input being of great importance to this master thesis.

I would also like to thank my family for the support and patience they have provided me during the semester while I was working on this master thesis.

Nomenclatures

CBL	- Cement bond logs
DEM	- Discrete element method
DDL	- Diffuse double layer
DCM	- Dielectric constant measurement
EGME	- Ethylene glycol monoethyl ether
Eq.	- Equation
FAB	- Formation as barrier
FBP	- Formation breakdown pressure
Fig.	- Figure
FPP	- Fracture propagation pressure
GoM	- Gulf of Mexico
ISIP	- Instantaneous shut-in pressure
LCR	- Used to measure the inductance (L), capacitance (C), and resistance (R)
LOT	- Leak-off test
LOP	- Leak-off pressure
LVDT	- Linear variable differential transformer
LWD	- Logging while drilling
MLR	- Multiple linear regression
NCS	- Norwegian Continental Shelf
NORSOK	- Norsk Søkkel Konkurransesystem
P&A	- Plug and abandonment
SSA	- Specific surface area
TOC	- Total organic carbon
USIT	- Ultrasonic imaging tool
VDL	- Variable density log
WBE	- Well barrier element
WBS	- Well barrier schematic
XLOT	- Extended leak-off test
XT	- Christmas tree
Å	- Angstrom (Å), unit of length, equal to $1 \cdot 10^{-10}$ meter, or 0.1 nanometer

Table of contents

Abstract	III
Acknowledgements	IV
Nomenclatures	V
Table of contents	VI
1 Objectives of this master thesis	1
2 History background	2
3 Introduction to P&A	4
4 Well barriers	6
5 Formation as barrier (FAB)	8
5.1 Formation sealability – Verification and identification of shale formation	10
5.2 Procedure for qualification of formation as barrier	12
6 Formation displacement mechanisms	13
6.1 Shear and tensile failure	13
6.2 Compaction failure and consolidation.....	13
6.3 Liquefaction	13
6.4 Thermal expansion	14
6.5 Chemical effects.....	14
6.6 Creep	14
7 Sedimentary structure and formations	15
7.1 Sedimentary structure	15
7.1.1 <i>Shale</i>	15
7.1.2 <i>Clay</i>	16
7.2 Clay mineralogy and shale instability	19
8 Salt rock formation as barrier	22
8.1 Establishment of salt rock as formation barrier	22
8.2 Challenges related to logging of salt.....	23
9 Measurements of formation petrophysical properties	26
9.1 Specific surface area.....	26
9.1.1 <i>Dielectric constant measurement</i>	27
9.1.2 <i>Shale strength correlation</i>	30
10 Formation movement behaviour	31
10.1 Collapsed formation.....	31
10.2 Creeping formation	33
10.2.1 <i>Process of creep</i>	35
11 Swelling formation	37
11.1 A review of conducted experimental works on swelling clay	40
12 Self-sealing and self-healing formation	44
13 Verification of shale formation	45
13.1 Logging	45
13.2 Pressure testing.....	45

14	Factors influencing creep	48
14.1	Mineralogy	48
14.2	Load and temperature	49
14.3	Pressure drop in annulus:	51
14.4	Chemical methods	52
14.4.1	<i>How brine exposure effects shale formation</i>	52
14.4.2	<i>Effects of KCl exposure on shale</i>	55
14.4.3	<i>How brines of Ca²⁺, Mg²⁺ and Zn²⁺ affects shale</i>	56
14.4.4	<i>Experimental example: Brine with KCl versus Brine with Ca²⁺, Mg²⁺ and Zn²⁺</i>	58
15	Modeling of creeping process	59
15.1	Empirical models	59
15.1.1	<i>Power law model</i>	59
15.1.2	<i>Modified Power law model</i>	60
15.2	Rheological models	62
15.2.1	<i>Burgers model</i>	63
15.2.2	<i>The FORMEL model</i>	72
15.3	Numerical model	76
16	Required geomechanical conditions for creep formation	78
17	Suggested laboratory experiments on shale	80
17.1	Hollow cylinder test.....	80
17.2	Shale barrier test.....	81
17.2.1	<i>Example from shale barrier test</i>	82
18	Summary	90
19	Future work	92
20	Appendix A	93
21	References	100

1 Objectives of this master thesis

This master thesis focuses on the following issues:

Objective 1

Is it possible to establish FAB by preparing for creep to occur, either already in the drilling of the well (the well construction) or to provoke this in connection with plugging of wells elderly where other barriers (such as cement) are insufficient compared to the current rules?

Objective 2

What are the central mechanisms related to behaviour of shale and salt formations when providing a self-healing annular barrier around a well?

Objective 3

Is there any procedure for estimating and improving the effectiveness of shale formation as a self-healing annular barrier where surrounding a well?

Objective 4

Is there any test procedure to study creep and investigate the barrier forming process?

2 History background

It all started with Oseberg oil and gas field located in the northern part of the North Sea where FAB concept was used in 2005 when Statoil observed good bonding signal from cement bond log (CBL) and ultrasonic imager tool (USIT) logs in areas where it was not suppose to be cement i.e. open annulus [1]. These intervals turned out to be related to clay rich intervals. Subsequently, the questions aroused: Is this a hydraulic isolating material in the same sense as cement and is it possible to use this material instead of cement? The material was tested out with a cut and pressure test, that showed no leakage in the interval. The concept of using formation material as an annular barrier, during plug and abandonment (P&A) operations, has since been developed, where cement evaluation logs showed long interval of solid material bonded to the casing, at depths significantly above the maximum theoretical top of cement. This solid material observed was identified as shale, which had moved in to "fill" the annulus and had bonded to the casing. It is believed this is primarily a creep process related to the plastic nature of the shale and resulting stress regime.

Shale formation material fulfils all the requirements with respect to properties of a well barrier specified in the NORSOK D-010 (2013):

- Impermeable
- Long-term integrity
- Non-shrinking
- Ductile – (non-brittle) – able to withstand mechanical loads/ impact
- Resistance to different chemicals/ substances (H₂S, CO₂ and hydrocarbons)
- Wetting, to ensure bonding to steel

Since shale was acknowledged as a potential barrier, an identification and verification procedure was established and ultimately accepted by the Norwegian authorities that allowed shale formation to be used as an annular barrier element [2].

The identification and verification procedure involves three principle steps:

- Confirm that the bonded formation is actually shale (with the above mentioned properties) or salt.

- Confirm that the shale/salt formation has bonded sufficiently with the casing, and that it has done so uniformly around the annulus over a sufficient interval length.
- Confirm that the mechanical properties of the formation material that has crept in to fill the annulus has the same mechanical properties as the virgin formation. This is to verify the sufficient integrity, such that it can withstand the required pressure without fracturing.

As salt formations are not relevant to the Norwegian sector of NCS, this master thesis will focus on shale formation as barrier material. Shale formation has been used as a barrier element to date in many wells on the Norwegian continental shelf (NCS). Planning traditional P&A operations (for slot recovery or permanent abandonment) on “old wells” often reveals a shortage of annular cement barriers or a lack of documentation supporting the existence of such barriers. Using formation as an annular barrier has on several occasions replaced the need for remedial casing retrieval, casing cutting, casing milling and remedial cement operations. This has resulted in significant cost savings for the petroleum industry.

3 Introduction to P&A

Wells constitute efficient flow channels between hydrocarbon reservoirs and the surface. When a well is no longer economically profitable to produce or there are technical difficulties of well completion, site tracking or water coning - it needs to be plugged and abandoned (P&A) with an eternal perspective to seal off the reservoir completely and prevent migration of hydrocarbons. It is possible that the annulus between the casing and the rock can evolve to undesired channels for leakage and thus required to be properly sealed, at least in certain sections of the well Fig 3-1.

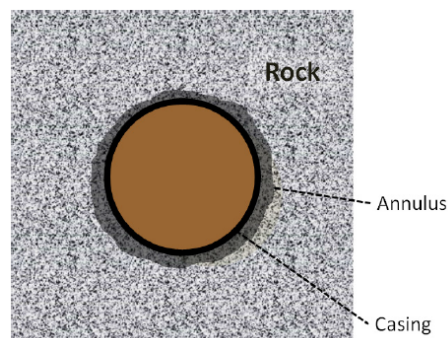


Figure 3-1: Schematic view of a cross section of a well , showing the rock (formation) forming a properly seal (barrier) of the annulus [1].

P&A operations are common operations performed on a large scale throughout the industry and there will be a strong wave of P&A operations in the near future. The operations are traditionally performed by retrieving the tubing followed by cutting the casing at an accepted depth and then mill it out to approach the formation. Cement plugs are thereafter established at required depths in the open hole to seal off and isolate the reservoir. Conventional milling is costly, laborious as well as including significant safety risks. To avoid milling, a qualified barrier behind the casing should be verified. If so, the P&A operation will be exceedingly more cost efficient, less time consuming and safer [3]. It has been established that older wells are more challenging to be plugged and abandoned due to lack of data, poor quality of cement behind the casing, etc. [4].

P&A operations can make up to 25% of the total drilling costs of exploration wells offshore on NCS [5]. Therefore, a more cost efficient P&A technology is necessary. There are no financial benefits associated with P&A operations, though it is exceptionally more cost

efficient than the financial obligations when re-entering a wellbore due to detection of leakage. The operators of the field have the obligation and responsibility to guarantee that rules and requirements are fulfilled in a safe and effective way so there is less chance of having to re-enter a well after previous permanent P&A operation.

Through the history, logging data has shown indications of good bond detection above theoretical depth of top of cement. Several interpretations of these signals exist as well as given potential causes for these incidents. The most dominant cause is assumed to be displacement of sedimentary formation, which may be suitable for use as a permanent barrier.

During the history of petroleum industry, there have been several accidents due to failed P&A operations. An example is the incident that happened in the Gulf of Mexico (GoM) [6]. The GoM accident shows us why knowing and verifying the quality barriers are important. However, even though the petroleum industry has strict regulations and requirements, there is no one who can predict if an accident will occur. Anything can happen anywhere.



Figure 3-2: Severe incident due to poor quality well barrier [6]

4 Well barriers

A barrier is defined as a measure that prevents an error from occurring such as release of energy or an leakage, Fig. 4-1. The more precise expression to well barrier is well barrier envelope. A barrier envelope is an enclosing system that prevents fluid from flowing unintentionally from the formation, into another formation or to the surface. Normally the requirement is two independent envelopes, a primary barrier (blue) and a secondary barrier (red), Figs. 4-1 and 4-2. The primary well barrier is the first well barrier envelope that prevents flow from a source. The secondary well barrier is the back-up barrier that presents flow from source in case of a failure of the primary barrier. Each barrier consists of several barrier elements [7] and each barrier element can be seen as the building blocks needed to form a barrier envelope.

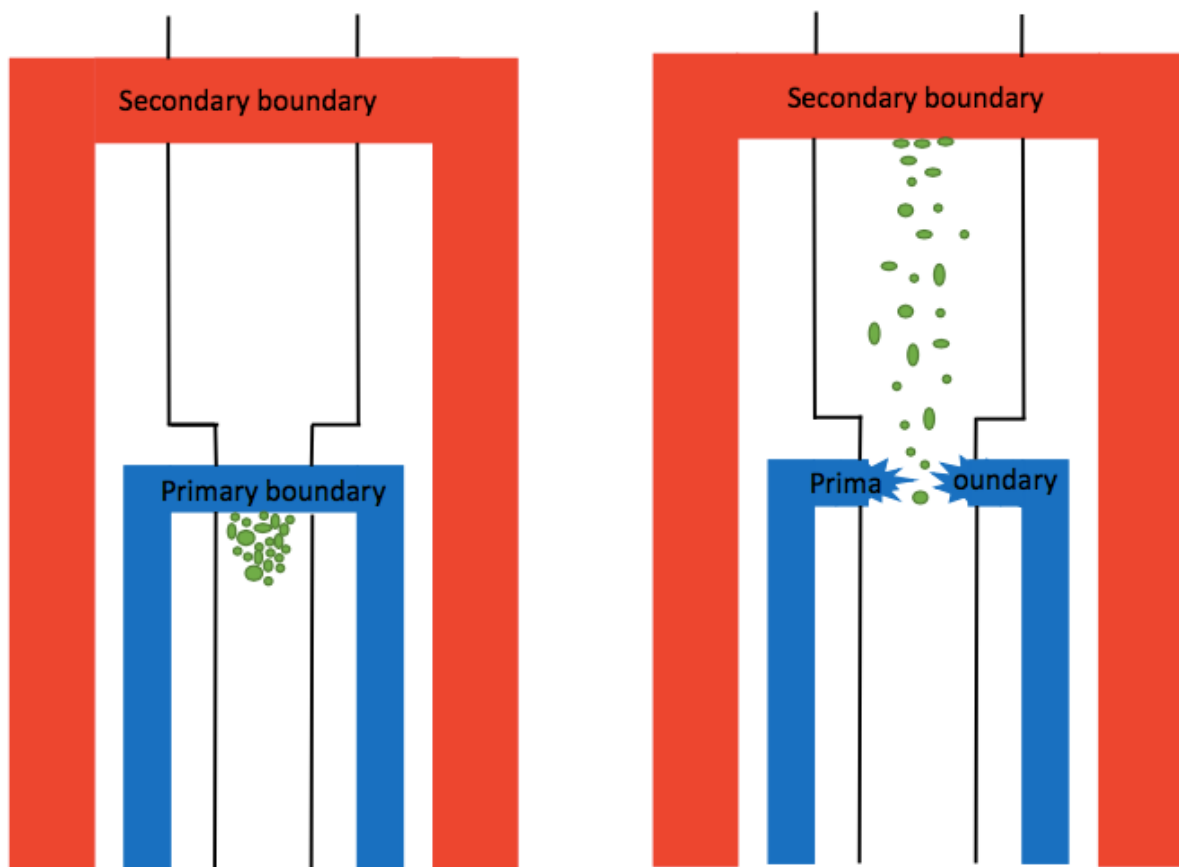


Figure 4-1: Principal of two independent barriers [7]

There are different types of permanent barrier elements (Khalifeh, M. et al. 2013):

- Formation
- Cement
- Cement derivatives
- Casing
- Grouts
- Thermosetting materials
- Gels
- Metals

This master thesis will focus on formation as barrier (FAB).

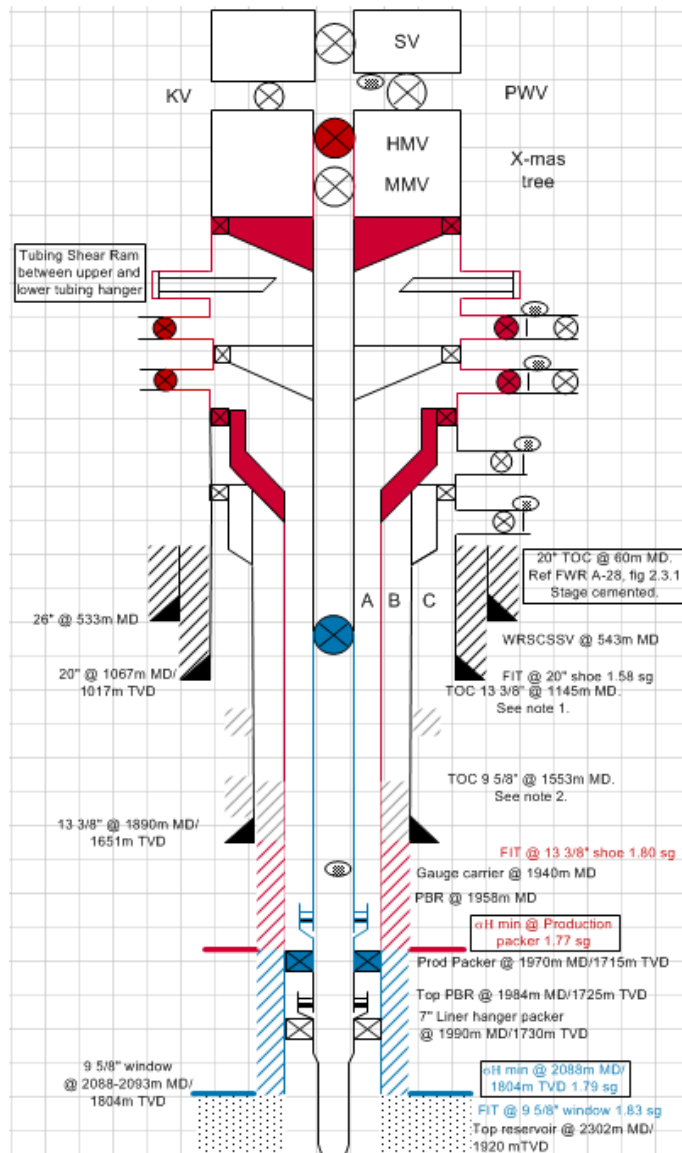


Figure 4-2: Well barrier schematic (WBS) of two independent barriers [8]

5 Formation as barrier (FAB)

There are different types of permanent barriers materials such as cement and formations (9). In the industry, cement is accepted as an annular barrier element. However, it has recognized that cement may not be optimal when it comes to ductility and shrinkage. Therefore, other materials are being developed and tested.

For wells to be permanently plugged and abandoned, rigid requirements for sealing barriers apply. Cement filling the annulus outside the casing may provide proper sealing, however in shale sections where the annulus is not filled with cement, the shale may start moving (creeping) towards the casing and eventually form an equally efficient sealing barrier. Bonded and impermeable in-situ formation (e.g. shale, salt) has sufficient formation integrity and is accepted as an annulus well barrier element. This is stated in NORSOK D-010 (2013). Creeping formation may be unfortunate during drilling process as it can lead to several drilling problems. Nevertheless, this phenomenon may be advantageous in certain-situation when P&A is desired as it creates a permanent annular barrier behind casing. This movement of shale formations is not predictable but if it happens, it is not fully understood why. It is necessary to have a contingency plan on using other types of barrier material for permanent P&A operation. However, if bonded shale is detected behind the casing, it would be the optimal barrier material.

The concept of FAB is to use earth itself as barrier material, which fulfils the regulations by creating a good seal around casing. It is desirable to exploit the displaced formation surrounding casing, which is cost efficient, saves time and operation is performed in a safe manner. When taking advantage of formation as an annular barrier, it is possible to eliminate processes such as milling operations.

Fig. 5-1 illustrates the experience related to FAB on NCS.



Figure 5-1: An overview of experience related to formation as barrier

It is important to point out that there has been found FAB from southern North Sea and all the way up to northern part of the Norwegian Sea, however not yet found in the Barents Sea (1)

Lithologies that have been qualified so far ranges in age from Oligocene (upper Tertiary) to Upper Jurassic.

It is common to use crept salt as exterior barrier in Gulf of Mexico (GOM). Salt is impermeable and has high tensile strength. Therefore, it is therefore considered as a good sealing material [6].

If a formation moves in towards the casing, surrounding the circumference and extends over a sufficient length along the casing in an equal and even form, then it is possible to consider this as a potential annular barrier if it has the particular properties. These properties involve for instance exceedingly low permeability to fluids. It is also important to understand the shale displacement mechanism taking place, as this has implications on whether the formation is capable of creating an annular barrier or not.

5.1 Formation sealability – Verification and identification of shale formation

When considering formation as barrier, logging and leak testing must be performed to determine the following two major factors that qualifies formation as barrier:

- The location of the barrier
- The sealability of the shale

The following indicators may be used to help identify formation bonding such as:

- Formation solids should be observed above the expected maximum theoretical total organic carbon (TOC), unless there were issues with the cement job (e.g. losses or channelling).
- Formation ‘bedding’ patterns on impedance image (often ‘sinusoidal’ in appearance due relative dip between the well path and the formation) in between intervals of good formation bond. These are often visible on the log images and typically correspond to stiffer formation beds (i.e. cemented sandstone or carbonate stringers), which do not creep in to fill the annulus. See Appendices A-1 to A-6 for detailed log examples of different sealing potential.
- Casing ovalisation caused by stresses being transmitted directly to the casing in the absence of cement. This is very commonly observed in deviated wells where the stress differential is largest around the casing azimuth.
- A sharp change from formation response to free pipe response at the previous casing shoe, going from a single to double (concentric) casings.

To act as a barrier the formation material must have the following general log acceptance criteria:

- The log must be of good quality such there is sufficient confidence in the interpretation.
- There must be sufficient interval length, in which the formation is interpreted as having a ‘high’ isolating potential. This is defined in NORSOK D-010 (2013). High isolating potential implies that the log is interpreted to show bonded formation with sufficient measured impedance, 360 degree around the annulus. The cement bonding log (CBL) amplitude should also be below expected threshold values and should be constant over the interval (i.e. show little variation versus depth).

When observing sufficient bonded formation material, with required log properties, the formation must be qualified by a number of requirements. To ensure the strength of shale observed on bond logs contacting the backside of the casing is sufficient to provide a barrier, it must be pressure tested. Pressure tests have through experimental observation shown that it is can be successful in some cases but not in all.

5.2 Procedure for qualification of formation as barrier

I have presented all requirements in the previous chapter in a procedure to understand how to qualify a formation as a barrier element or not, Fig. 5-2.

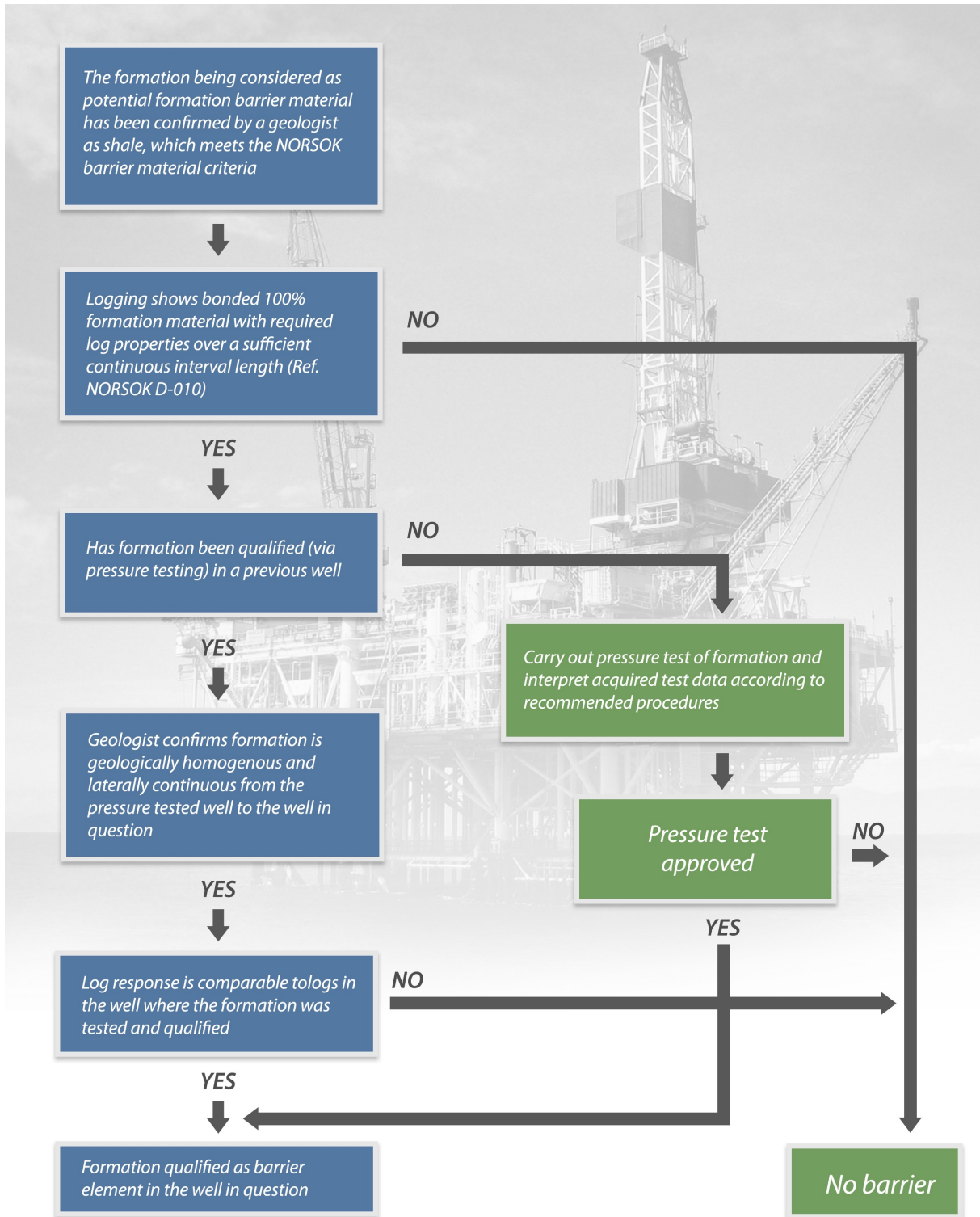


Figure 5-2: FAB qualification procedure for formation as a barrier element [8]

6 Formation displacement mechanisms

Theoretical studies and drilling observations have revealed that shale formation can be deformed and moved in towards the well casing. Formation displacement is detected as a decreased diameter of the wellbore. This process may occur both slowly or rapidly during and after the drilling.

There are various displacement mechanisms, which may take place in a combination or separately. The following displacement mechanisms are described below [10]:

6.1 Shear and tensile failure

Shear and tensile failure is most often detected in shale arrangements where it is required mud weights higher than the pore pressure to stay balanced at the same time being equivalent to shear failure calculations. One of the major influences that may start this process is the reduction of density of the mud located behind the casing over a period of time. It is likely to create permeable rubble filled annulus.

6.2 Compaction failure and consolidation

Compaction failure and consolidation does occur once the formation starts moving in towards the casing. This is to be considered as a consequence response rather than an important triggering process [10].

6.3 Liquefaction

Liquefaction is another deformation mechanism that is stimulated by static shear stress and may result in severe deformations. It is induced by rapid loading and could be an important process that can be utilized for the purpose of creeping formation, given that the shale is soft. However, it is unlikely to form annular barrier alone. It would show as a liquid on logs [10].

Liquefaction is a phenomenon that occurs during earthquakes or alternative rapidly applied loadings causing reduced strength and stiffness of the soil. The structure of the saturated sand breaks down resulting that the soil particles seek to move into a denser structure (configuration) [11]. In case of an earthquake, the water becomes trapped in the pores of the soil due to the limited time for it to be squeezed out. The water is therefore being “trapped”

and hinders the soil particles from gathering together. Increasing water pressure, which leads to weakening and softening the soil deposit as the contact forces between the particles lowers, follows this. However, there is nothing from the logs or drilling experience that implies that liquefaction is connected to this process [10,11].

6.4 Thermal expansion

Thermal expansion is defined as the tendency of a body to experience transformation in volume when temperature is changed [12]. It would tend to affect all types of formations equally and it is not considered to have a significant impact on the displacement. From production, thermal expansion may be of less importance, as the change in temperature from formation temperature to the phase of production is normally small. However, it may be of importance when it comes to increasing the process in the shallower areas [10,11,13].

6.5 Chemical effects

Chemical effects are of minor importance when it comes to contribution to the process of displacement. This is established through bonding logs, which indicates an indifference of what kind of mud that is used while drilling [10].

6.6 Creep

This phenomenon is summarized as a displacement process of formation with high content of clay where formation moves in a hydraulic way. It is considered to fit best the observations, likely in combination with section 6.1, shear and tensile failure. In addition, it must have a very low permeability and sufficient rock strength [10]. Although other formation displacement mechanism may contribute to a greater or lesser extent, the predominant displacement mechanisms for establishment of sealing annular shale formation barriers is presumably creep.

7 Sedimentary structure and formations

7.1 Sedimentary structure

In order to understand the mechanisms behind establishing FAB, it is necessary to obtain knowledge regarding the sedimentary structure of the formation considered suitable as sealing annular barrier.

7.1.1 Shale

Shales are basically sedimentary rocks that have been laid down over geological time in marine basins. They are usually composed of quartz, feldspar, calcite, and a number of clay fractions in varying proportions. Shales play a major role in petroleum exploration and production because they are commonly considered to be both source rocks and seals. Their ability to exhibit good sealing characteristics arises from their small, water-wet pores. These small pore throats are responsible for generating high capillary pressures, which excludes hydrocarbons [14].

Shales are defined as sedimentary rocks with low permeability and porosity [15]. Since shale is the optimal formation to benefit as annular barrier, it is of great importance to know what shales are and their properties.

Shales are significantly fine-grained sedimentary rocks consisting of a large amount of clay minerals that were generally deposited in marine basins. They consist of compacted beds of clays, muds and silts. Different types and amounts of minerals result in different structures. Shales evolve denser at increased depth because of the compaction induced by overburden weight from the layers above. Due to the overload of weight and stresses, further alteration of shale may occur.

Fundamental factors that have essential impact on mechanical and chemical behaviour of the shale are the various kinds and quantities of clay in the shale including the degree of clay hydration. It is necessary to establish the swelling clay content seeing that over 75 % of drilled formations are shale, and over 70% of the borehole problems are related to shale instability [16]. It is one of the most significant technical problems in petroleum exploration

and a major source of lost time and revenue. Other describes that more than 90% of wellbore instability problems are caused by problematic shales [17,18].

Knowing the clay mineralogy during drilling is helpful to:

- Determine water and hydrocarbon saturations in shale reservoir formations and in similar formations.
- Establish the type and amount of shale inhibitor needed in the drilling fluid in order to establish wellbore stability.
- Provide information about different drilling problems such as:
 - Hole cleaning problems
 - Torque
 - Stuck pipe
 - Instability in wellbore
 - Bottom-hole fill
 - Mud rings
 - Drag
 - Solids build-up in the drilling fluid
 - Bit balling
- Provide information and prevent various types of completion problems which are attributable to the hydratable clay content of the formation:
 - Formation damage in shale sands
 - Well logging and coring failures
 - Hole wash outs
 - Poor cement jobs - Information provided during drilling may be helpful in P&A operations. See Appendix A for log examples

7.1.2 Clay

Clay is a common term for different fine-grained natural rock or soil material. It is known for being plastic because of its water content and evolves into non-plastic, fragile and hard material as a consequence to air drying or firing, Fig. 7-1.

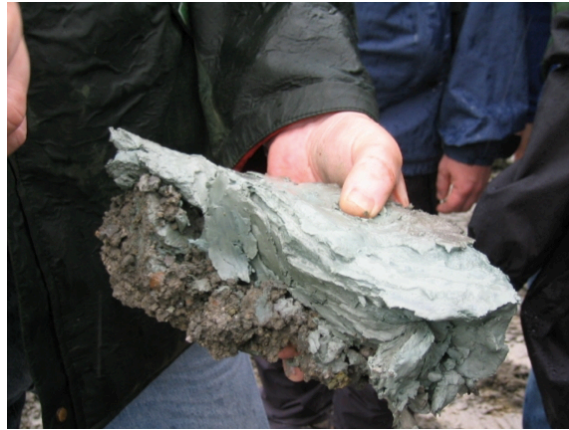


Figure 7-1: Clay from Denmark [1]

Clays minerals can be divided into three main groups, where each group has its own characteristics (19):

- Smectite or Montmorillonite
 - Includes bentonite and vermiculite.
 - Formed by the alteration of mafic igneous rocks that are rich in calcium and magnesium.
 - Weak linkage by cations (e.g. Na^+ , Ca^{2+}) results in high swelling/shrinking potential.
- Illite
 - Includes glauconite (a green clay sand).
 - The most common clay minerals.
 - Formed by the decomposition of some micas and feldspars.
 - Predominant in marine clays and shales.
- Kaolinite
 - Includes dickite and nacrite; formed by the decomposition of orthoclase. Feldspar (e.g. in granite).
 - Kaolin is the principal constituent in China clay.
 - Purest clay – stable composition.

Chemically, clay particles are charged due to isomorphous substitution, incomplete occupation of the positions available for metal ions and release of protons from hydroxides. As a consequence of the negative charge at the surface of clay particles, electrostatic forces exist between the negative surface and exchangeable cations such as iron, calcium, sodium, potassium and magnesium [20,21]. For example, aluminium (Al^{3+}) may be replaced by iron (Fe^{2+}) or magnesium (Mg^{2+}), leading to a net negative charge.

The different types and quantity of clays in a shale formation has the most severe impact on the mechanical and chemical behaviour of the formation. The ability to absorb water and swelling of confined or compacted shales develop internal stresses that may cause a reduction of compressive strength, fracturing, sloughing and spalling. The most water-sensitive clays are montmorillonites, illites, and interlayered varieties, which may constitute as much as 80% of the total weight of the shale [18,21]. When in contact with water-based drilling fluids, these types of clays adsorb the water by the means of two hydration mechanisms:

- The first mechanism represents a small consumption of water commonly resulting to a deposition of only four molecular layers. During the compaction process, free water is forced from the shales and when contact between their surfaces and liquid occurs, a potential for crystalline adsorption of water is established. Even if the degree of adsorption is quite small following that there is little to no apparent swelling as well as loss of strength, the hydration energies involved are relatively high.
- The second mechanism of the hydration process involves considerably larger alterations in the dimensions of the clay particles. The hydration follows imbalances between the solute content of the contacting moisture and the amount of ions at clay surface. The magnitude of hydration is therefore dependent on the volume of electrolyte of the drilling fluid. This does not imply that swelling of clay can be discarded simply by rising the ionic level to saturation. It is only possible to avoid swelling when a semipermeable membrane is present.

Disintegration of the shale matrix may cause the shear stress around the wellbore to go beyond the formation strength because of hydration of clays minerals in the shale formation. This increases the risk of various forms of wellbore instabilities that may occur as for instance hole closures leading to undergauge due to plastic deformation of ductile rocks and tight hole wellbore problems [22,23].

The breaking up of the shale matrix into more finely and divided particles can also cause serious formation damage in shale reservoir sands. And if the quantity becomes too high, it may have an unfortunate impact on the rheological properties of the drilling fluids. A second important cause of shale problems is dispersion of shale cuttings. Drill cuttings of shale with a high tendency to hydrate may become soft in water and start attaching to drill

collars, stabilizers, forming mud rings in the annulus or get stuck to the drill bit causing crucial bit balling problems. Accordingly, clay hydration may lead to problems that causes reduced drilling rates and stuck pipe.

A trustworthy, significant measure of clay content for clay with tendency to hydrate and shale hydration characteristics may be determined from the specific surface area.

7.2 Clay mineralogy and shale instability

As previously mentioned, the instability of shales in drilled formations leads to serious operational problems with major economic consequences for petroleum exploration and production. Shale instability appears in several different ways, which results in a variety of problems: [17].

- The wellbore may collapse through caving, sloughing or heaving unavoidably leading to enlarged holes.
- Plastic shrinkage, which involves change in volume with an alteration in effective stress, commonly due to change of water content.
- Fracture leakage caused when fractures connects, then leading the formation to break along those fractures.
- Cuttings from the drilled shale may disintegrate and disperse through the drilling fluid
- The shale may agglomerate around the drill bit (bit-balling) and drill pipe, accreting onto the walls of the wellbore and significantly reducing its diameter.

These problems can result in tight holes and stuck drill pipes that may even lead to bore hole abandonment.

The clay minerals considered to be most active towards shale instability are classified as smectite, illite and mixed-layer clays (primarily mixed-layer illite/smectite). Chloritic clay minerals are considered to be of secondary importance and kaolinite is considered relatively inactive. O'Brien and Chenevert (1973) were among the first to try to directly relate the instability of shales to their clay mineral composition as presented in the following table, which gives a classification of the different problem shales according their characteristics and clay mineralogy [17].

Table 7-1 Influence of mineral compositions on shale characteristics [17]

Class	Characteristics	Clay minerals
1	Soft (less stable), highly dispersive. Mud making.	High smectite, some illite.
2	Soft, fairly dispersive. Mud making.	High illite, fairly high smectite.
3	Medium hard, moderately dispersive, sloughing.	High in mixed-layer, illite, chlorit.
4	Hard (stable), little dispersion, sloughing.	Moderate illite, moderate chlorite.
5	Very hard, brittle, no dispersion, caving.	High illite, moderate chlorite.

It is generally agreed upon that the nature of the clay minerals in shale formations is a primary factor leading to their instability, though the specific mechanism involved is more debateable. The affect of interacting factors that correlates to shale clay mineralogy, such as structure, texture and fabric, are determining along with pore size distribution, the nature of water in clays and how these alter with increasing depth of burial [17].

Since clays are aluminosilicates, the clay particles become surrounded by a hydrosphere of adsorbed water that contains a thin layer of adsorbed cations when suspended in an electrolyte. Outside the layer, ions of opposite polarities create an electrically neutral diffuse layer. The adsorbed cations are affected by electrostatic attraction, while two identical opposing forces affect those in the diffuse layer: electrostatic attraction and diffusive forces. This ionic structure containing the negative surface charges, adsorbed cations, and diffuse layer is known as the diffuse double layer (DDL), which occurs at the interface between the clay surface and the soil solution [24]. Overlap of the DDLs related to exposed outer surfaces of clay minerals on opposing sides of micropores (up to 2nm in diameter) and mesopores (2-50 nm in diameter) in a lithostatically compressed shales would result in electrostatic repulsion and lead to increased pore/ hydration pressure in smectitic, illitic and even kaolinitic shales. This pressure would be restrained by the use of more concentrated K-based fluids, which effectively shrink the thickness of the DDL towards the clay mineral surfaces in the pore walls. The effectiveness of K⁺ ions in minimizing swelling pressures is related to the

small degree of hydration of these ions in water, resulting in low ion repulsion [25,26]. The effects of ion hydration, however, are non-trivial. Application of polymers could also encapsulate the clay mineral surfaces and inhibit hydration.

Even though the nature of clay mineral composition that makes up shales, together with the overall shale texture, structure and fabric, is most often thought to be the primary causes of wellbore instability, there are often a variety of interacting mechanical factors, which can potentially worsen the situation [17]. This can for instance be contact between the drill string and the shale formation, fluid erosive action and pressure rushes. Also the distribution of the overall in-situ vertical and horizontal stresses, and particularly overpressure, can play a major role regarding instability. Nevertheless, the central cause of shale instability is considered to be the hydrophilic and charged properties of clay minerals, which makes it possible for them to swell and take part in cation exchange reactions.

Swelling pressure is invariably present in clay-rich shales, where it functions as a tensile force on clay platelets. On the other hand, the magnitude of this may alter due to chemical reactions provoked by interactions between the shale formation and the drilling fluid (either positively or negatively). In consideration of expandable clays (smectites), the swelling pressure will increase either directly due to hydration of clay or indirectly when osmotic pressure increases due to cation exchange. It may also increase when the shale rock acts as a semi-permeable membrane [17]. To date, the dominant cause of shale instability is considered to be volume expansion following the osmotic swelling of Na-smectite. On the other hand, shales that are non-smectite such as illitic and kaolinitic shales may also be unstable, which makes it reasonable to dismiss the theory of interlayer expansion to be a universal causing mechanism of shale instability.

8 Salt rock formation as barrier

Creep is particularly dominant phenomenon in salt formations, where drilling problems as well as salt loading on casing has been studied. Salt formations have a tendency to dissolve and leach out, causing drilling-fluid contamination or pipe sticking. As previously mentioned, salt formations are not relevant to the Norwegian sector of NCS, which is the reason for focusing on shale formation as barrier material in this master thesis. On the other hand, rock salt has been known for its excellent isolation capacity and the potential to heal fractures because of its mechanical properties and it is a common reservoir seal worldwide. As a ductile material, salt can creep, surrounding matter, develop traps as well as performing as a sealing material since it is impermeable to hydrocarbons [27]. It is impermeable and has high tensile strength and therefore it is considered as a good sealing material. However, not all types of salts are suitable barrier material, whereas simple salts, such as halite, maintain relatively stable during drilling while more complex salts, particularly tachyhydrite, may creep and seal around a drillstring rapidly [28].

8.1 Establishment of salt rock as formation barrier

The process of salt creep may re-establish the integrity of salt caprocks and create an additional well barrier. The barrier is formed by the closure of an openhole section of the well by the natural process of creep. An openhole section can be created during well abandonment by milling out a few tens of meters of well casing across a salt caprock. Fig. 8-1 illustrates the stresses around the open wellbore initiating the natural process of creep in the rock salt, which would eventually close the uncased section of the wellbore [28,29].

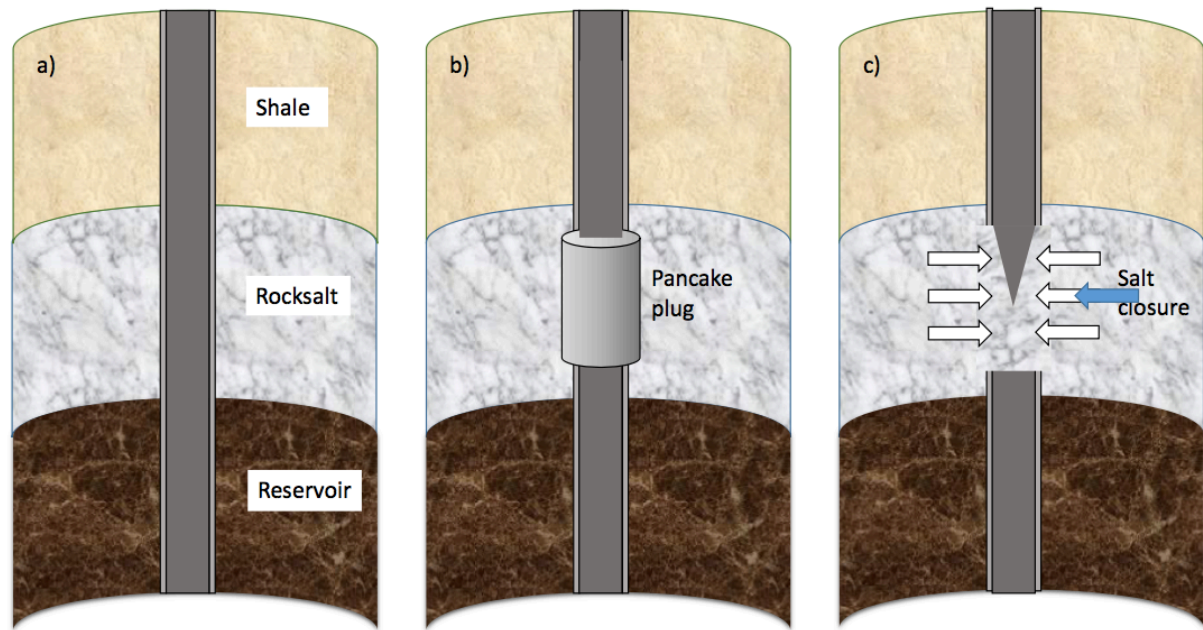


Figure 8-1 a: A well penetrating the salt deposits abandoned, b: Using a pancake plug set across the caprock, c: Using an alternative way of well abandonment based on the closure of an open wellbore by the creep of rock salt

Using salt as well barrier can also be possible when combining with a pancake plug to create an additional barrier to improve the sealing of well.

8.2 Challenges related to logging of salt

In well logging, sound waves are generally characterized by their slowness (v^{-1}), typically expressed in s/ft or s/m. Acoustic properties of the formation influence acoustic logs [30]. Fast formation and slow formation are terms that refer to sound velocity of a specific formation.

- A fast formation is a rock in which the shear velocity travels faster than the compressional velocity of the fluid in the borehole. The so-called “fast-formation effect” is recognized as transit-time decrease. When the formations have higher velocities than the casing, the refracted formation compressional waves may arrive before the casing wave. In this case, the transit time is shorter than expected, and the amplitude characterizes the formation instead of the casing/cement bond.
- A slow formation is a rock in which the shear velocity is equal to or slower than the fluid velocity. In this case, there is no significant alteration in the direction of the wave front of the shear wave and no shear head wave generated.

If there is sufficient sound energy propagating through the formation to interfere with the early part of the waveform, it indicates the presence of solid material between the casing and the formation. In some cases, the transit time does not reflect fast formation while the variable density log (VDL) data is able to detect a potential formation arrival before the casing arrival. When logging salt formations, which are highly plastic and have little heterogeneity, the obtained VDL data of the area is very regular most of the time, sometimes appearing similar to that of free pipe.

Due to plastic properties of salt, salt formation may act as slow formation and therefore, the emitted acoustic wave may not arrive to the receiver at the right time. Subsequently, logging of salt formation or verification of creeping salt may require special consideration.

Another issue regarding rock salt as plugging material are the timescales on which closure takes place and the change in porosity/permeability of the salt when creeping into an open hole section. As logging of salt formation is known to be challenging, it is necessary to obtain different types of information through logging while drilling (LWD) tools, in order to identify salt or salt zones, such as [19]:

- Drilling rate
- Condition of the mud and mud resistivity
- Response of resistivity logging methods
- Response of radioactivity logging methods
- Cuttings or sideall cores

However, it may still be difficult or not possible to obtain positive identification when these types of information are acquired.

Important measurements used to identify salt formations include:

- EcoScope spectroscopy to determine salt composition
- Seismic-while-drilling measurements that can be used to correlate with existing seismic data to help update geomechanics models and plan salt exit.
- Resistivity, and sonic-while-drilling for pore pressure modelling
- Formation-pressure-while-drilling together with resistivity and sonic-while drilling to provide a measurement of pore pressure immediately above the salt body.

Table 8-1 shows the values that will be obtained when using some of these measurements [31].

Table 8-1: The physical and electrical properties of salt.

Electrical resistivity	High
Porosity	Low
Travel time	67-70 usec/ft
Natural gamma ray Radioactivity	Low
Natron radioactivity	High

Seismic logging of salt zones is particularly difficult due to [32].

- The complicated form of precipitously dipping sides
- Position adjacent to overburden strata
- The typical strong acoustic impedance along with velocity contrasts at the interface of evaporite

Compared to other rocks, the creeping limit or elasticity of salt rocks are extraordinary low and subsequently it is difficult to measure their true creeping limits [33].

Due to significant logging limitations regarding detection of formations, poor illuminations and poor sampling are the fallout. It is necessary to do further work on measurements of formation properties, development of acquisition and eliminating source and receiver ghost notches.

9 Measurements of formation petrophysical properties

9.1 Specific surface area

Specific surface area (SSA) is defined as the total surface area of all the particles in a unit of a rock mass:

$$SSA = \frac{Surface}{Volume} \text{ or } \frac{Surface}{Mass} \quad (\text{Eq.9.1})$$

It is mainly defined by the quantity of hydratable clays in the soil and it has a great impact on the physical and chemical characteristics of the formation. The SSA also determines the strength of shale, the hydration tendency of clay particles and the swelling pressure [22]. Soils have a wide variety in their reactive surface due to the differences in mineralogical and organic composition and in their particle-size distribution. Table 9-1 presents relevant soil particles and their SSA [34] and the Fig. 9-1 illustrates the relation between the size and surface area of different soil particles.

Table 9-1 Relevant soil particles and their SSA

Particle	Effective diameter (cm)	Mass (g)	Area (cm²)	Specific surface area (cm² g⁻¹)
Gravel	$2 \cdot 10^{-1}$	$1.13 \cdot 10^{-2}$	$1.3 \cdot 10^{-1}$	11.1
Sand	$2 \cdot 10^{-3}$	$1.77 \cdot 10^{-7}$	$7.9 \cdot 10^{-5}$	444.4
Silt	$2 \cdot 10^{-4}$	$1.13 \cdot 10^{-11}$	$1.3 \cdot 10^{-7}$	$1.11 \cdot 10^4$
Clay	$2 \cdot 10^{-4}$	$8.48 \cdot 10^{-15}$	$6.3 \cdot 10^{-8}$	$7.4 \cdot 10^6$

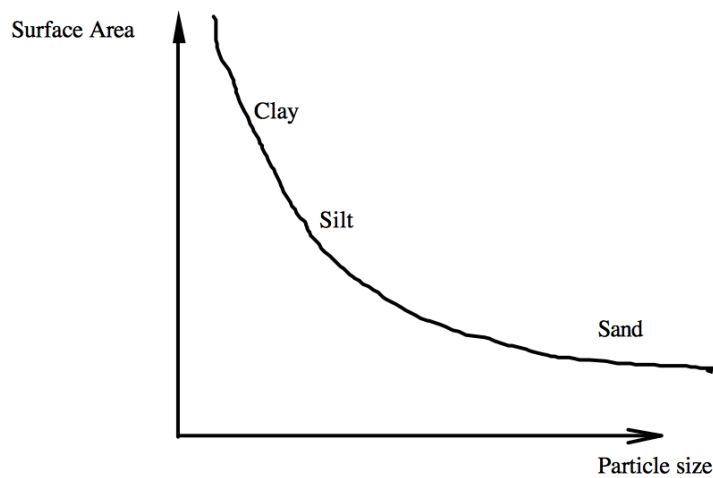


Figure 9-1: Surface area versus particle size for relevant soils [34]

There are several methods to measure specific surface area such as gas phase or liquid phase adsorption, cation exchange capacity, X-ray analysis and chemical analysis [22].

The measuring techniques are time consuming and challenging or field inconsistent values for surface areas. The results from the various methods also differ significantly from different analytical laboratories and analysts.

One of the methods is performed by using ethylene glycol monoethyl ether (EGME) as a liquid adsorbate and it is considered to be the most useful quantifying method as it provides the most accurate and trustworthy surface area measurements for shales. This particular experiment takes 24-48 hours to complete and must continuously be under controlled conditions supervised by experienced laboratory technicians. Even though this method delivers sufficient results, it is not considered suitable for wellsite operation. The new dielectric constant measurement (DCM) solves this dilemma and makes it possible to perform shale characterization tests at the wellsite on a regular basis. It can also define specific surface area of shales.

9.1.1 Dielectric constant measurement

A material is defined as “dielectric” if it can store electrical energy. Dielectric constant measurement (DCM) is performed to quantify swelling clay content and to determine the specific area. The new method was established when taking advantage of dielectric constant measurements from drill cuttings to measure swelling clay content. The dielectric constant of

a certain rock is determined by quantifying the electric capacitance of a sample of the rock in a coaxial sample cell, Fig. 9-2.

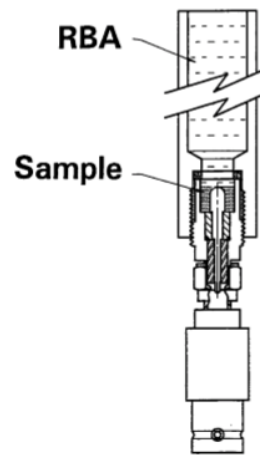


Figure 9-2: DCM cell

The capacitance of the dielectric material is a function of the dielectric constant as given in the following equation:

$$C_0 = \frac{A}{t} \quad (\text{Eq.10.1})$$

$$C = C_0 \kappa' \quad (\text{Eq.10.2})$$

$$\kappa' = \epsilon'_r = \frac{C}{C_0} \quad (\text{Eq.10.3})$$

where

- C = capacitance with dielectric
- C_0 = capacitance without dielectric
- $\kappa' = \epsilon'_r$ = real dielectric constant or permittivity
- A = area of the capacitor plates
- t = the distance between the plates

These parameters are shown in Fig. 9-3 [22].

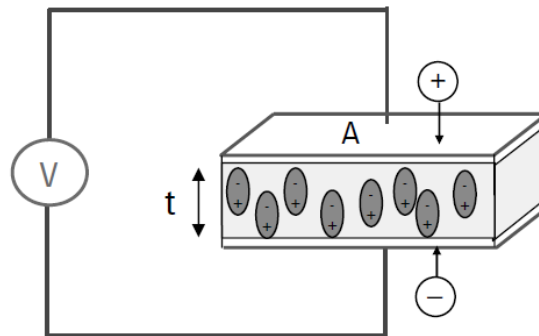


Figure 9-3: Dielectric constant [22].

A complete system for DCM contains of an inductance, capacitance and resistance (LCR) meter, the dielectric cell and connecting adapters and cables. The dielectric constant of a mineral increases proportional with the surface area [22].

The surface area and dielectric constant measurements are useful when distinguishing between sand and shale formations as well as different shale formations. DCM and surface area may also help defining the downhole rock strengths at different depths, which follows a wellbore stability analysis that can be performed on a regular basis. This analysis can be used to:

- Forecast the densities of drilling fluid needed to provide wellbore stability.
- To detect stuck pipe problems and create guidelines for new wells to decrease the wellbore instability.

9.1.2 Shale strength correlation

The development of standard triaxial testing methods has evolved through the last 30 years with the objective of quantifying strength and pore pressure of maintained cores of shale formation. For stability analysis, formation strength is an essential parameter and is traditionally identified by the parameters cohesive strength, S , and friction angle ϕ . These values are normally established from several rock mechanics testing of various core plugs from the same depth.

The outcome is that shale strength increases with the downhole stress or mean effective stress of the shale. The relationship between the shale strength and the strength to mean effective stress explain that a rock placed at a lower depth in the ground in a high rate of stress will have a higher value of strength compared to the same rock if it was placed under normal conditions [22].

If two types of shales were exposed to the same mean effective stress condition, that is: identical downhole stress circumstances, the shale with the lower specific surface area have the higher strength. In a related aspect, the dielectric constant also has a mutual connection with mean effective stress and shale strength. Due to these interactions we are able to find the downhole rock strengths at deeper depths by using SSA or DCM from drill cuttings.

10 Formation movement behaviour

10.1 Collapsed formation

The barrier formation process can generate large load on the casing. If this load is uneven, ovaling and collapse of the casing may occur. Borehole collapse is normally caused by shear failure of the rock near the hole, and thus controlled by the stress alteration taking place as a result of drilling, which may lead to tight hole/stuck pipe incidents which are very costly for the oil industry [5].

Collapsed formation is a common term, which refers to all forms of creeping, whereas most cases are not suitable for use as a barrier. This is because the collapsed material often is considered to permeable along contacts between blocks.

Fig. 10-1 shows a collapsed mine (at the top section). This form of filling of the annulus will not be considered sufficient to be used as a barrier on production wells. It is desirable to use formations that creep inwards, and not pieces of collapsed material [10].



Figure 10-1: Collapsed formation [1].

To use collapsed formation as a barrier, there are certain requirements that need to be fulfilled. The table below tabulates the given requirements and solutions for using a collapsed formation as permanent barrier [10].

Table 10-1 Requirements and solutions using a collapsed formation as permanent barrier

Requirements	Solutions
Must prove the collapsed formation is shale with the correct qualifications: <ul style="list-style-type: none"> • Impermeable • Long term • Non-shrinking • Ductile • Chemical resistance • Wetting 	We ensure the qualifications by collecting geological data that indicates good shale presence surrounding the well
Must prove the formation has collapsed all around the casing over a sufficient interval (50m).	We ensure the qualifications by collecting geological data that indicates good shale presence surrounding the well
We need a high enough formation strength to avoid propagating upward fracture propagation	By running ultrasonic and cement bond log (CBL)
Need to know formation fracture pressure (leak-off).	Performing a leak-off test of the formation

10.2 Creeping formation

One of the fundamental geological processes in the evolution of basins is compaction of sediments. Compaction and chemical reactions and physical conversions that occur in deposited sediment during diagenetic processes causes evolution of physical and mechanical properties. These properties are permeability, compressibility and porosity of sediments. Compaction of sediments is a time dependent process and this deformation of sediments has been connected to pore fluid expulsion under drained condition or to pore pressure redistribution under undrained condition [35]. Time-dependent deformation is further visible in dry unconsolidated reservoir formations, which is discovered by creep and stress relaxation under constant stress and strain conditions.

Creep is defined as deformation under constant load and the creeping rate is the rate of deformation. It is a complicated process, being hypersensitive to stress as well as temperature. During and after drilling operation, certain formations may start moving (creeping) inward and begin to close off the well. It is related to the viscoelastic response of the solid framework and can be observed both in dry and wet rocks. In consideration of wet rocks, consolidation may be incorrectly interpreted as creep because it is also a time dependent effect. Both of the effects can be detected both in the laboratory and the field, but the timescale can be very different [36].

Basically, when applying constant load to a sample of a saturated soil, it will start changing its shape. This type of deformation is time dependent and generated by displacement [36,37,38]. In this case, the displacement is the process of forcing pore fluid or gas out of the saturated soil, called pore pressure diffusion. This is the primary consolidation, a geological process where volume of the soil decreases. The following phase consists of a deformation development of the soil due to applied load below a material's yield strength during an extended amount of time. This time-dependent deformation does not fall under primary consolidation since this phase is not always characterized with expulsion of pore fluids. This stage is therefore called secondary consolidation, also recognized as creep.

Using creeping shale as annular barrier material is at the moment acknowledged as a reasonable alternative to cementing in the petroleum industry. Acceptance criteria for

creeping formation are given in NORSOK D-010 (2013). It is proven that some formations can start creeping enough to seal and isolate the annular gap in a safe and efficient matter. On the other hand, the consequences of creep may vary. Whereas a limited amount of primary creep typically results in a uniform deformation that has only a limited impact on the rock permeability, accelerating creep through failure is likely to produce localized failure zones with significant higher permeability. Thus, delayed deformation, which brings the shale in contact with the casing, does not necessarily produce a sealing barrier.

The occurrence of this phenomenon only happens in some cases due to massive variations concerning creep properties between different shale formations and even within a particular formation.

Scenario to consider [38]:

- a) After the borehole is drilled and cased, the gap between the rock and the surface of the outer casing is filled with a certain mixture of drilling fluid and formation fluid.
- b) The formation rock starts to move toward the annulus. Development of fractures in the creeping rock can occur during this process.
- c) Eventually, the annulus is filled and sealed with creeping rock behind the casing.
- d) Viscous deformation proceeds further. However, the casing applies support, and contributes to open area in the rock formation, as well as the fractures developed in stage (b). This type of deformation contributes to sealing available space in shale, including the fractures caused by the creeping process during stage (c) or the excavation damage caused by drilling during stage (a). The radial stress that is applied on the casing by the surrounding shale formation will continuously increase up to the point where annulus is sealed and equilibrium is established.

In an optimal scenario, creeping can be a tool to reach optimal drilling operation due to the creation of a natural, solid and eternal perspective barrier for flow along the outer surface of the casing.

It should be noted that the timescale of the formation creeping into the annulus appears to vary considerably. Bonded formation has been observed in some cases after only a number of days while in other cases no formation bond is observed after many years [1]. More work is required in order to better understand the controlling mechanisms behind formation bonding.

10.2.1 Process of creep

Theoretically, a fully developed creep process contains three phases; primary, secondary and tertiary as shown in Fig. 10-2. (Fjær et al. 2008). The process may alter entirely from a time restricted movement with small amplitude (i.e. transient creep) to a clear constant process (i.e. steady-state creep) and ultimately to a swiftly process ending in failure (i.e. accelerating creep) [39].

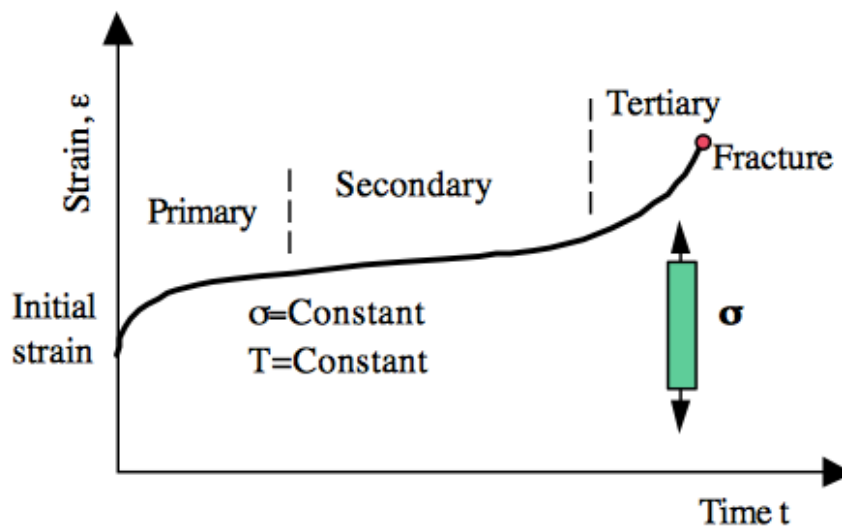


Figure 10-2: The three phases during the creep process [40]

Phase 1

The primary, initially or transient stage involves an large incensement of strain at an accelerated rate that lasts until the strain rate eventually starts to decrease monotonously and becomes relatively constant. The mechanism causing creep in the transient period is the creation of stable microfractures spreading at a decaying rate (Fjær et al. 2008). This decrease of strain is caused by a quickly receding number of available dislocations and the material strain hardens. This material hardening increases proportionally with deformation which is counteracted by the recovery of dislocations [41]. At higher stresses and/or temperatures, strain hardening acts together with "stress relieving" of the material due to reorganization of the dislocations. This phase is caused by thermally activated grain boundary slip. If the applied stress is removed, the rock acts elastically and will go back to its initial size. The deformation will be reversed and approach zero (Fjær et al. 2008).

Contrarily, if the stress or temperature continue to be sufficiently high, the transient creep stage will be followed by the second stage called steady state creep, where the deformation rate will stabilize and approach a final value.

Phase 2

The secondary creep is characterized by the strain hardening being eliminated by the "stress relieving", accordingly leading to a constant creep rate. It consists of the slowest creep rate during the test, also known as the minimum creep rate or steady-state creep rate. Steady state creep is defined as increasing deformation with constant strain rate, and will eventually lead to failure. If the applied stress is reduced or removed during the steady state stage, the deformation derived from this phase will not recover. This is classified as plastic deformation.

Contrarily, if the stress is sustained for sufficient period of time and the stress and/or temperature is high enough, the deformation will proceed into the third and final stage called tertiary or accelerating creep.

Phase 3

The same mechanisms are working in the final phase called tertiary or accelerating creep. It consists however of a rapid increasement of strain rate and the deformation rate increases exponentially as unstable microfractures spreads at a rapid rate just before it reaches the point of failure.

After creep tests are performed, the results are schemed and plotted in a diagram as initial strain versus time up to the point of rapture/failure [35,38].

11 Swelling formation

Most reservoirs contain both interstitial waters/ formation water and swelling clay minerals. The common class of shale problems presented in the introduction results from the following interrelated factors [42]:

- Shale hydration and swelling
- Dispersion of shale cuttings
- Abnormal pressure

In addition, other processes and borehole conditions tend to intensify the instability of the formation. These include

- Time spent in the open shale zone
- In-situ stresses and formation characteristics
- Mechanical and erosive action

Swelling occurs when the pore fluid chemistry changes (e.g., it is soaked in water) or the confining stress is below the swelling pressure. Swelling pressure is the average pressure in pores that cause material to swell. Some elements, such as clay, are especially sensitive to water and swell to take in the extra mass. The swelling process can be divided into three phases, as shown in Figs. 12-2a to 12-2c [43,44]:

- Phase 1: Water flows from outside into intramatrix pores by hydraulic flow
- Phase 2: Water migrates from the intramatrix pores to the interlamellar pores by ionic gradient. Water interacts with clay minerals and cations by hydration and swelling occurs
- Phase 3: Fluid in interlamellar pores reaches equilibrium. The effective confining stress is sufficient to prevent both water osmotic movement and hydration

The following graph shown in Figs. 12-2a to 12-2c presents an example of the swelling phases of a specimen in salinity [44]:

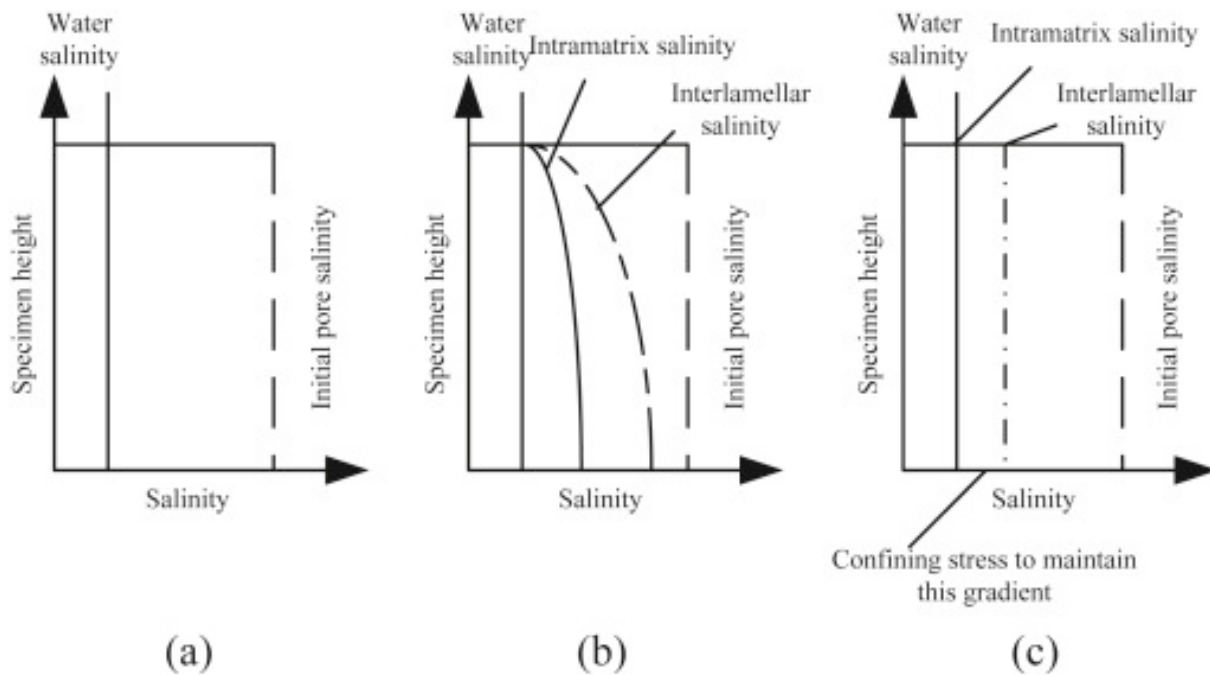


Figure 11-1: Swelling phases of a specimen in salinity a: initial, b: intermediate, c: final equilibrium [43]

There are two types of swelling that can occur in smectitic minerals [43]:

- The first is “crystalline” swelling where expansion of the interlayer spacing takes place in discrete steps which are related to the number of water layers in the interlamellar space, Table 11-1 [17].

Table 11-1 Basal spacing related to water layer

Water layers	Basal spacing [Å]
One- water-layer	≈ 12.5
Two-water-layer	≈ 15.0
Three-water-layer	≈ 20.0

- The second type is “osmotic” swelling and is thought to occur in nature environment when the smectitic clay is Na^+ -saturated and where the external fluid has a very low ionic concentration. In osmotic swelling, the basal spacing of the swollen smectite usually exceeds 40 Å and may reach much higher values. As previously mentioned, osmotic swelling of Na^+ smectite is thought to be the main cause of shale instability. Therefore, swelling pressure should be highly clay-specific and the effectiveness of inhibitors in reducing swelling pressures should be different for different clays, with

the strongest effects being confined to smectites and mixed-layer clays with expandable interlayers. There should be little effect on illite and other non-swelling clays [26].

To a certain degree, higher initial water content implies lower adsorbed water content. Consequently, shale swelling potential is negatively related to initial water content. Clay minerals are characterized by small particle size. A higher clay fraction will produce more pores and clay surface, which are suitable for cation exchanging. However, the swelling of clay is determined by water adsorption. Therefore, initial water content has a higher influence on shale swelling potential than the clay fraction.

Swelling clay minerals or migration can lead to formation damage during the production of oil and gas. For that reason, it is important to have a good understanding of the damage mechanisms of clays to avoid and fix possible formation damage in reservoirs [44]. Even if swelling clays only constitute a few percent of the reservoir rocks, they are predominant in regards to surface area. The clays are originally hydrated to a certain degree and are in a state of equilibrium with the connate water/fossil water (water trapped in the pores of a rock during its formation). The equilibrium in the clay-water system is disturbed during drilling, when water from mud penetrates the sand, as the water is not in chemical equilibrium with the initial interstitial water. This results to swelling of the clay particles, obstruction of pore spaces and reduction in effective permeability. The same problem can take place if there is incompatibility between injected water during water flooding and formation water.

When clay rich shale adsorbs water, the surface of the clay mineral reduces the chemical potential of the water, generating a gradient in the chemical potential that leads to further water to flow into the shale.

Shale swelling is also influenced by other elements, i.e. temperature, water, salinity and content of total organic carbon (TOC) [43].

11.1 A review of conducted experimental works on swelling clay

During this master thesis, I have done a literature review on clay rich shales and their properties, especially mechanisms behind swelling. Several laboratory studies performed by many researchers have examined clay swelling [43]. The essence in the reports is as described below:

- Grim (1939)
 - Stated that kaolinite has little impact on EOR and the montmorillonites have the greatest influence [45].

- Mooney and Keenan (1952)
 - Determined osmotic swelling transpire as a result of the exchange of cations between layers. When the concentration of cation in the interlayer area is greater than that in the water nearby, water molecules infiltrates the area to dilute the concentration of cations and re-establish the cationic balance. Thus, the interval between layers of clay begins to grow and the clay swells.
 - Osmotic swelling increases the volume more compared to crystalline swelling [46].

- Skempton (1953)
 - Analysed the relation between clay content and plasticity index, which showed that for a specific clay, the ratio between clay content and plasticity index is constant, which was called activity [47].

- Norrish (1954), Foster (1954), Madsen and Vanmoos (1989), Lal (1999) and Fink (2015)
 - Concluded that clay swelling occurs by two mechanisms: crystalline swelling and osmotic swelling. Crystalline swelling occurs in all types of clay minerals, especially in the smectite group, as a result of hydration of cations located between the layers of clay. The hydration of cations by water increases the distance between the layers of clay [48,49,50, 51].

- Ezzat (1990)
 - Stated that smectite is 100% expandable and it causes tremendous loss of micro-porosity and permeability. However, smectite is not as common as the other clay minerals in most of the reservoirs currently being developed [52].

- Karaborni, et al., (1996)
 - The effectiveness of K^+ ions in minimizing swelling pressures in montmorillonite is considered to be related to the small degree of hydration of these ions in water, resulting in low ion repulsion [53].

- Chenevert (1970)
 - Studied the swelling alteration of montmorillonite shales, illitic shales and chloritic shales after adsorbing fresh water. The results showed that all the three types of shale presented a significant swelling percentage.
 - Stated that modifying the water activity of oil-based drilling fluid could prevent water adsorption into shale formation during drilling operation i.e. water activity of drilling fluid equals water activity of pore fluid, which is referred to as the balanced water activity concept [54].

- O'Brien and Chenevert (1973)
 - Were among the first to try to directly relate the instability of shales to their clay mineral composition [55].

- Wang et al. (1994)
 - Researched the swelling of five shales under a temperature range from -10°C to 23°C . The results showed a quadratic relationship between them. When the temperature is less than 10°C , the swelling potential of shale will decrease with the increase of temperature. When the temperature is higher than 10°C , it has a promotion effect of shale swelling. As the variation of swelling against temperature was not high].
 - Measured the swelling of four pure clay minerals, which often occurs in shales, by determining the relationship between stress and void ratio (water content) by using an odometer test.
 - Swelling index found characterises the hydration stress of a specific clay mineral/fluid combination and the results signifies that inhibition basically influences hydration of smectitic clays, but not for other clay minerals tested [56].

- Holsrud (1998)
 - Studied the swelling pressure phenomenon in shale formations. Conclusion was that shale swelling develops because of capillary pressure as the main driving mechanism (capillary suction) [57].

- Van Oort (2003)
 - Described what is considered to be a common situation where swelling pressure that occurs after interlamellar expansion and hydration of smectitic clay minerals, combined with pore pressure overcomes in-situ vertical and horizontal stresses and any cementation bonds holding the mineral particles together.
 - Specified the chemophysical nature of shale-water interactions by examine the transport phenomena associated between the wellbore and the shale formation.
 - Studied shale drilling fluids that had been qualitatively classified in five different categories of increasing shale-stabilizing ability based on their effect on swelling pressure, shale water content and pore pressure.
 - Suggested that shale-fluid system could act as a “leaky osmotic membrane” and the ability maintain chemical osmosis when the diffusion of solutes and the direct Darcy flow of water are studied individually. Therefore, by using high-salinity fluids (e.g. KCl, NaCl, CaCl₂, KCOOH) it is possible to stimulate osmotic backflow of shale pore water towards the wellbore, efficiently offsetting the hydraulic inflow of mud filtrate.
 - Proved that if the salinity of water in the drilling mud is greater than that in the pores of the shale then osmosis acts to dehydrate and stabilize the shale [26].

- Schlemmer et al. (2003)
 - Detected that the interactions of shales with various drilling fluids developed pore pressures generally compatible with osmotic theory, but depending on their clay mineralogy, porosity, pore water salinity and especially the composition of the drilling fluid. Water-based muds resulted the lowest osmotic effect whereas silicate-based muds, which formed impermeable deposits or precipitates, as well as invert emulsions, produced the greatest effect [58].

- Sabtan (2005)
 - Presented a multiple linear regression (MLR) model to do calculation of the expansion of 30 undisturbed shale core samples. The linear empirical equation which involve incorporates plasticity index, the clay fraction and initial water content is written as follows [59]:

$$S = 1 + 0.06 (C + PI - W) \quad (\text{Eq.11.1})$$

where

- S = Swell
- PI= Plasticity Index (ranges: 8-79)

- C = Clay presentage
- W= Moisture content

- Ewy and Morton (2009)
 - During the drilling process, the drilling fluids and the ground water are absorbed by shale. These fluids are not pure water; they usually contain salts such as K, Na and Ga. The concentrations of these salts will affect shale swelling and strength [60].

- Gomez-Gutierrez et al. (2011)
 - Performed slake durability and swell tests on unweathered shales, and developed the prediction equation, which is written:

$$S = 29.33e^{-0.064\sqrt{\frac{Id_2}{c}}} \quad (\text{Eq.11.2})$$

where

Id₂ = slake durability index and it is a function of water content.

- The confined pressure affects the swelling potential when shale underground absorbs water. The initial water content and shale water adsorption potential are related.

However, the effect of in-situ pressure was not included, which makes it incorrect to estimate the swelling of shale. [61].

- Zhao et al. (2014)
 - Studied the effect of aqueous solution chemistry on the swelling of clay rock, they concluded that swelling of clay rock was clearly dependent on the concentration of the aqueous solution. The more concentrated the solution, the weaker the swelling [62].

As swelling is a mechanism, which makes the barrier, any induce fracture or failure of the barrier may be re-sealed or re-healed. Therefore, it is important to consider FAB concept self-sealing and self-healing barrier.

12 Self-sealing and self-healing formation

A self-healing material have a natural ability to naturally repair damage on itself without any external diagnosis of the problem or human interventions and is accompanied by loss of memory of the pre-healing state [10,63]. It is more likely to take place in a weak, soft and ductile material. With respect to safety analysis and performance evaluation for a potential repository, it is of great interest to prove whether the interaction of clay with infiltrated water from overlying aquifers can lead to a self-healing of fractures by processes such as swelling and creep. However, it is still unknown if chemical reaction can be a major factor that causes creep, which makes it reasonable to state that shale formation has self-sealing ability, not self-healing.

It is crucial to point out that shale formations are able to self-seal damaged formation and fractures. Self-sealing is determined as the reduction of fracture permeability by any hydro-chemical or mechanical process. This property enables the use of shale formation as barrier, which is a result of a delayed deformation of the shale that occurs when the boundary conditions are reasonably stable. Delayed formation is a common phenomenon in many rock types, with a wide variation of rate and amount. It is less likely to happen in over-consolidated shale because of the brittle structure of such material. Self-sealing can be linked to consolidation, e.g. pore pressure diffusion. However, it is more likely that a result of creep. External conditions like stress, pore pressure and temperature are expected to have a significant impact on the self-sealing process. Also the chemical properties of the borehole fluid that the rock is exposed to may have an impact on this process, although there are incidents that indicated otherwise. Some of these conditions can be modified to some extent, which implies that there may be room for improving the sealing efficiently of the shale barrier in a given situation.

13 Verification of shale formation

13.1 Logging

By testing the formations through logging, it is possible to identify shale formations and positioning of sufficient length and azimuthal coverage in order to determine sufficient collapse all around the casing.

There are currently two logging tools that must be applied for this: ultrasonic imaging tool (USIT) and cement bond logging (CBL) tool. The logs operate independent and are normally run when evaluating the cement behind the casing. Available logging tools do not directly distinguish between liquid and solid (cement, formation). These tools measure acoustic properties. An understanding of these acoustic properties for expected annular liquid and solid materials allows us to interpret what is present in the annulus. To use FAB on a larger scale, improved logging tools is needed to log beyond a single casing string.

VDL is normally performed in addition to CBL as it provides an improved understanding regarding detection of formation arrivals behind the casing in addition to differentiate between a fluid- filled annulus and cement in the presence of a large microannulus. CBL and VDL complement each other and should therefore always be run in combination [10].

However, it is not sufficient only to detect good bonding by the use of logs. Some additional and essential observations are [1]:

- Sections with good bonding (detected by low CBL-values) appear to collate with high content of smectite. Conventional logs show nothing special in the zones with good bonding, but the clay type is different in these areas.
- Possible leakage into nearby permeable zones may have enabled reduced annulus pressure in sections where good bonding has been detected.
- Prefer pressure testing in addition to logs, for verification. Such tests have 30 minutes duration, and are performed over 30 m intervals.

13.2 Pressure testing

If the bond log detects shale formation behind the casing, it is necessary to perform a pressure test to control if the formation has acceptable strength as a barrier.

The minimum formation stress is a highly important parameter since it determines the most desirable depth of barrier placement. As stated by NORSOK D-010 (2013), a primary and secondary barrier should be situated under the conditions where the estimated formation pressure is above the potential internal pressure. Another rule is to place a barrier at a depth under the conditions where the potential pressure does not extend the minimum formation stress, also known as the fracture closure pressure.

To determine the quantity of pressure a specific formation may sustain before fracturing, it must be identified how strong the formation surrounding the wellbore is. This information is acquired by an extended leak-off test (XLOT) performed after completed drilling operation of the set cement below the casing shoe. The process is initiated by pumping mud at a constant rate into the wellbore while monitoring the pressure. As long as the pressure increases at a constant rate as mud is pumped into the wellbore, the formation is intact and there is no leakage of fluids present. This phase represents the straight increasing line at the beginning of the diagram, Fig. 13-1 [64], also constituting what is known as a formation integrity test (FIT) [65,66].

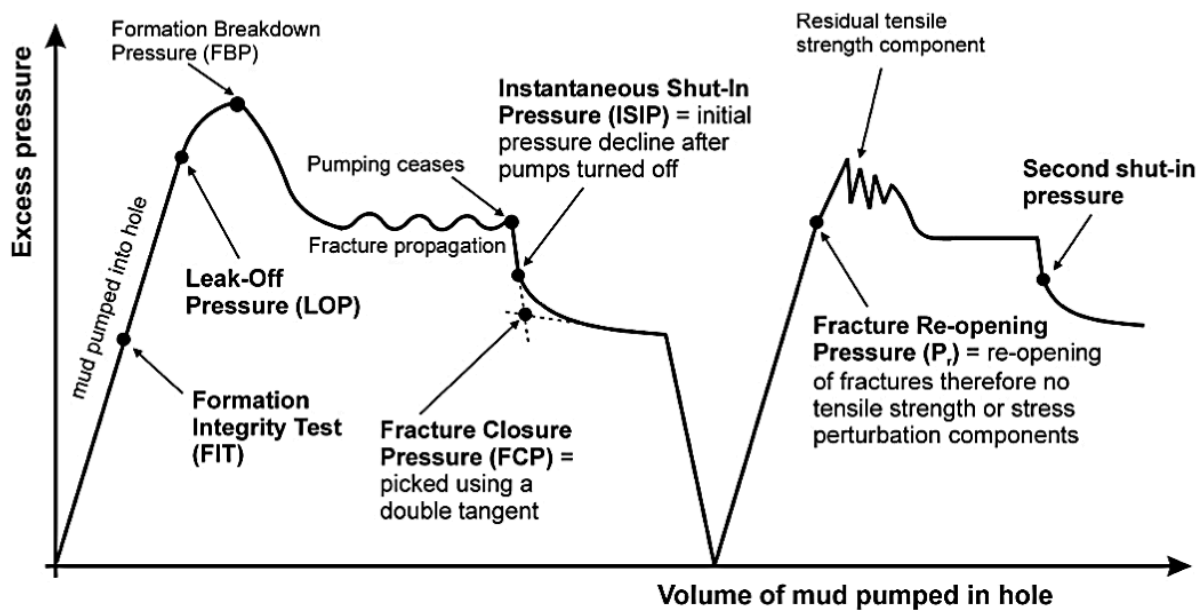


Figure 13-1: Significant points during an extended leak-off test [64].

As the pressure increases, mud will eventually start to seek into the formation rock either through fractures or along the cement around the casing. This is illustrated in the diagram as the point where the linear line ends, where the pressure begins to decrease and the leak off pressure (LOP) is achieved. The maximum pressure is generally referred to as the formation breakdown pressure (FBP). The formation will at this point ultimately fracture causing a rapid drop of pressure as the mud leaks into the formation. Due to the massive load of the rock applied on top, the fractures are not able to crack upwards. The formation will therefore open where it finds the least resistance, which is sideways. A fracture will evolve equally in a vertical direction and grow as more fluid is pumped into it. After the fracture has grown further into the formation for a period of time (fracture propagation), the pumping stops when the pressure becomes relatively stable. This pressure is called the fracture propagation pressure (FPP). The instantaneous shut-in pressure (ISIP) is reached when the pumps are turned off and a pressure declination occur as the frictional pressure loss disappears might be detected. Leak off in the formation or backflow into the well reduces the pressure and the fracture in the formation closes. This pressure is the minimum formation stress, which gives information on where to place barrier in the well. If the same procedure is performed one more time, the fracture will open at the minimum formation stress since it has already been broken down before [64,65,66].

14 Factors influencing creep

Since not all shale formations creates seals, the question is if its possible to stimulate shale creep and seal formation to avoid the need for casing removal, e.g. by applied load, heating or pressure drawdown in the annulus around the casing.

14.1 Mineralogy

Knowing the mineralogy (from mineralogy data) is highly important to estimate where creeping shale may appear. Fig. 14-1 shows an example of mineralogy data, the left side shows the total amount of clay and the right side shows typical types of clay; green is smectite, yellow is illite, red is kaolinite and black is chlorite. It also shows intervals where formation has proven to close in and become barrier that contain a lot of clay and smectite. However, a formation does not necessarily need to have a lot of smectite to create a barrier. From the previous sample from Oseberg Shetland formation in section *History background*, the smectite content was quite low and the clay was predominantly illite clay. But one thing is certain: The formation needs a lot of clay to work as formation barrier.

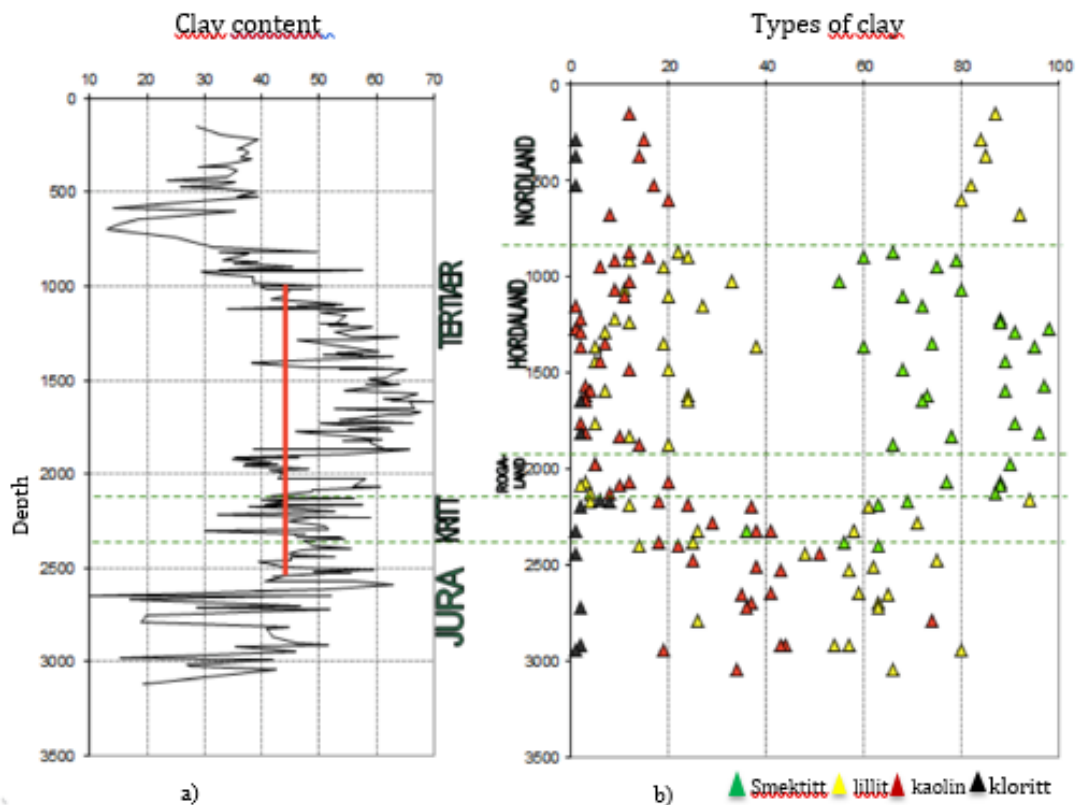


Figure 14-1: Mineralogy data example a: Clay content, b: Types of clay [1]

It appears that the clay content must be larger than 40%, quartz content less than 5%, and the total carbonate content less than 5%. The presence of smectite appears to be important, as it have been seen good bonding correlated with high content of smectite. However, as previously mentioned, it may not be directly necessary, as good bonding has also been observed in formation with low smectite content [1]

Table 14-1 Content requirements for shale barrier

Mineral	Content (%)
Clay	>40%
Quartz	<25%
Carbonate	<5%
Smectite	No specific number defined

14.2 Load and temperature

High load and high temperature is known to accelerate the creeping process. It is the outcome of temperature, applied load and time that determines if a creep process is suitable for a specific application. Fig. 14-2 shows three different scenarios after primary consolidation with three different loading scenarios applied to the material while Fig. 14-3 shows the effect on the creeping process from change in temperature and stress [38,67].

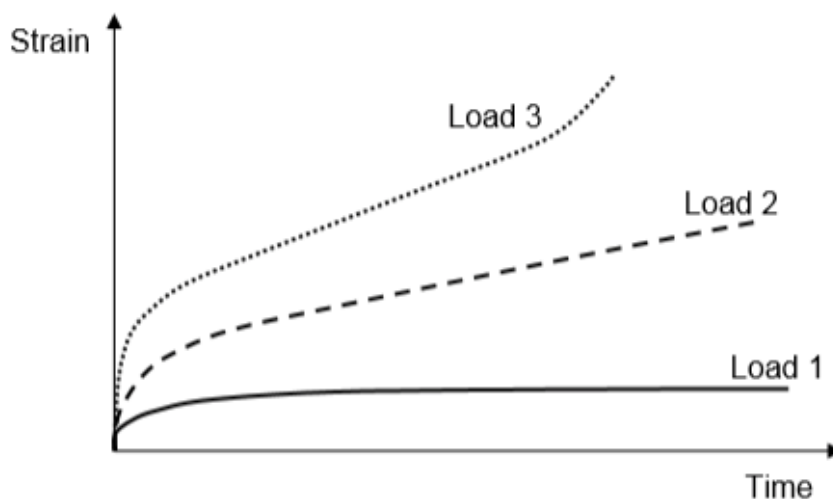


Figure 14-2: Three different loading scenarios applied to a material [67].

- Load 1: Low load applied. Consist only of the first phase of creep process: primary creep or also called transient creep. The strain rate eventually decreases and stays at zero. The creep deformation stabilizes.
- Load 2: Higher load applied. Consist of two phases. Initially the primary phase with decreased strain rate followed by steady-state creep/ secondary creep, where the creep rate remains at a constant rate.
- Load 3: Highest load applied. All phases are present consisting of decreased strain rate, constant creep and incensement of strain until point of rapture (tertiary creep).

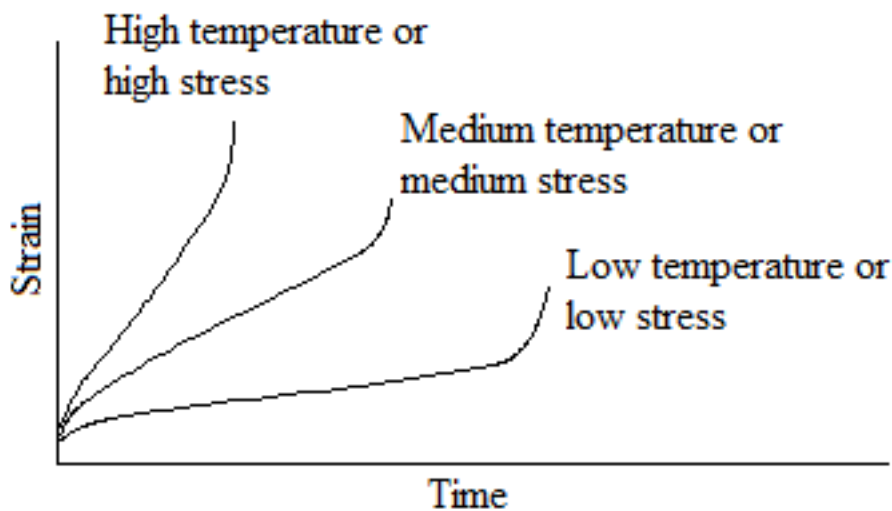


Figure 14-3: The effect on the creeping process from change in temperature and stress [67]

Rising temperature can yield enhanced creep rates and/or reduced rock strength. Even more substantial is the fact that heating low permeability shale formation gives increased pore pressure due to the thermal expansion of pore fluid is greater than that for the rock matrix. This can lead to a reduction of effective stress, which under the shear stresses present around a wellbore, can produce plastic shear deformation.

Several laboratory experiments with core plugs from different field-shale facies as well as numerical simulations advocate that heating helps stimulate plastic deformation in shale formation, which could optimally result in shale barriers. Experimental results demonstrate how undrained heating under deviatoric stress can result in large plastic shear strains. Thermo-hydro-mechanically coupled finite-element simulations show that heating of a well

can give a adequately strong reduction of the borehole radius to close the gap between the casing and formation [68].

Even though temperature may be a good method in many cases, more work is needed to understand the limitations regarding to heating the shale formation to induce creep.

14.3 Pressure drop in annulus:

The understanding of the activation of shale barriers using pressure drop in annulus is maturing. However, the best experience regarding initiating creep has so far been by performing a rapid pressure drop in the annulus. High fluid pressure in the annulus may however prevent the establishment of shale barriers. In the situations where shale barriers have been detected the annulus, pressure has been bleed off either through an open annulus valve, or into nearby permeable zone. Whereas good bonding has been observed after only a few days in such cases, no bonding has been observed after as much as 14 years in cases where the annulus fluid has not been able to escape during compression [1].

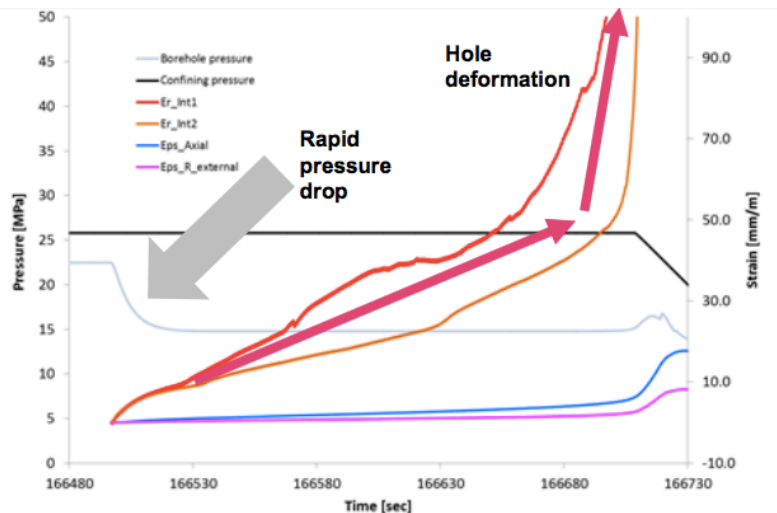


Figure 14-4: Shale deformation response, shale is closing annulus around casing [69].

Fig. 14-4 shows an illustration from an experiment performed by SINTEF in Shale Barrier JIP sponsored by Aker BP, ConocoPhillips, Shell, Statoil and Total on how a shale cylinder is reacting to a pressure drop in the annulus of a well. The plot is showing a typical development

in an annulus in a well where a drilling liner is used to drill into a depleted reservoir. The pressure increase is typically caused by flow restrictions starting to form in the annulus as shale material is closing the annulus [69].

14.4 Chemical methods

It has been studied and experienced that under given circumstances, creeping process seems to be connected to drilling fluid. However, chemical methods may take some more time than typically needed with the pressure drop in annulus method.

The petroleum industry has found a few wells over the last year where the formation has moved in and sealed around the pipe. These incidents are linked to water-based drilling fluid. Sufficient formation bond has not been found where wells was drilled with oil based mud. This is so far not proven yet and still under research.

14.4.1 How brine exposure effects shale formation

Bore hole collapse/ creep is normally caused by shear failure of the rock near the hole, and thus controlled by the stress alteration taking place as a result of drilling. Mainly the pressure in the borehole, i.e. the mud weight, therefore controls borehole stability. Wellbore instability is in fact the most significant technical problem area in drilling and one of the largest sources of lost time and trouble cost. The mud composition may however be adjusted so that interaction between shale and drilling fluid may help stabilize the borehole. Otherwise, if the mud interacts in a non-favourable way with the formation, chemically triggered borehole collapse may occur [67,70,71].

During drilling it is common to encounter water-sensitive shale zones, where the selection of the fluid becomes even more important. Thus, it is necessary to understand the mechanisms of shale-fluid interaction [5] to improve the foundation for selecting the optimum drilling fluid density and composition fluid (in particular water-based mud) to avoid borehole instabilities or, if desired, potentially contribute to formation movement.

The stress conditions in shale are altered through chemical interaction between the formation and the drilling fluid. Water and ion movements in shales affect the alteration of the mechanical and physicochemical characteristics of shales, which leads to wellbore instability

and potentially hole collapse [72]. This process is known as osmosis by which a semipermeable membrane splits a solvent into two zones of dissimilar water activity. The water molecules of a solvent will then pass through the membrane from the less concentrated to the more concentrated water activity zone until concentrations are equalized on each side of the membrane.

As mentioned in *Clay mineralogy and shale instability* section, the traditional view of the industry has been that clay swelling is responsible for chemically induced instabilities, and that adding salt to the drilling mud prevents swelling. The stress conditions in shale are altered through chemical interaction between the formation and the drilling fluid through the process known as osmosis where a semi-permeable membrane permits water and rejects ionic flow between the drilling fluid and the formation. In terms of osmotic theory, a semipermeable membrane splits a solvent into two zones of dissimilar water activity. The water molecules of the solvent will then pass through the membrane from the less concentrated to the more concentrated water activity zone until concentrations are equalized on each side of the membrane. In the case of water-based drilling fluids, the shale itself is thought to be the membrane, whereas with oil-based mud, the membrane properties are associated with the mud. If the chemical activity of the mud is low compared to chemical activity of the pore fluid (usually associated with high mud salinity), then water will be sucked out of the shale to establish chemical equilibrium, Fig. 14-5. This implies a reduction of the pore pressure near the borehole wall, and thus has a stabilising effect on the borehole.

Contrary, if the mud activity is high (low salinity), then the borehole may be destabilised. The osmotic effect is time dependent. At the time $t = 0$ (start of fluid exposure), there is no chemical effect. The characteristic time for establishing the osmotic potential is given by water transport into or out of the shale near the borehole; i.e. by shale permeability, and the range of the zone behind the borehole wall where pressure changes are required to have influence on borehole stability.

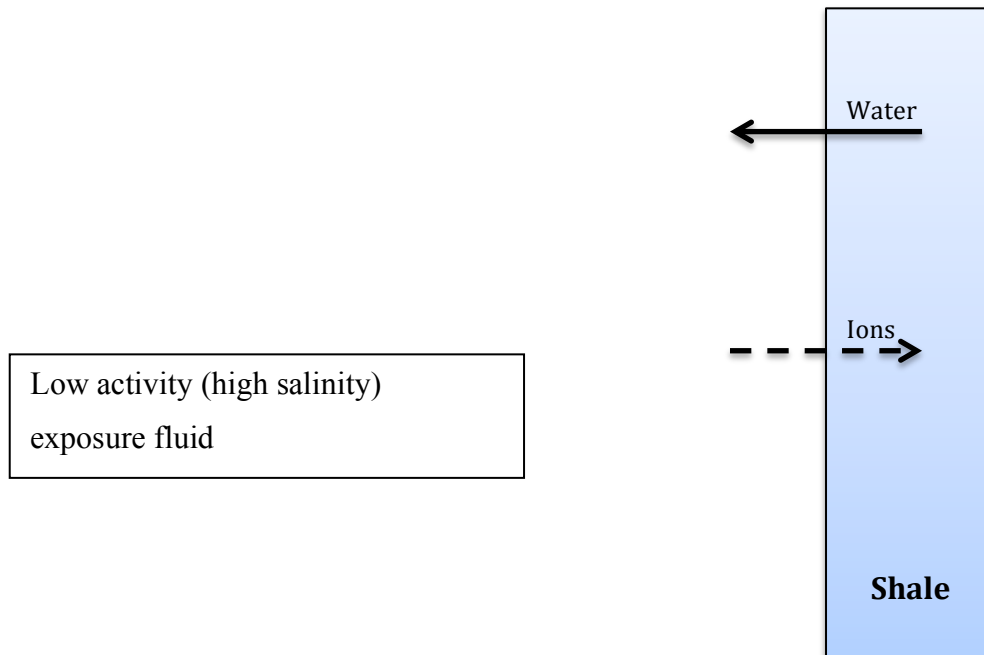


Figure 14-5: Schematic illustration of water and ionic transport between exposure (e.g. borehole) fluid and shale [71]

Mathematically, the osmotic potential (the maximum increase in pore pressure) is given as

$$\Pi = \frac{RT}{V_w} \ln \frac{a_{w,df}}{a_{w,sh}} \quad (\text{Eq.14.1})$$

where

- Π = osmotic potential
- R = the molar gas constant
- T = temperature
- V_w = the molar volume of water
- $a_{w,df}$, $a_{w,sh}$ = water activities of the exposure (drilling) fluid and of the pore water in the shale, respectively.

Literature shows strong evidence from experiments that shales do not act as semipermeable membranes [17,71]. Since ions moves through shales (nearly at the same rate as water) the effect described above is reduced. This is most simply done by introducing membrane efficiency < 1 , which means that ions move in the opposite direction of water in Fig. 14-5.

The osmotic potential in Eq.14.2 is multiplied by this efficiency. Literature also directs to values of membrane efficiencies for typical drilling problem shales between 0.1 and 0.3 [73].

The introduction of a leaky membrane also means that there is a second time scale, dominated by ionic transport in shale. In other words, as time goes by, the osmotic potential will reduce.

The osmotic (“swelling”) influence versus the influence of ionic diffusion is slightly a question of membrane efficiency. If the membrane efficiency $\ll 1$, then the concept of osmosis becomes relatively irrelevant. While if ions in addition to moving through shales also interact directly with the shale, by e.g. ionic exchange, then the osmotic model becomes insufficient for mud design.

Ions diffusing into shales will transfer at clay sites, changing the swelling pressure. The invading mud pressure will increase the pore pressure. In the case of osmosis, the shale can become dehydrated in the near-wellbore zone. These alternations can influence the stress state and/or the strength of a freshly drilled shale subsequently [26].

14.4.2 Effects of KCl exposure on shale

Potassium chloride (KCl) exposure on smectite-rich shale has been studied by various experimental techniques, both under atmospheric and simulated downhole conditions [26,74,75]. Laboratory and field studies have demonstrated that potassium cations at sufficient concentrations in water-based drilling fluids can effectively reduce the swelling and dispersive tendencies of clay-containing shales. It is probably the best-known inhibitor in the oil-industry on account of several particular effects as a consequence of potassium intruding shale. It is also preferred for field use due to low cost and high temperature stability.

One remark is that shale shrinks, mainly due to ion exchange. This will make the permeability increase, alter the deformability and possibly the shale strength. Through simulations of the shrinkage effect around a borehole, it is observed how compressive stresses starts to decrease with increasing KCl concentration, and this will improve the stability. The possibility of borehole instability problems may increase if tensile stresses are developed in the rock at high concentrations. This can also increase the risk of potential destructive effects such as ion transport, pore pressure diffusion [57].

K^+ is considered much more effective than Ca^{2+} or Mg^{2+} in reducing the swelling pressure in for instance the dioctahedral smectite montmorillonite. The effectiveness of K^+ ions in

minimizing swelling pressures in montmorillonite is believed to be related to the small degree of hydration of these ions in water, resulting in low ion repulsion [25,26].

However, the main performance limitation of KCl is its inability to prevent filtrate invasion and mud pressure penetration in shales. The viscosities of KCl solutions are close to that of water, even at salt-saturation levels. KCl cannot plug pore throats or modify shale permeability [26].

Osmotic pressures generated by concentrated KCl solutions are moderate (< 20 MPa) and membrane efficiencies are low (1 – 2%) due to the relatively high mobility of KCl in shale. Accordingly, osmotic backflow of shale pore fluid induced by KCl muds (with effective osmotic pressures in the range 0.1 – 1.0 MPa) will be negligible. As a result, KCl-based mud systems usually are not suitable for drilling older, less-reactive shales. First, ion diffusion is lagging behind mud pressure diffusion. Secondly, these shales have gone through a process of diagenesis which has changed the smectites into less swellable clays such as illites. Concomitantly, there is less swelling pressure in these shales for KCl to act upon. These shales will typically fail due to the effects of mud pressure penetration at prolonged exposure to the invading mud filtrate. Thus, KCl is recommended for primarily for cuttings-stabilization of relatively young, more reactive shale types that contain significant amounts of smectites [26].

Through laboratory and field studies, it is assumed that the concentration of KCl is important for the behaviour of shale [57].

14.4.3 How brines of Ca^{2+} , Mg^{2+} and Zn^{2+} affects shale

Concentrated brines of Ca^{2+} , Mg^{2+} and Zn^{2+} are popular as base fluid for high-density, low-solids drilling and completion fluids. Two factors make them suitable for shale drilling: (i) their filtrate viscosities are high which will slow down hydraulic flow, and (ii) they can generate very high osmotic pressure (on the order of 1000 bars; however, membrane efficiencies are on the order of 1–10% so that the effective osmotic pressure acting is attenuated to 10 – 100 bars) that may be used to (partially) offset the hydraulic mud overbalance. The disadvantage is however that divalent ions will diffuse into the shales as the

fluid, shale membrane is leaky and allows for ion transport from the mud to the shale. When these ions exchange at clay sites for more inhibitive ions such as K^+ , then the swelling pressure may increase, leading to shale instability. When these muds are used, one should carefully balance their beneficial effect on shale water content and pore pressure, and their potentially detrimental effect on the swelling pressure [26].

Whatever the interlayer cations are (for example sodium, calcium) or a mixture of sodium with calcium), the elastic and creep properties of clay skins depended on relative humidity/water content. Increasing the water content makes the clay skins less stiff and make them creep more [76].

14.4.4 Experimental example: Brine with KCl versus Brine with Ca^{2+} , Mg^{2+} and Zn^{2+}

O'Brien and Chenevert (1973) clearly demonstrated that K-based fluids dramatically affected the clays swelling and dispersion behaviour, especially when the fluid included a polymer. As a part of their test Wyoming montmorillonite was saturated with strongly hydrated divalent cations such as Ca^{2+} and Mg^{2+} , which gave a interlayer spacings of approximately 15 Å over a wide range of relative humidities (30-80%) related with a double layer of water. In the case of saturation with the less strongly hydrated monovalent such as K^{+} and NH_4^{+} ions gives smaller interlayer spacings of 12.0-12.4 Å related to a single water layer under the same conditions [17]. Such observations are entirely consistent with the inhibiting effects of K-based drilling fluids on shale instability. Many unstable shales have similar clay mineralogical composition to the specific shales O'Brien and Chenevert (1973) tested and showed how K- based fluids drastically influenced the swelling clay effect and dispersion behaviour, particularly when the fluid included a polymer, Table 14-2.

Table 14-2: Swelling and dispersion behaviour of shale sample in various fluids (after O'Brien and Chenevert, 1973)

Solution	% Linear Swelling	Appearance	% Shale recovery
Water	-	Total disintegration	1.3
10% CaCl_2	2.18	Partial disintegration	5.0
10% NaCl	2.00	Intact, easily crumbled	8.8
10% KCl	1.49	Intact, firm	46.0
10% KCl + Polymer	0.00	Intact, firm	91.6

Seeing that swelling pressures are highly clay-specific, the effectiveness of “inhibitors” in swelling pressures will vary for different clays. For instance, whereas potassium has a strong effect on swelling of montmorillonite, it has hardly any effect on illite and may actually increase the swelling of kaolinite.

15 Modeling of creeping process

Understanding the connections between analytical and numerical tools is important for up scaling to field conditions when studying the mechanisms for use of FAB. Analytical solutions are derived assuming either a linear creep law or a non-linear creep law, while the numerical solution can combine both linear and non-linear creep components in the same creep law.

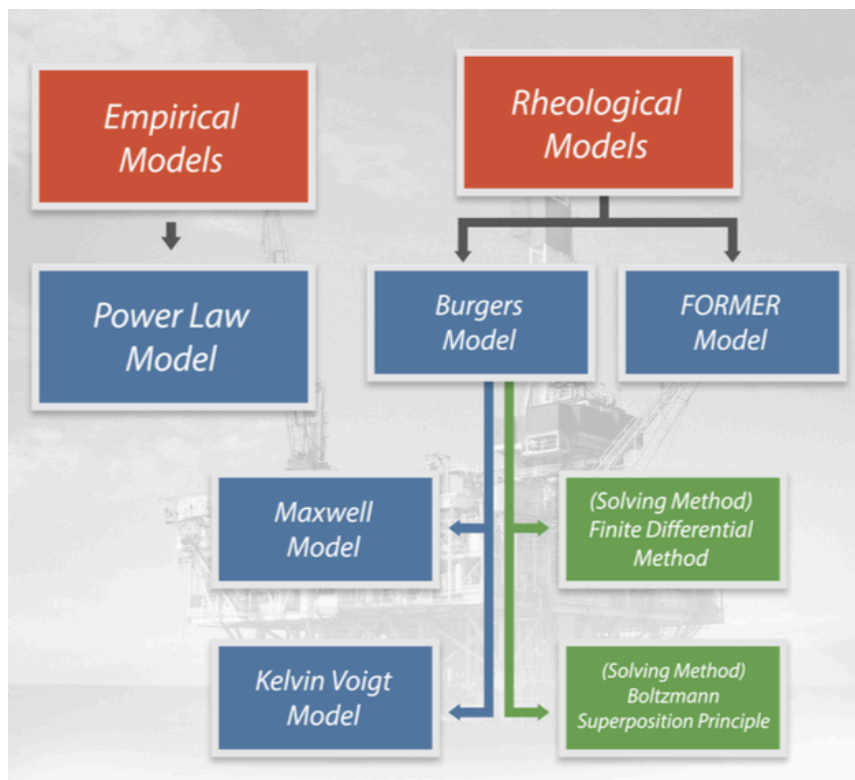


Figure 15-1: Overview of modelling of creeping process

To predict creep, a proper mathematical model is required. Relevant constitutive models can be classified as empirical models, rheological models, and general theories as illustrated in Fig. 15-1 [77].

15.1 Empirical models

15.1.1 Power law model

Sone and Zoback (2014) established a simple empirical power law model to fit the time-dependent deformation data in their tests. This specific model is interesting because it

involves only two constitutive parameters and fits sufficiently to observations of creep with deaccelerating rate at low and moderate stress levels. The original power law model is an empirical strain-time relation defined as:

$$\varepsilon(t) = B_0 \left(\frac{t}{t_{ref}} \right)^n \tau \quad (\text{Eq.15.1})$$

where

- ε = Strain
- B_0 = Constitutive parameter (represents instantaneous elasticity of the rock)
- n = Constitutive parameter (power law exponent)
- $\tau = \sigma_z - \sigma_r$ = Shear stress
- σ_z = Axial stress
- σ_r = Confining stress
- t = Time
- t_{ref} = Reference time

The creep compliance $J(t)$ of viscoelastic materials is an established measure of the rate at which strain increases for a constant applied stress. $J(t)$ is defined as the change in strain as a function of time under instantaneous application of a constant stress, or [77]:

$$J(t) = \frac{\varepsilon(t)}{\tau} = B_0 \left(\frac{t}{t_{ref}} \right)^n \quad (\text{Eq.15.2})$$

15.1.2 Modified Power law model

The original power law model provided a satisfactory analysis of the physical purpose of the two constitutive parameters. However, Fjær et al. 2017 observed that the original power law model could underrate long-term creep when the model was suited for short-term creep data, particularly evident in cases of moderate and high stress levels.

For that reason, the original power law model for the description of short-term creep (transient creep) was extended through inserting a feedback mechanism to detect strength degradation with increasing deformation. This is also expressed in fiber bundle theory [78]. Uniform distribution and Weibull distribution (Weibull, 1951) [79] are two common descriptions in fiber bundle theory and Fjær introduced Weibull distribution (Weibull 1951) as a specific model to characterize strength degradation in the modified power law model.

Fjær et al. (2014) [80] included creep in the FORMEL model (Fjær, 1999) [81] by connecting a delay time with local failure events, which was used to identify an important parameter in the Weibull distribution.

The feedback mechanism that was introduced in the new power law model involved replacing the parameter B_0 with a modified B, defined as following:

$$B \rightarrow \frac{B_0}{1 - P(J(t))} = \frac{B_0}{e^{-\left(\frac{J(t)}{\lambda}\right)^\rho}} \quad (\text{Eq.15.2})$$

where

- λ = Scale parameter
- ρ = Scale parameter

As the creep compliance $J(t)$ increase, B also increases, particularly when $J(t)$ approaches the same value as the scale parameter λ .

With the alternative constitutive parameter B, the modified power law model is defined as:

$$\square(t) = \frac{B_0}{e^{-\left(\frac{J(t)}{\lambda}\right)^\rho}} \left(\frac{t}{t_{ref}}\right)^n \quad (\text{Eq.15.3})$$

When the value of the creep compliance $J(t) < \lambda$, creep is developed with deaccelerating rate. Otherwise, when $J(t) > \lambda$, accelerating creep takes place before ultimately ending in failure.

Therefore, assuming that a corresponding critical creep compliance J_c and λ are equivalent parameters and substitute λ by J_c in the modified expression for $J(t)$, which yields the final version of power law model that will be applied to predict long-term creep by data fitting of short-term creep

$$J(t) = \frac{B_0}{e^{-\left(\frac{J(t)}{J_c}\right)^\rho}} \left(\frac{t}{t_{ref}}\right)^n \quad (\text{Eq.15.4})$$

where

- $J_c = \frac{\varepsilon_c}{s}$ is corresponding critical compliance J_c , which can be calculated based on the FORMEL creapy model
- $\varepsilon_c = \frac{1 - \sqrt{\Delta\sigma_z \frac{q}{E^*}}}{q}$ = critical strain

where

- $E^* = \text{constant}$

As conclusion, the modified power law model has proved to forecast long-term creep based on short-term creep data with remarkably improved precision compared to the original power law model. It is also capable of anticipating accelerating creep and failure.

15.2 Rheological models

The definition of viscoelastic is derived from the words "viscous" + "elastic". A viscoelastic material that exhibit both viscous and elastic characteristics when undergoing deformation – a bit like a fluid and a bit like a solid [82]. A model of linear viscoelasticity can be created based on combinations of linear elastic springs, plastic sliders and the linear viscous dashpot. These are known as rheological models or mechanical models.

The spring complies with Hooke's law as a mechanical model with an elastic element and the dashpot complies with Newton's law of viscosity as a mechanical model with a viscous element [26]. The mechanical model which consists of a Hookean spring and a Newtonian dashpot in series is a Maxwell element (Fig. 15-3) and in parallel is a Kelvin-Voigt element (Fig. 15-4), and the characteristics of the elements are changed to best match the viscoelastic and elasto-viscoplastic behaviour [15].

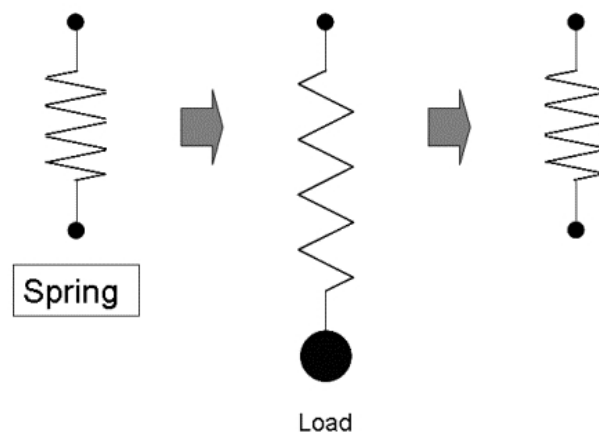


Figure 15-2: A spring which represents an elastic material [83]

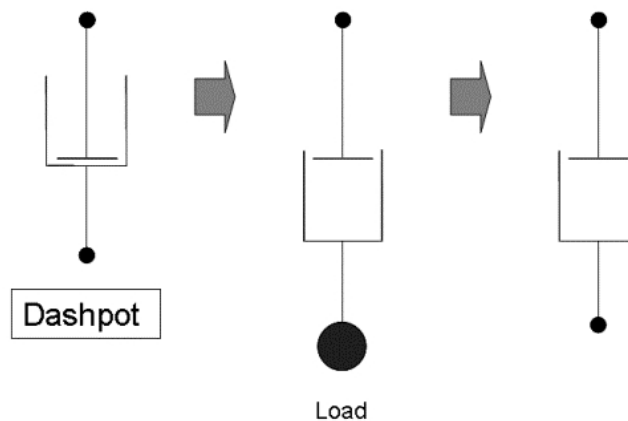


Figure 15-3: A dashpot ,which represents a viscous material [83]

15.2.1 Burgers model

The Burger's model can obtain good comprehensive predictions for deformation in cases where an acceptable number of free variables are used. In situations where only one set of parameters are applied, the model is unable to anticipate deformation of tests involving stress paths with loading, unloading and reloading.

These types of models are quite basic and does not account for normal stress, shear stress, temperature and intrinsic structure. The elasto-viscoplastic substance shows time dependent behaviour in which the deviatoric stress give rise to viscous behaviour, or plastic behaviour if the instantaneous elastic strength of the material is temporarily exceeded [36].

The Maxwell- material (elstoviscous) and the Kelvin-Voigt- material (viscoelastic) are two models that are typically applied when representing a viscoelastic material.

15.2.1.1 The Maxwell- material model

Fig. 15-4 illustrates the Maxwell-element, where a spring and a dashpot are set up in series. The strain of the spring remains constant if the force is unchanged at the same time as the dashpot absorbs more strain with time. The dashpot is made out of a viscous container and a piston arm with enough space for a fluid to pass through to the other side. The fluid flows

from one side of the piston to the other as a function of time. Therefore, the strain absorbed by this element is time dependent and increases with time.

In the Maxwell model, the strain is given by Eq.15.6 [36].

$$\varepsilon = \frac{\sigma_{spring}}{E} \tag{Eq.15.5}$$

where

- ε = the strain
- σ_{spring} = the stress absorbed by the spring
- E = the spring characteristics (an analogue to Young’s modulus in rock mechanics)

Stress-relaxation test

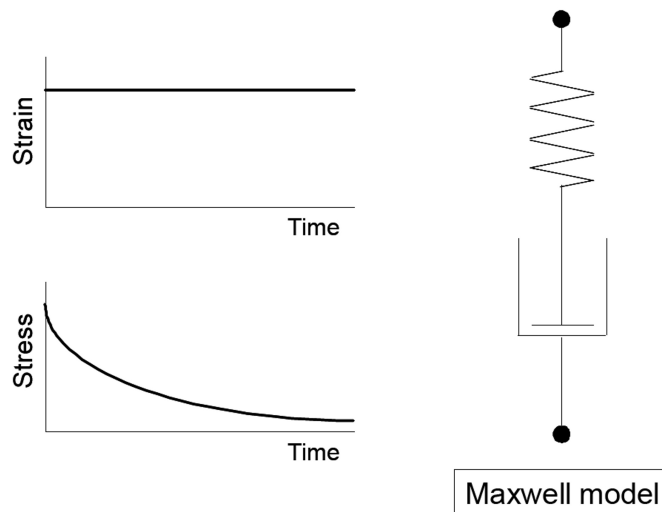


Figure 15-4: Stress-relaxation test and a Maxwell model [83]

The strain absorbed by the dashpot is time-dependent and can be determined from the relation in the Eq.15.7:

$$\varepsilon_{dashpot} = \frac{\sigma_{dashpot}}{\eta} \tag{Eq.15.6}$$

where

- $\varepsilon_{dashpot}$ = the strain rate in the dashpot

- $\sigma_{dashpot}$ = the stress acting on the dashpot
- η = the material coefficient of viscosity

The total strain of the Maxwell model is assumed to be the combined strain of the dashpot and the spring and is represented by adding Eq.15.6 and Eq.15.7, which results in the following Eq.15.8:

$$\dot{\varepsilon}_{total} = \dot{\varepsilon}_{spring} + \dot{\varepsilon}_{dashpot} = \frac{\sigma_{dashpot}}{\eta} + \frac{\dot{\sigma}_{spring}}{E} \quad (\text{Eq.15.7})$$

where

$\dot{\sigma}_{spring}$ = the derivative of Eq.15.6 with respect to time.

Integration of the Eq.15.6 gives:

$$\int d\varepsilon = \frac{1}{E} \int \frac{d\sigma}{dt} dt + \frac{\sigma}{\eta} \int dt \rightarrow \varepsilon = \frac{\sigma}{E} + \frac{\sigma}{\eta} t + C \quad (\text{Eq.15.8})$$

In case the strain rate is non-zero and the material behaves elastic at $t = 0$, $\varepsilon_0 = \frac{\sigma_0}{E}$ and $C=0$.

Assuming the stress is increased instantly before the strain is held constant and the strain rate $\dot{\varepsilon}$ is zero, the relaxation for the stress absorbed by the spring would be:

$$\int \frac{1}{\sigma} d\sigma = -\frac{E}{\eta} \int dt \rightarrow \sigma_0 e^{-\frac{E}{\eta}(t-t_1)} \quad (\text{Eq.15.9})$$

where

- $t - t_1$ = the time when $\varepsilon \rightarrow 0$ and $\sigma = \sigma_0$ gives $C = \ln \sigma + \frac{E}{\eta} t_1$

This indicates that the stress inside the material will decrease once the strain rate starts to approach zero, and relaxation will be non-linear. The reason for the relaxation is that the dashpot takes up strain from the spring.

15.2.1.2 The Kelvin-Voigt model

The Kelvin-Voigt model (also known as the Voigt model) exemplified Fig. 15-5 is another model applied to specify the rheology of a material. It involves the same elements as the Maxwell-element only the spring and dashpot elements are set in parallel instead of series, which provide the material diverse properties. Creep test measures strains caused by a specific load (i.e. a definite force) in a certain range of time. This phenomenon is analysed using a Kelvin-Voigt model.

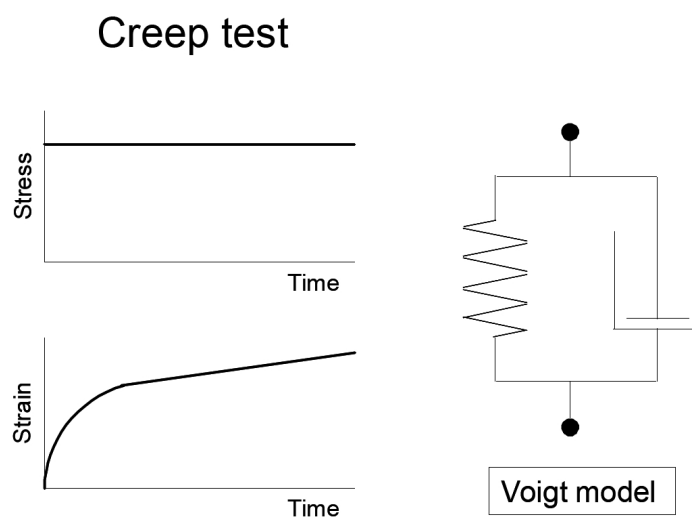


Figure 15-5: Creep test and a Voigt model [83]

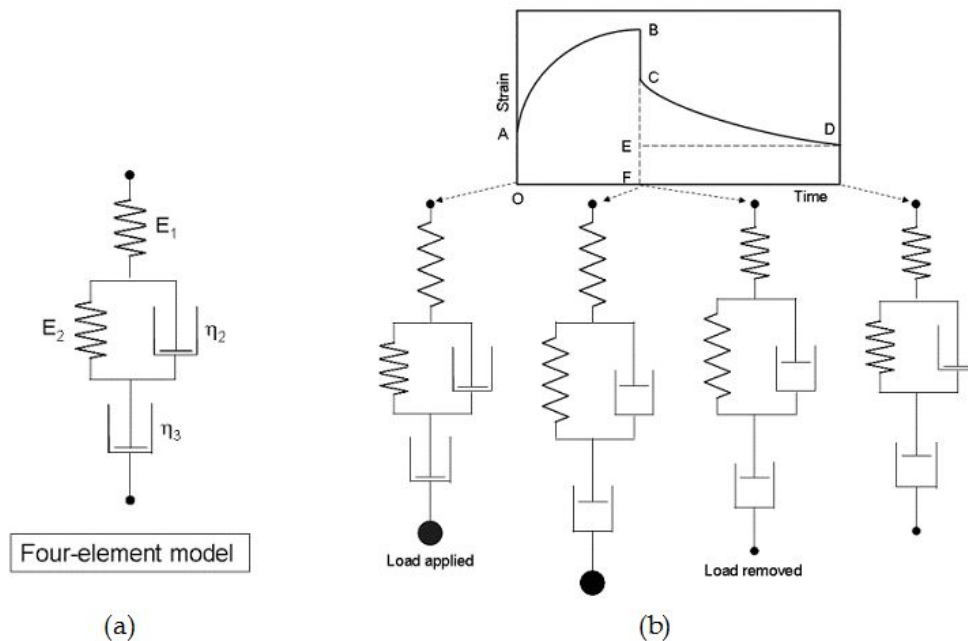


Figure 15-6 a: Four-element model for creep and creep recovery b: Creep and creep recovery. OA: Instantaneous strain; AB: Time-dependent opening; BC: Instantaneous recovery (=OA); CD: Slow recovery; EF: Permanent deformation [83]

Furthermore, a four-element model can analyse creep and creep recovery of a material. Fig. 15-6 illustrates the following:

- a) Four-element model for creep and creep recovery
- b) Creep and creep recovery.
 - OA: Instantaneous strain
 - AB: Time-dependent opening;
 - BC: Instantaneous recovery (=OA)
 - CD: Slow recovery
 - EF: Permanent deformation

When a constant stress is applied at $t = 0$, the material shows an instantaneous increase in strain (the spring E_1), followed by a gradual increase in strain (the spring E_2 / dashpot η_2 and dashpot η_3). On removal of the stress, the spring E_1 recovers instantaneously followed by gradual recovery of the spring E_2 / dashpot η_2 . Some permanent deformation remains as a consequence of the dashpot η_3 .

The dashpot absorbs nearly all stress at the time right after a force is applied to a system illustrated in Fig. 15-6. As the piston in the dashpot is pulled through the cylinder the spring is also extended, which determines that the stress absorbed by the spring increases with time.

The strain development is also dissimilar between the Kelvin-Voigt model and the Maxwell model. For the Kelvin-Voigt model the strain increases simultaneously in both elements as a function of time while in the Maxwell model the strain is instant in the spring and time-dependent for the dashpot.

The Kelvin Voigt model can be defined mathematically by reorganizing Eq.15.6 and Eq.15.7 set apart the stress on one side and adding the stresses:

$$\sigma_{total} = \sigma_{spring} + \sigma_{dashpot} = E\varepsilon + \eta\dot{\varepsilon} \quad (\text{Eq.15.10})$$

If the stress is assumed to be constant (σ_0) for the entire period the differential Eq.15.12 would describe the deformation rate:

$$\frac{d\varepsilon}{dt} = \frac{\sigma_0 + E\varepsilon}{\eta} \quad (\text{Eq.15.11})$$

If Eq.15.12 is modified and integrated the solution would be:

$$\frac{1}{\eta} \int dt = \int \frac{d\varepsilon}{\sigma_0 - E\varepsilon} \rightarrow \varepsilon = \frac{\sigma_0}{E} (1 - e^{-\frac{E}{\eta}t}) \quad (\text{Eq.15.12})$$

since $\varepsilon = 0$ at $t = 0$, giving $C = \frac{1}{E} \ln\sigma_0$ [36].

Eq.15.13 shows that the deformation for the Kelvin-Voigt substance is non-linear.

When the Maxwell and Kelvin-Voigt substances are combined in a series, the product substance is called Burgers substance and is illustrated in the Fig. 15-7. This model can explain the immediate strain, transient creep and steady state creep, for both loading and unloading.

Fig. 15-7 illustrates the way the Burger substance reacts to sudden loading to a constant stress as well as rapid unloading back to zero. The stress σ_0 is applied to the Burger's substance from $0 < t < t_c$. After t_c , the stress is removed and the strain recovery follows in opposite

order as loading. Another difference from the loading phase is that the steady-state deformation is permanent and leaving a non-recoverable deformation. Deformation in the Burger’s substance can be represented mathematically by sets of equations given by presented by Fjær et al. (2008):

$$\varepsilon = 0, t < 0 \qquad t < 0 \qquad \text{(Eq.15.13)}$$

$$\varepsilon = \frac{\sigma_0}{E_2} + \frac{\sigma_0}{E_1} \left(1 - e^{-\frac{t}{t_1}} \right) + \frac{\sigma_0}{\eta_2} t \qquad 0 < t < t_c \qquad \text{(Eq.15.14)}$$

$$\varepsilon = \frac{\sigma_0}{E_1} \left(e^{\frac{t_c}{t_1}} - 1 \right) e^{-\frac{t}{t_1}} + \frac{\sigma_0}{\eta_2} t_c \qquad t > t_c \qquad \text{(Eq.15.15)}$$

where $t_1 = \frac{\eta_1}{E_1}$

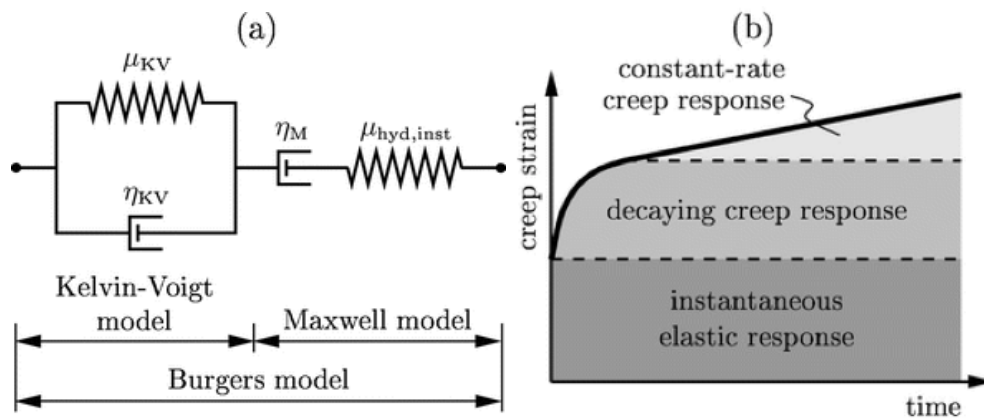


Figure 15-7a: Burgers model, b: Strain response in a Burger’s substance (84)

15.2.1.3 Solving Burgers Model– Finite Difference Method

The Burgers model consists of two basic differential equations based on the Maxwell and Kelvin-Voigt models. To solve the Burgers equations analytically, the two differential equations must be solved separately followed by adding the solutions. A finite difference method makes it possible for the solution to be approximated for the entire equation.

The two simple models in the Burgers model are discretized using backward difference as a way to yield the two following expressions:

$$\dot{\epsilon}_{maxwell} = \frac{\sigma}{\eta_2} + \frac{1}{E_2} \dot{\sigma} \rightarrow \frac{E_{M,i} - E_{M,i-1}}{\Delta t} = \frac{\sigma_i}{\eta_2} + \frac{1}{E_2} \frac{\sigma_i - \sigma_{i-1}}{\Delta t} \quad (\text{Eq.15.16})$$

rearranging gives the Maxwell part:

$$E_{M,i} = E_{M,i-1} + \frac{\sigma}{\eta_2} \Delta t + \frac{\sigma_i - \sigma_{i-1}}{E_2} \quad (\text{Eq.15.17})$$

$$\sigma = E_1 \epsilon_{K-V} + \eta_1 \dot{\epsilon}_{K-V} \rightarrow \sigma_i = E_1 \epsilon_{K-V,i} + \eta_1 \frac{\epsilon_{K-V,i} - \epsilon_{K-V,i-1}}{\Delta t} \quad (\text{Eq.15.18})$$

rearranging gives the Kelvin-Voigt part:

$$\epsilon_{K-V,i} = \frac{\sigma_i + \eta_1 \frac{\epsilon_{K-V,i-1}}{\Delta t}}{\frac{\eta_1}{\Delta t} + E_1} \quad (\text{Eq.15.19})$$

Thereafter, Eq.15.18 and Eq.15.20 can be inserted into two different columns in Excel spread sheets and combined to one model. Next, the squared difference between the model and the linear variable differential transformer (LVDT)-data is determined and minimized by applying a built-in solver function, which adjusts the four parameters (E1, E2, η1, η2) in the equations above. This process is illustrated in Fig. 15-8.

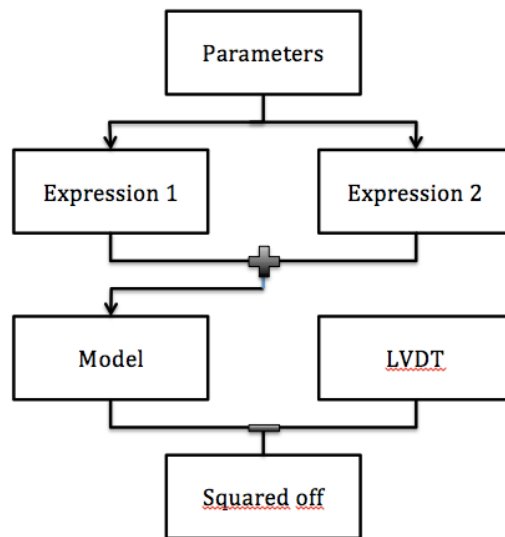


Figure 15-8: Fitting process [36].

15.2.1.4 Solving Burgers model - Boltzmann Superposition Principle

The basic Burgers model can describe the concept in Fig. 15-7. This is the basic model for that specific stress path. This does not solve the stress path used for other experiments where the stress path is varying from a non-zero value to another non-zero value. To deal with this situation, Boltzmann Superposition Principle may be useful since it breaks up the stress path in assorted increments. When a viscoelastic material is linear, the output strain (or stress) response scales linearly with the stress (or strain) input, and the principle of linear superposition holds (Boltzmann Superposition Principle). The method declares that a materials reaction to a given stress is independent of the stress previously applied to the material and gives the following expression [36].

$$\varepsilon(t) = P(t - t_{c1})\sigma_1 + P(t - t_{c2})(\sigma_2 - \sigma_1) + \dots + P(t - t_{ci})(\sigma_i - \sigma_{i-1}) \quad (\text{Eq.15.20})$$

or

$$\varepsilon(t) = \int_{-\infty}^t P(t - t_{c1})d\sigma(t) \quad (\text{Eq.15.21})$$

where

- $P(t) = \frac{1}{E(t)}$ = the compliance function, which is a characteristic of the polymer at a given temperature and initial stress.

Fig. 15-9 shows the creep curve by Boltzmann superposition principle:

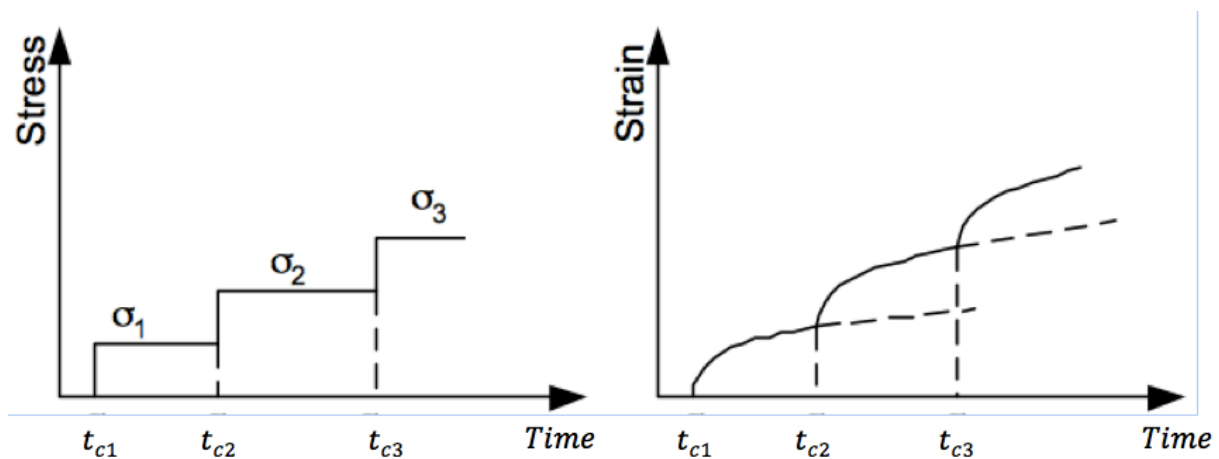


Figure 15-9: Stress and strain curves using Boltzmann Superposition Principle (36)

giving the general form for discrete changes:

$$\varepsilon(t) = \sum_i \varepsilon_i = \sum_i P(t - t_{ci}) \Delta\sigma_i \quad (\text{Eq.15.22})$$

where

- $P(t)$ is the time-dependent compliance of the rock
- t_{ci} is the time where the stress is changed.

This expression can model the stress path and strain curves as illustrated in Fig. 15-9. It is able to use three terms of “compliance” from the Burgers equation yielding:

$$\varepsilon_{i+} = \sum_{i=0} \frac{\Delta\sigma_i}{E_2} + \frac{\Delta\sigma_i}{E_1} \left(1 - e^{-\frac{t-t_{ci}}{t_1}}\right) + \frac{\Delta\sigma_i}{E_2} (t - t_{ci}) \quad (\text{Eq.15.23})$$

Eq.15.24 is one of the addend in the sum of Eq.15.23.

Eq.15.24 can only model the stress path given in Fig. 15-9. Therefore, it is necessary to acquire another term in order to model the decreases in stress applied during the test. By taking Eq.15.14 to Eq.15.16, which consists of two parts; one for the increases in stress and one for decreases in stress, and applying the Boltzmann Superposition principle to the term for $t > t_c$, the following expression is obtained:

$$\varepsilon_{i-} = \sum_{i=0} \frac{\Delta\sigma_i}{E_1} \left(e^{\frac{t_{ci}}{t_1}} - 1\right) e^{-\frac{t_i}{t_1}} + \frac{\sigma_0}{\eta_2} t_{ci} \quad (\text{Eq.15.24})$$

15.2.2 The FORMEL model

Raaen et al. (1996) published the first version of the FORMEL model in 1996. The objective was to define the in-situ mechanical characteristics from logs based on specifying the internal processes existing in the rock when applied mechanical loading. Through further research, Fjær, E (1999) presented an updated FORMEL model in 1999, where the project focused on dynamic and static mechanical characteristics of weak sandstones. As a further work, Fjær.

et.al (2014) presented as a developed model that described the time-delayed deformation of rocks (i.e. creep process).

The FORMEL model application in creep modelling uses the relation between the static and dynamic Young's and Bulk modulus described in Eq.15.26 and Eq.15.27 [36]. According to Fjær (2014) the F- parameter depends on the shear strain and the stress level according to Eq.15.26:

$$E = \frac{E_e}{1 + P_z E_e} (1 - F) \quad (\text{Eq.15.25})$$

$$K = \frac{K_e}{1 + 3PK_e} \quad (\text{Eq.15.26})$$

where

- e = the dynamic moduli
- P = a measure for the non-elastic compliance due to normal loading a process which involves crushing of asperities at the grain contacts.
- F = a measure of the additional non-elastic deformation caused by shear loading and is believed to be proportional to the density of sliding cracks

$$F = A \frac{\varepsilon_z - \varepsilon_r - \varepsilon_0}{\sqrt{\sigma_z + \sigma_r + S}} \quad (\text{Eq.15.27})$$

where

- A and S = material dependent constants
- ε_0 = the shear strain at the start of axial loading
- F = associated with local failure caused by shear stress, e.g. friction controlled slip along crack surfaces, which is the source of creep in the model

As stated by Hook's law: a step increase in axial stress ($\Delta\sigma_z$) leads to an immediate strain ($\Delta\varepsilon_z$), following Eq.15.29:

$$\Delta\varepsilon_z = \frac{\Delta\sigma_z}{E} \quad (\text{Eq.15.28})$$

The increase in stress further generate the F-parameter to increase because the axial strain increases to $\varepsilon_z \rightarrow \varepsilon_{z,0} + \Delta\varepsilon_z$. This results to a decrease in Yong's modulus, following Eq.15.26, which causes an additional increase in ε_z . This leads to initiating another full cycle that reruns until $d\varepsilon_z \rightarrow 0$ or the sample breaks, where each cycle is completed according to the characteristic time. For low stress levels where F is significantly less than 1, the chain of cycles will converge to a finite strain. If stress levels are increased to high values where F is close to 1 the series will diverge and the strain rate will increase to the point where $E \rightarrow 0$. From this point the strain rate increases and quickly leads to failure. Strain-time relationship is given by Eq.15.30 and describes the axial strain induced by a step increase in the axial stress:

$$\frac{d^2\varepsilon_z}{dt^2} + \frac{1}{\tau} \left[1 - \frac{\Delta\sigma_z}{(1 - q\varepsilon_z)^2} \frac{q}{E^*} \right] \frac{d\varepsilon_z}{dt} = 0 \quad (\text{Eq.15.29})$$

where

$$E^* = \frac{E_e}{1 + PE_e} \quad (\text{Eq.15.30})$$

$$q = \frac{A(1 - \nu)}{\sqrt{\sigma_z + \sigma_r + S}} \quad (\text{Eq.15.31})$$

$$(1 - \nu)\varepsilon_z = \varepsilon_z - \varepsilon_r \quad (\text{Eq.15.32})$$

where

- E^* , ν , and q = constants

The creep characteristics are depending on the factor in the brackets in Eq.15.30. If this factor remains positive up until the strain rate approaches zero the total strain will converge to a final value. On the other hand, if the factor turns negative before the strain rate approaches zero, the deformation will accelerate towards failure. The parameter controlling the sign of the bracket is the axial strain and if ε_z becomes sufficiently large the value of the bracket turns negative.

The characteristic creep time in the FORMEL model, τ , is also believed to be a function of the strain contribution from each cycle. The extended model is believed to follow the relation:

$$\frac{d^2 \varepsilon_z}{dt^2} + \frac{1}{\tau^2} \left[1 - \frac{\Delta \sigma_z}{(1 - q \varepsilon_z)^2} \frac{q}{E^*} \right] \tau \frac{d \varepsilon_z^{\frac{1+2n}{1+n}}}{dt} = 0 \quad (\text{Eq.15.33})$$

where

- n = the parameter controlling the strain contribution from each cycle.

For $n = 0$ Eq.15.29 is equal to Eq.15.33.

On discrete form the equation becomes:

$$\varepsilon_z^{n+2} = \varepsilon_z^{i+1} + (\varepsilon_z^{i+1} - \varepsilon_z^i) \left[1 + \frac{\Delta t^{\frac{1}{1+n}}}{\tau} \left[\left(\frac{\Delta \sigma_z}{(1 - q \varepsilon_z^i)^2} \frac{q}{E^*} \right)^{1+n} - 1 \right] (\varepsilon_z^{i+1} - \varepsilon_z^i)^{\frac{n}{1+n}} \right] \quad (\text{Eq.15.34})$$

15.3 Numerical model

Creep is introduced by adding a time-dependent plastic shear deformation at the grain contacts. This implies that the plastic deformation part is mainly distortion rather than change in the volume.

A study done by Fjær et al. (2016) used a commercial code called Particle Flow Code in 2-dimensions to simulate creeping shales [85]. The code is based on the discrete element method (DEM). To simulate creeping shales, it was assumed that the elements are initially bonded. Depending on how the interactions between the elements are defined through the constitutive contact law, the 2D DEM model can be used to simulate materials with different mechanical properties.

In the DEM model, the interactions between the elements (including normal and shear contact forces and rotational moments) are functions of the relative displacements (including angular displacements) between the elements. If those displacements are decomposed into elastic parts and plastic parts, the change of the plastic displacements should not induce the changes of the interacting forces or moments. If the total displacements between two elements are remained unchanged, creep induces an increase in the plastic part while the elastic part and the associated stress is correspondingly reduced. This is called stress relaxation. It results in the time dependent reduction of the interaction forces between the discrete elements.

If the total deformation is maintained unchanged and reduce τ to τ' after a time period Δt , then we have:

$$\tau > \tau' > \tau_0 \quad (\text{Eq.15.35})$$

where

- τ = the average shear stress at a contact between two discrete elements
- τ_0 = the threshold for creep

It is assumed that creep will not happen if the stress magnitude is below this threshold.

If the plastic deformation in the time period Δt is $\Delta \varepsilon_p$, it gives:

$$\tau' = \tau - M\Delta\varepsilon_p \quad (\text{Eq.15.36})$$

where

- M = a modulus.

The ratio of the stresses after and before relaxation is therefore:

$$\alpha = \frac{\tau'}{\tau} = 1 - \frac{M\Delta\varepsilon_p}{\tau} \quad (\text{Eq.15.37})$$

The creep strain in time period Δt can be assumed as:

$$\Delta\varepsilon_p = V_0 e^{-\frac{\beta}{T}} \left(\frac{\tau}{\tau_m} \right)^n \Delta t \quad (\text{Eq.15.38})$$

where

- V_0 , β , τ_m and n = constants
- T = the temperature.

Thus, Eq.15.38 becomes:

$$\alpha = 1 - \frac{MV_0 e^{-\frac{\beta}{T}}}{\tau_m^n} \tau^{n-1} \Delta t \quad (\text{Eq.15.39})$$

Eq.15.40 describes the general way to calculate the contact force reduction in a time step Δt due to creep induced stress relaxation. It applies to the contact forces if they are larger than a threshold. The constants have to be determined through a calibration study by simulating simple creep tests on shale specimens and comparing the simulation results with the laboratory measurements.

16 Required geomechanical conditions for creep formation

The geometry of the problem is illustrated in Fig. 16-1, it shows the borehole (radius R) and the casing (external radius R_c). A common scenario involves a 12^{1/2}" diameter hole and 9^{5/8}" diameter casing whereas the gap $\Delta R/R$ is approximately 23%. The equivalent value for a 17^{1/2}" diameter hole and 13^{3/8}" diameter casing is approximately 24%. This shows the quantity of shear deformation that must be applied to the rock at the borehole wall to close the gap to be sealed. The displacement of the borehole wall due to drillout in a linearly elastic formation is [85]:

$$\frac{\Delta R}{R} = \frac{\sigma_h - p_w}{2G} \quad (\text{Eq.16.1})$$

where

- σ_h = the formation stress
- p_w = the wellbore (i.e. annulus) pressure, and G is the shear modulus of the rock

If there is a pressure reduction of $\sigma_h - p_w = 25$ MPa, then it is necessary to have $G \approx 0.05$ GPa or less to form a shale annular barrier by elastic deformation [56]. Since this is typically a low value, plastic deformation is therefore necessary to create formation barrier.

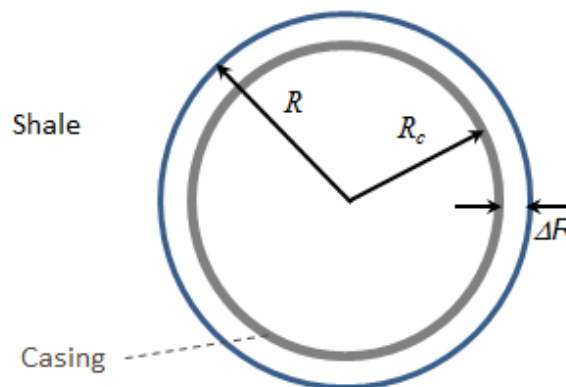


Figure 16-1: Borehole with casing [82]

A gap in a visco-plastic material will eventually close the gap, given the assumption that the threshold for plastic flow is sufficiently low, and that the annulus pressure can be reduced considerably. Contrarily, the pressure drop $\sigma_h - p_w$ will be absorbed by the elastic formation and the gap will remain open. Shales are typically plastic to some degree. But the properties

for shales with a low content of quartz are more likely to have a lower threshold for plastic flow and a higher ability to preserve considerable plastic deformation without disrupting. These types of shales are considered better candidates for annular barrier [85].

In consideration of stress conditions at a borehole wall, plastic flow provoked by large shear stresses at low confinement tends to be dilatant, which can be advantageous for the formation establishment process because the required shear deformation of the surrounding rock will be reduced. On the other hand, it is necessary to mention that the concept of FAB is to seal the annulus around the casing. Therefore, if the process of establishing formation barrier causes fractures and/or high permeable regions around the well, the objective of establishing FAB will not be accomplished.

To measure the quantity of shear deformation that must be applied on to a formation to close the annulus gap, laboratory experiments may help obtaining this information and identify if a specific shale is suitable barrier material.

17 Suggested laboratory experiments on shale

17.1 Hollow cylinder test

Hollow cylinder (HC) test is often used for studies related to borehole stability problems. The hollow cylinders are then often considered to represent the rock around a borehole, and the HC test are expected to reproduce the processes involved when a borehole fails. The benefit of using a hollow cylinder test as compared to uniaxial or triaxial tests combined with modelling, which is usually the alternative, is that the stress distribution around the hole of a hollow cylinder is similar to around a borehole. This stress distribution implies a coupling between deformation and stress, unlike the situation in uniaxial/triaxial tests, and plasticity effects are therefore implicitly accounted for in the HC test. In other respects, the resemblance between an HC test and real downhole conditions is limited. The hole size is down-scaled in an HC test, and the rock volume involved is much smaller. Stress geometry, magnitude of stress and pore pressure, and temperature may be different from in-situ situations, as well as loading rate and stress history. It is therefore a number of parameters that have to be considered in order to establish a quantitative link between lab and field conditions for HC tests [86].

Since shales are porous, fluid saturated and often weak rocks with very low permeability, the scaling effects have to be considered for several phenomena, such as the coupling between elastic and non-elastic deformations and stress, consolidation, creep, pore pressure diffusion and thermal diffusion, boundary conditions, etc. For studies on borehole stability, an additional complication is that there is no unambiguous definition of borehole failure in the field nor in a laboratory test.

There are basically two ways to run a HC test to failure: by keeping the pressure in the hole constant while increasing the external stress, or by establishing a fixed external stress and lowering the pressure in the hole. There are advantages and disadvantages both ways with respect to scaling. In both cases, the rate of change of external parameter plays a significant role, since the pore pressure distribution around the hole depends on this rate as well as hole diameter. On the other hand, creep effects sets other requirements for the strain rate in order to obtain the best match between laboratory test and field conditions [86].

In general, it is not possible to fully reproduce field conditions in a laboratory test by adjusting the external parameters. A sufficiently complex and properly calibrated theoretical model may however give good indications of the corrections needed to bring laboratory results in line with field observations.

17.2 Shale barrier test

This laboratory experiment determines the qualification of shale as barrier and gives us the answer to the two following questions:

- When does the cap close?
- If the gap is closed, is it completely sealed?

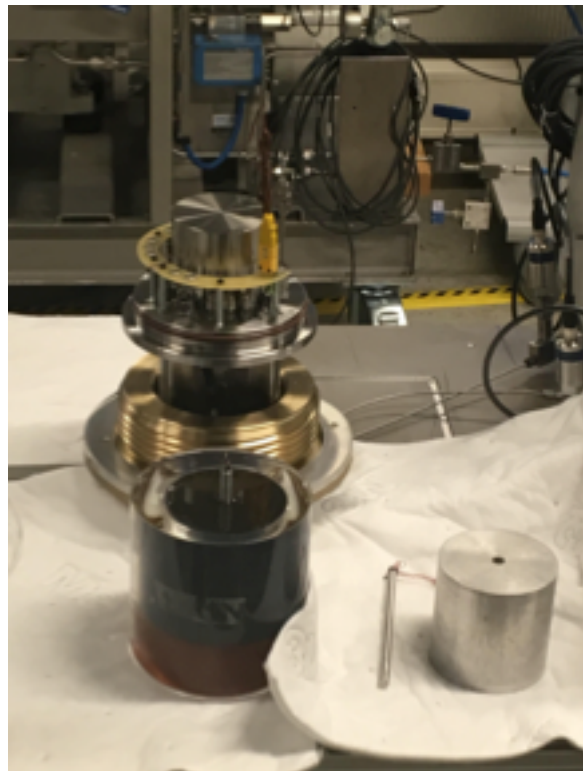


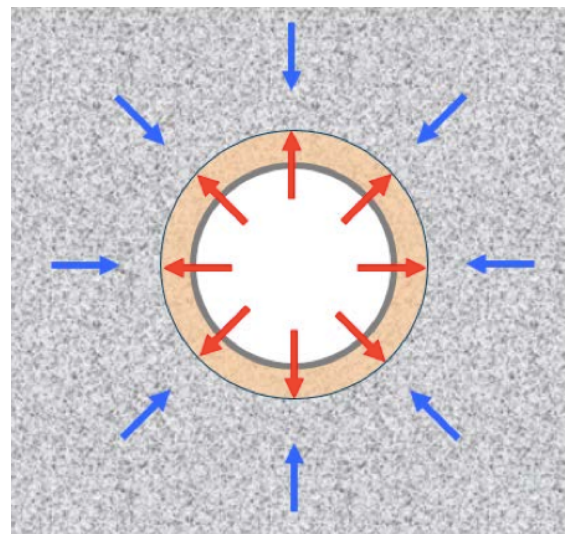
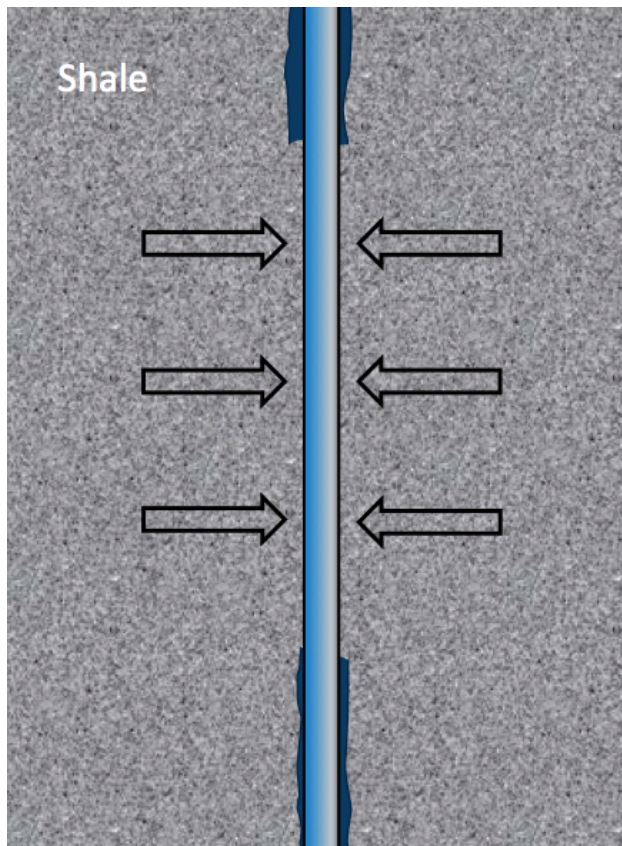
Figure 17-1: Test setup from SINTEF laboratory in Trondheim [86]

The Shale Barrier Test is a specific version of the hollow cylinder test, which is constructed to examine the process of formation of a shale barrier (creep) and qualify the resulting barrier. The creep process involves very large deformations (>20%) of the material located near the casing. This means a region of a considerable size around the drilled hole must be subjected to a substantial plastic deformation in order to close the gap [87].

During the experiment, the fluid pressure communication along the annulus is checked as well as monitoring of the load on a aluminium cylinder, which represents the casing. Theoretical descriptions of the process involve theories of plasticity, consolidation and creep. For numerical simulations, discrete element methods may be useful.

17.2.1 Example from shale barrier test

If looking at a situation in the field, we have formation and a drilled hole. Thereafter a casing is set. The objective is to create a movement of the formation to squeeze in on casing after a while. There are basically two types of forces or stresses when considering the force balance; the in-situ stress, that drives the formation inwards to the drilled hole and the annulus pressure, which is contracting the process.



- In-situ stress
 - drives the shale barrier forming process
- Annulus pressure
 - counteracts the shale barrier forming process

Figure 17-2: Illustration of field scenario [87]

Figure 17-3: Illustration of force balance [87]

A shale barrier map is developed as shown in Fig. 17-4. The map is divided into two sections: One section represents a situation where there is open gap and the other one represent a closed gap situation. When creating a barrier, it is desired to be located in the green area (closed gap) as illustrated in Fig. 17-4. It is undesirable to be in the lower part of this diagram where the hole is collapsing. After the casing has been set, we move downward and end up in the green area.

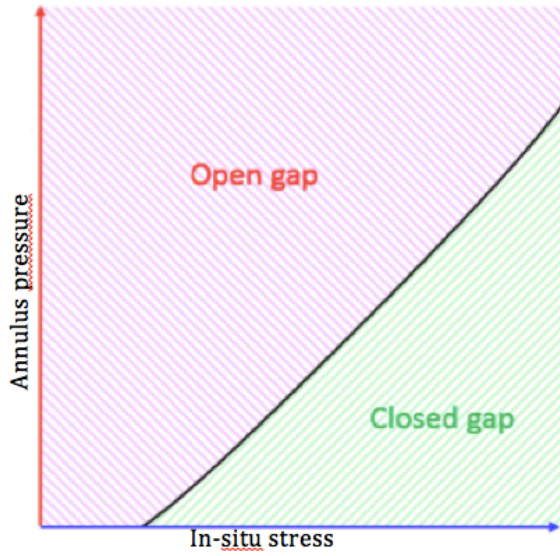


Figure 17-4: Shale barrier map [87]

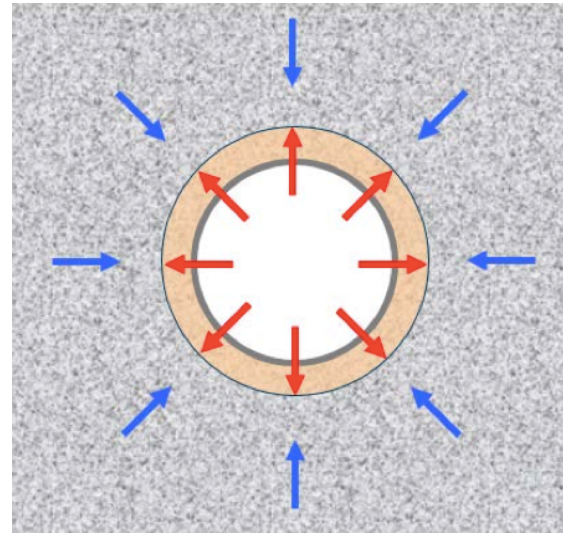


Figure 17-5: Illustration of force balance [87]

However, when during drilling situation is the opposite; to stay in the stable hole part.

During drilling:

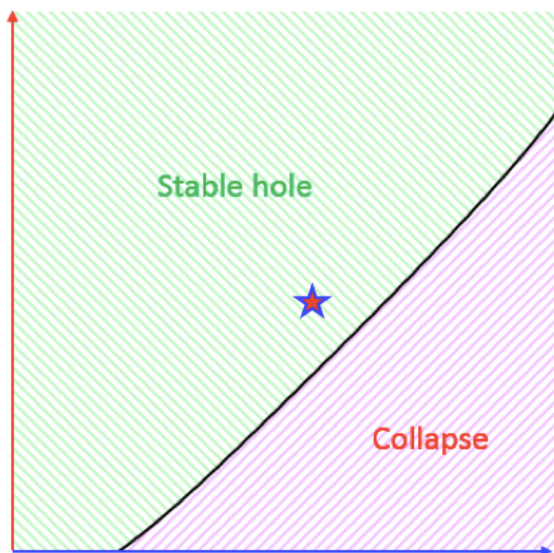


Figure 17-6: Shale barrier map [87]

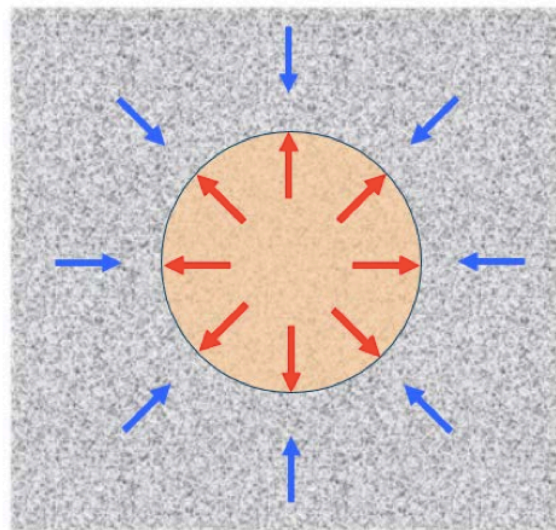


Figure 17-7: Illustration of force balance [87]

After casing has been set:

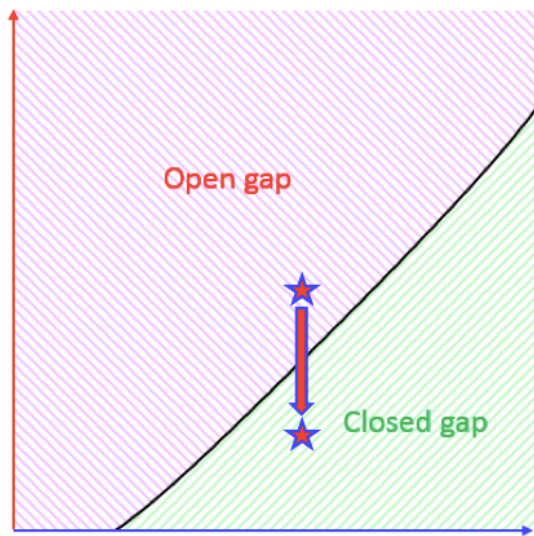


Figure 17-8: Shale barrier map [87]

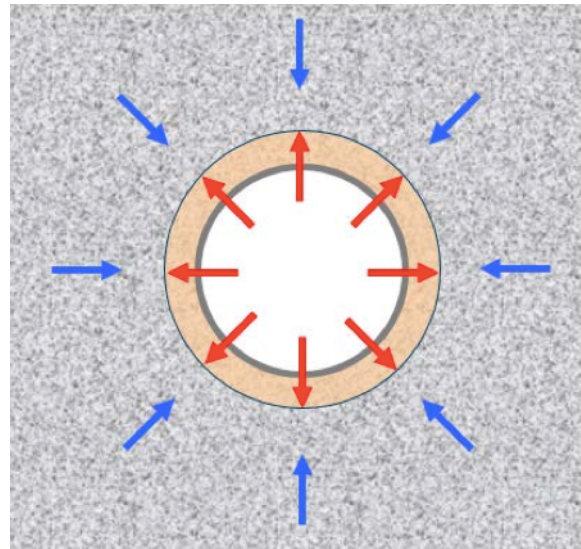


Figure 17-9: Illustration of force balance [87]

In this specific laboratory experiment, a piece of rock is sampled from the field and thereafter involved in creating a shale barrier test set up. First a hollow cylinder is created to represent the situation around the hole. The dimension of the sample is 4-in. as it is the maximum size from the field. Next step involves running an aluminium cylinder into this hole that will represent the casing. Thereafter, the test condition is created to simulate what is happening in-situ before applying confining pressure on the cylinder and pressure in the annulus. Fig. 17-10 illustrates the final test setup for when a potential barrier should be formed and completed installation of a shale barrier test, which simply consist of moving from the open gap area to the closed gap area.

The test may give relevant estimates for the sealing capacity of the shale barrier if the shale permeability is less than about $0.1 \mu\text{D}$.

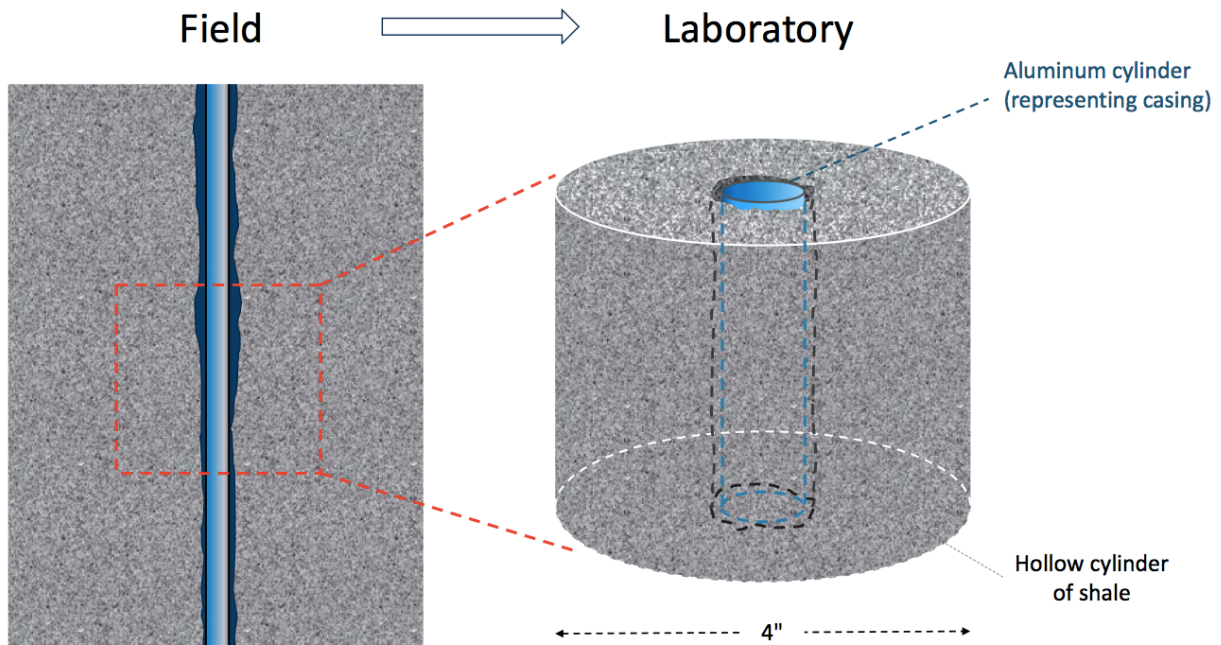


Figure 17-10: Illustration of taking a field sample to laboratory [87]

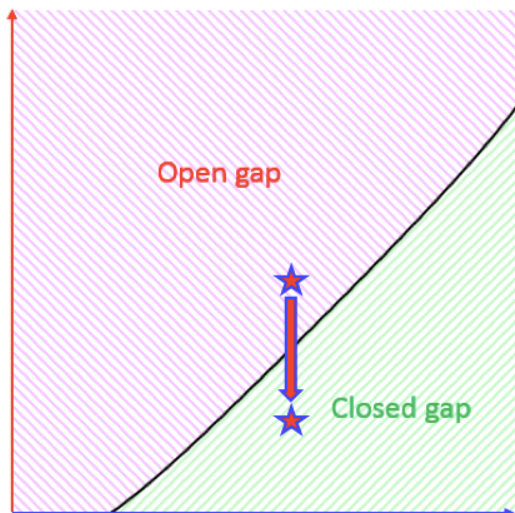


Figure 17-11: Shale barrier map [87]

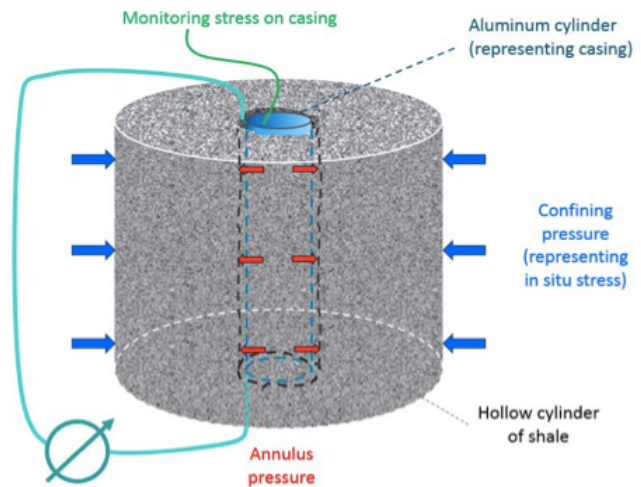


Figure 17-12: Shale barrier test set up [87]

The experiment is quite time consuming because the process of creating a barrier involves consolidation, which is very slow in shale. In addition, it involves creep, which is triggered by stress changes. Stress changes are triggered by deformation, which is again triggered by consolidation. These are mixed processes and typically difficult to analyse [87].

Figs. 17-13 to 17-16 are μ CT scanning images taken after completion of the test that can investigate fractures, voids and other density variations of the barrier [87].

The green coloured zones represent an indication of the range that has been affected by the process (i.e. implies higher porosity). Change in density is caused by volumetric deformation. In borehole geometry volume deformation represent the same as plastic deformation. If volumetric deformation is detected, we can deduce that it has to do with plasticity. The theoretical model assumes that material is linear elastic up to a given point and after that is perfectly plastified.

Plastic deformation is permanent (irreversible). Elastic deformation is reversible, which means it is possible to squeeze a rock, but it can “bounce back” to its original state. And as previously stated: A barrier has to be permanent.

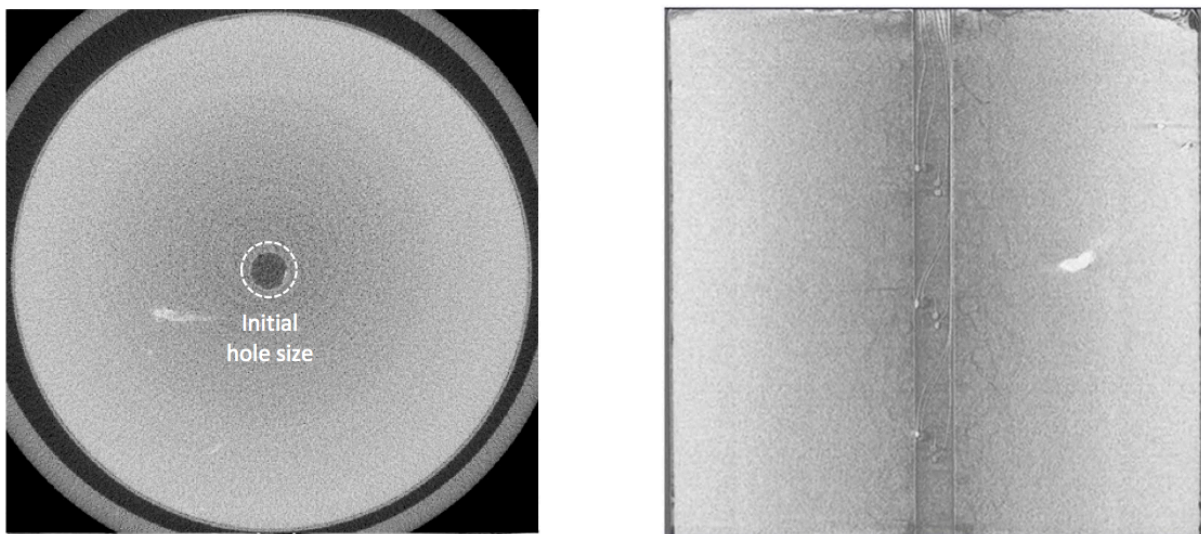
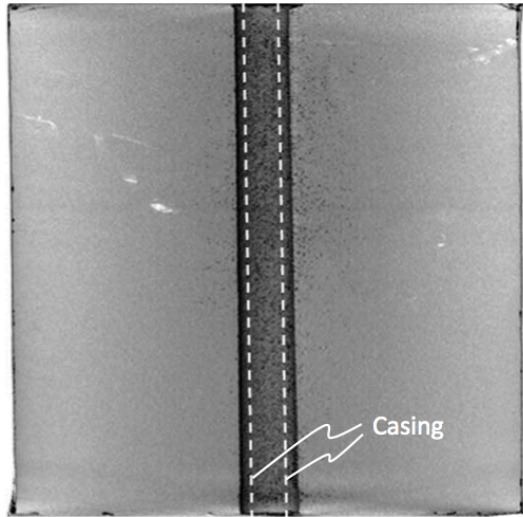


Figure 17-13: CT scan before test [87]

Before the test



After the test

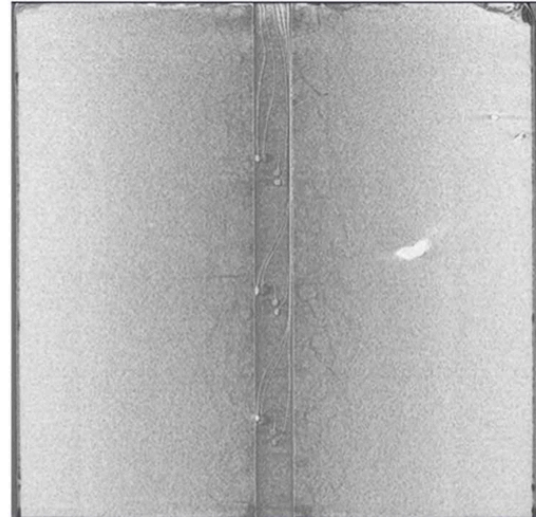
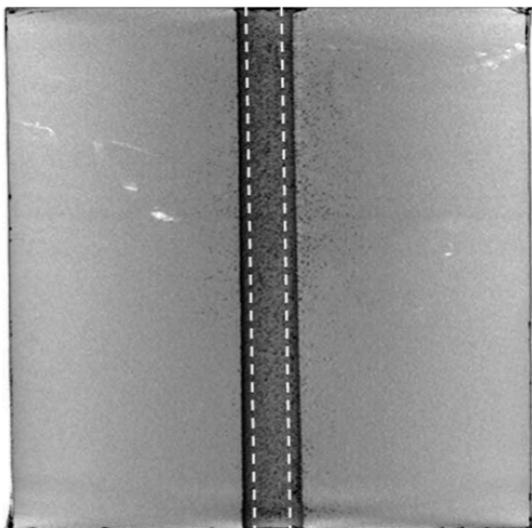


Figure 17-14: CT scan before versus after the test [87]

Before the test



After the test

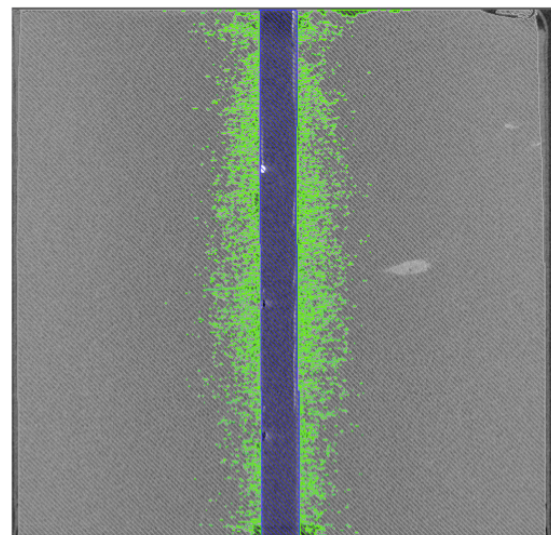


Figure 17-15: CT scan after test [87]

After the test

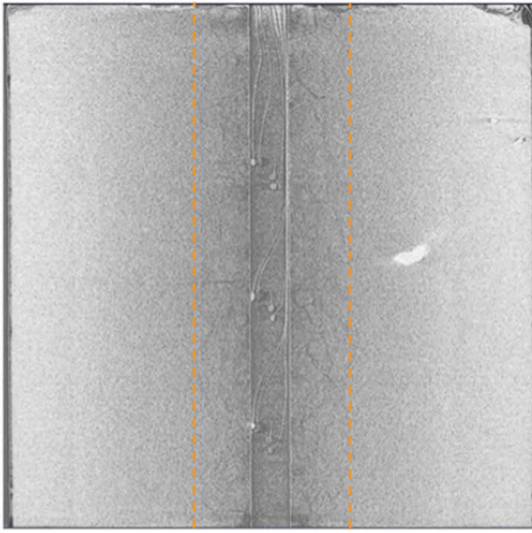


Figure 17-16: CT scan after test [87]

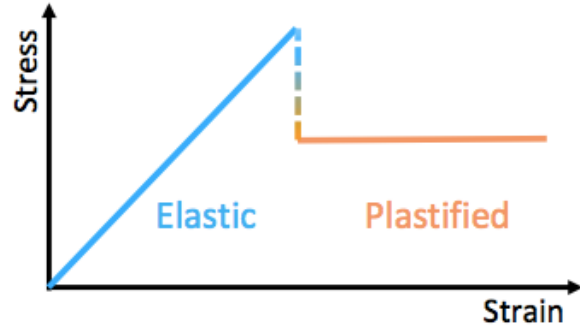


Figure 17-17: Theoretical model [87]

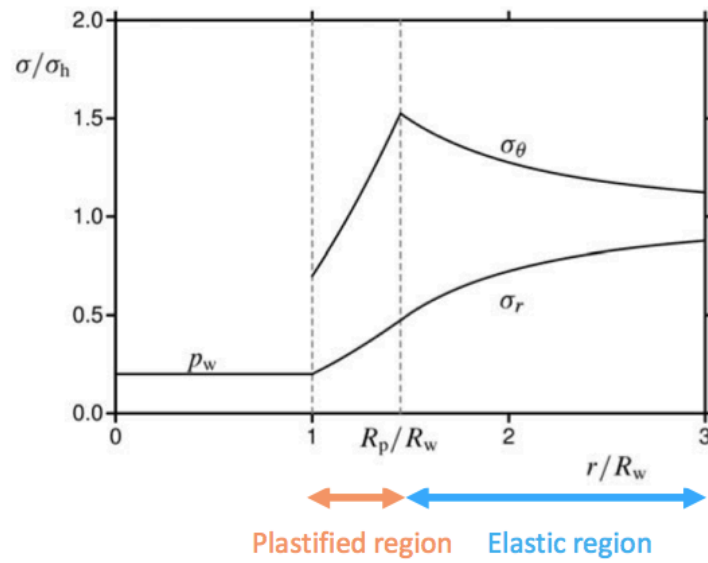


Figure 17-18: Theoretical model [87]

18 Summary

The summary presents objectives of the project and their possible answers as following:

Objective 1

Is it possible to establish FAB by preparing for creep to occur, either already in the drilling of the well (the well construction) or to provoke this in connection with plugging of wells elderly where other barriers (such as cement) are insufficient compared to the current rules?

Findings 1

To establish FAB, the crucial factors are:

- Formation with plastic properties.
- Having a lower pressure in annulus (it is the well pressure that ensures that the crawl does not occur during drilling) or that there is a formation that can absorb the excess of annulus fluid when the camp crawls.
- It is also clear that the creep is strongly dependent on temperature so that an increase in well temperature can trigger initiation of insects.
- Optimal drilling fluid composition.

Objective 2

What are the central mechanisms related to behaviour of shale and salt formations when providing a self-healing annular barrier around a well?

Findings 2

- Temperature, applied load and time are mechanisms that determines if a creep process is suitable for a specific application
- Initiating creep has so far been by performing a rapid pressure drop in the annulus. In situations where shale barriers have been detected the annulus, pressure has been bleed off either through an open annulus valve, or into nearby permeable zone.
- Creeping processes seem to be connected to drilling fluid. The petroleum industry has found a few wells over the last year where the formation has moved in and sealed around the pipe. These incidents are linked to water-based drilling fluid. Sufficient

formation bond has not been found where wells was drilled with oil-based mud.

Perhaps swelling process is the mechanism rather than creeping mechanism.

- Regardless of the interlayer cations (for example sodium, calcium), the elastic and creep properties of clay depend on relative humidity/water content. Increasing the water content makes the clay less stiff and make them creep more

As the mechanisms involved during creeping processes are not fully understood, there are currently no methods or procedures that can improve the possibility of success using this method.

Objective 3

Is there any procedure for estimating and improving the effectiveness of shale formation as a self-healing annular barrier where surrounding a well?

Findings 3

- Thorough mineralogy, pressure and temperature mapping is necessary to understand which formations will creep under different conditions and where they are located.
- Lab testing of creeping formations will be able to pinpoint what measures and degree of accuracy (how fast the pressure can be reduced, with, for example, how many bars) to be inserted and perhaps what time to devote to the purpose.
- A procedure has been established for all relevant requirements to understand how to qualify a formation as a barrier element or not.
- Available logging tools do not directly distinguish between annulus liquid and solid (cement, formation)

Objective 4

Is there any test procedure to study creep and investigate the barrier forming process?

Findings 4

- The shale barrier test can identify the sealing capacity through investigating various rock characteristics and determine which external conditions that may be of importance for the efficiency of shale as an annular barrier.

19 Future work

There is currently no possibility to predict when a formation barrier is established, or possibly how fast the process goes. It is of this reason no possibility to influence the process in a predictable manner. Several empirical interpretations for creep are published in literatures and lab studies regarding creep; however such interpretations have a limited value in borehole geometry where further complications are added due to the stress gradients and the coupling between stress and deformation. When it comes to lab studies, not everything is directly relevant since there is deficiency of some components in addition to inaccurate estimates for many parameters in the mud over the reservoir.

Because of the limited knowledge about shale as barrier, and the exceptional potential cost savings related with the use of this sealing method, there is necessary to predict under which conditions this process is able to work or not work, and for measures that can better the chance of successful sealing.

Changing behaviour around a hole is influenced by many parameters (internal forces, mineralogy etc.). A reasonable starting point for students or companies that is interested to do further research on formation as barrier in P&A operations would be to find the parameter(s) that is most important for the creeping process. If this is accomplished, it is possible to design the wells or process well production so that formation collapse can be actively used as a barrier element. Especially new wells, but also for old wells may be relevant for use of the concept. Future P&A work may also provide insights that can be used in adjacent areas such as drilling, cementing and completion.

20 Appendix A

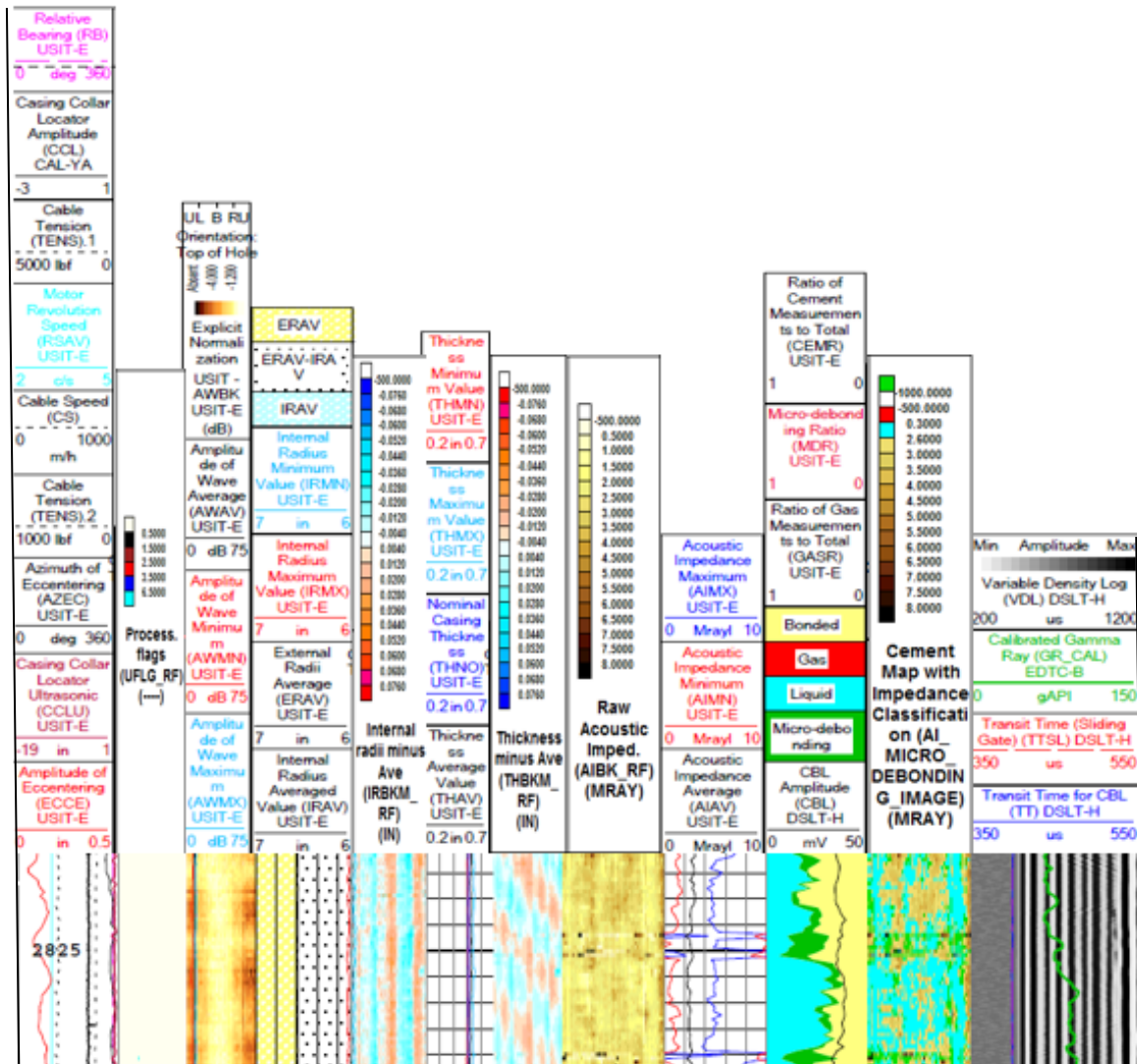


Figure A-20-1: Standard Log header insert (showing tracks, curves, scales etc) for the following figures

- All azimuthally measured impedances plotted at each depth sample 36 or 72 points
- Light Blue = Liquid
- Brown = Solid scaled
 - Light brown = lower impedance (poorer bond)
 - Dark brown = higher impedance (better bond)

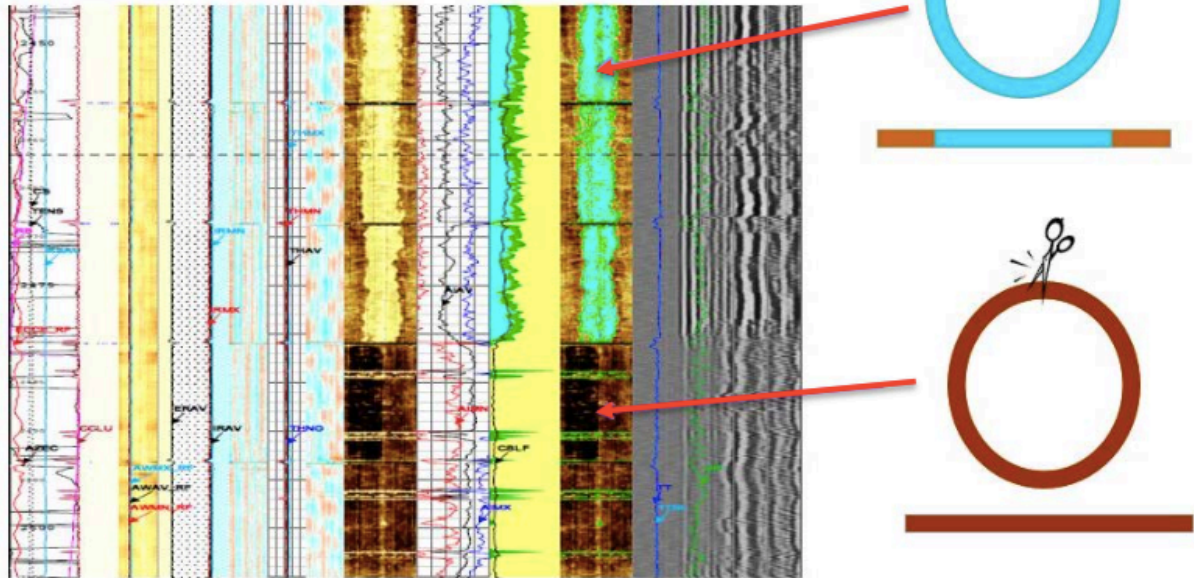


Figure A-20-2: Illustration of interpretation of USIT Log display

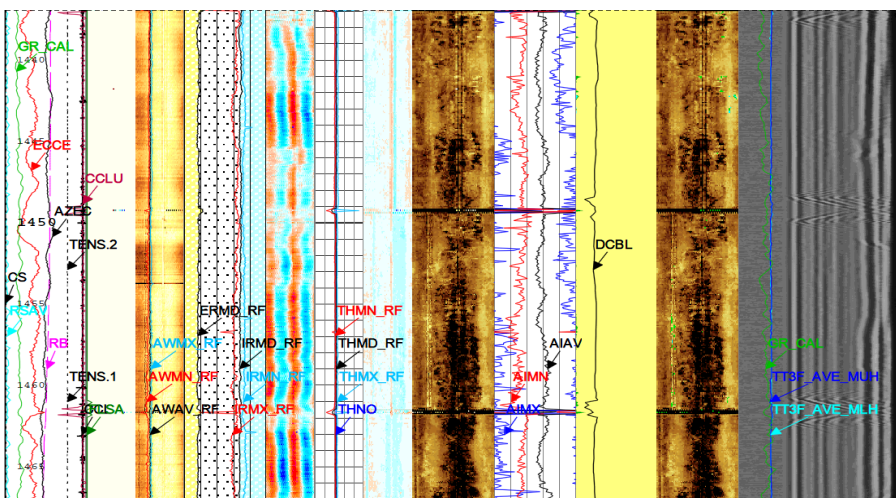
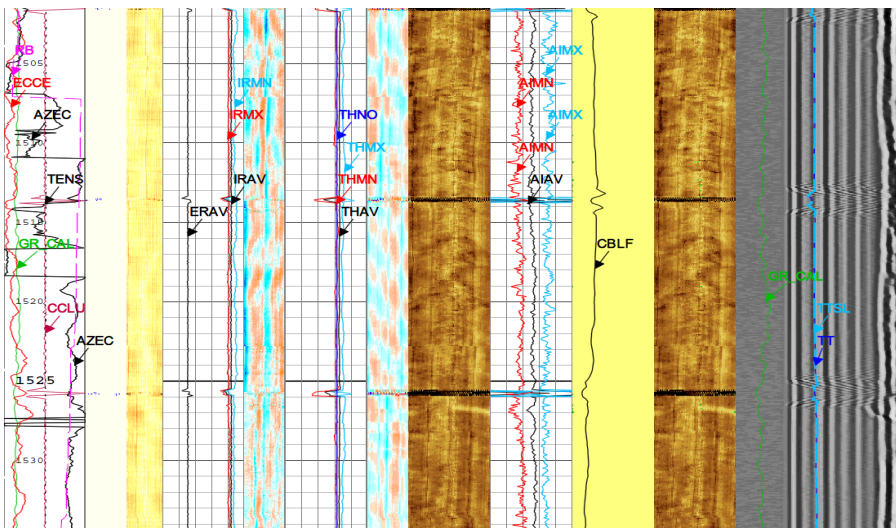
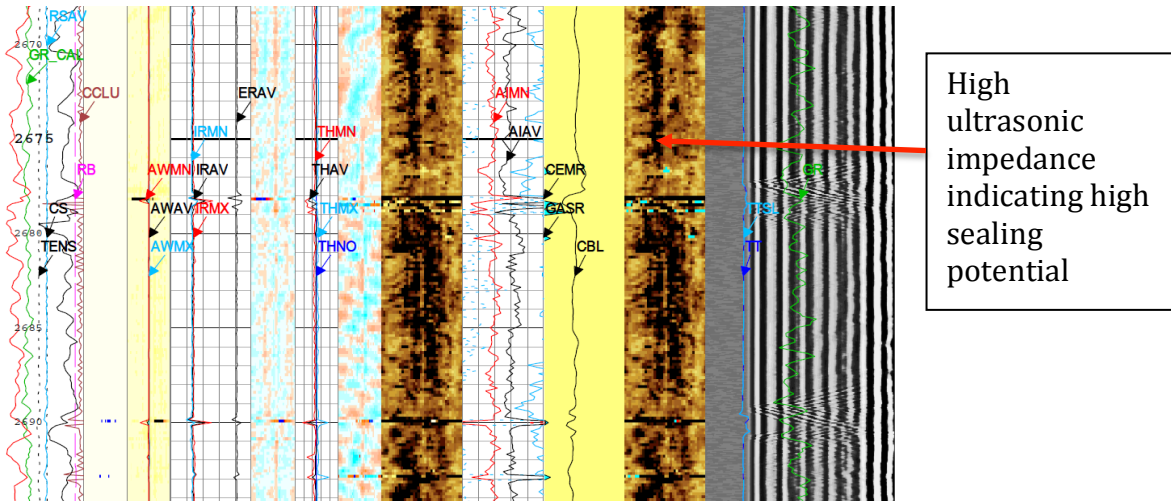


Figure A-20-3: Examples from three different wells (Hordaland and Shetland formations) of bonded formation material that would be classified as having high sealing potential (and where isolation was subsequently confirmed by pressure testing)

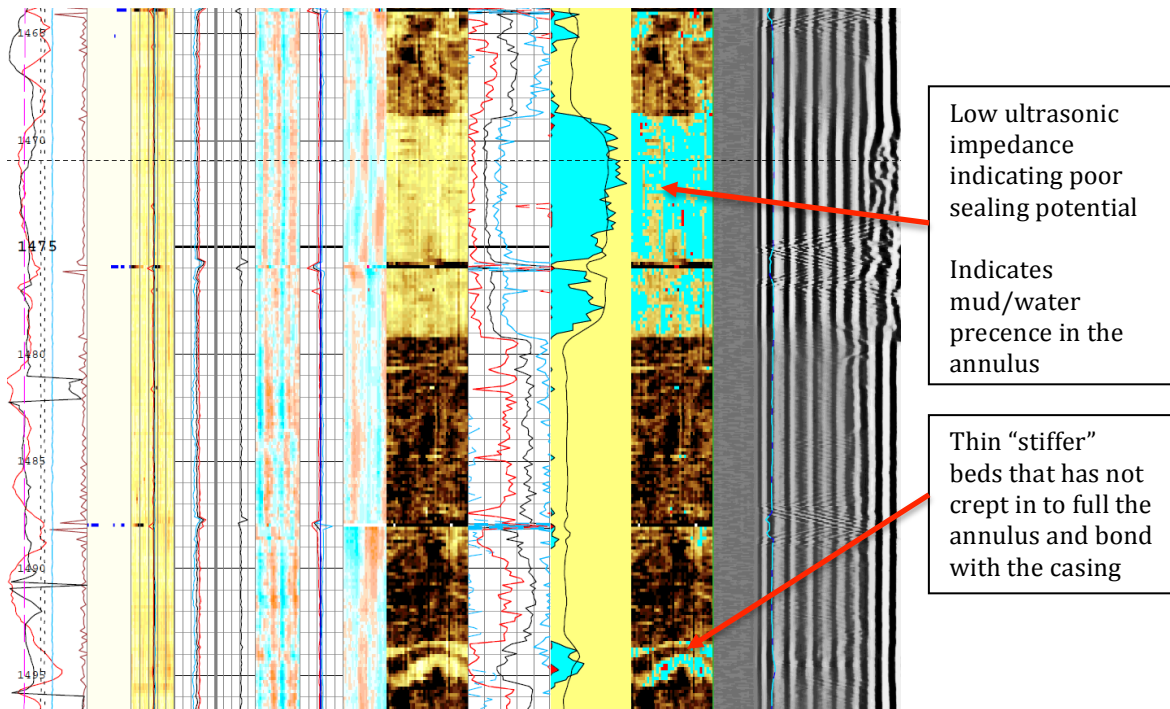
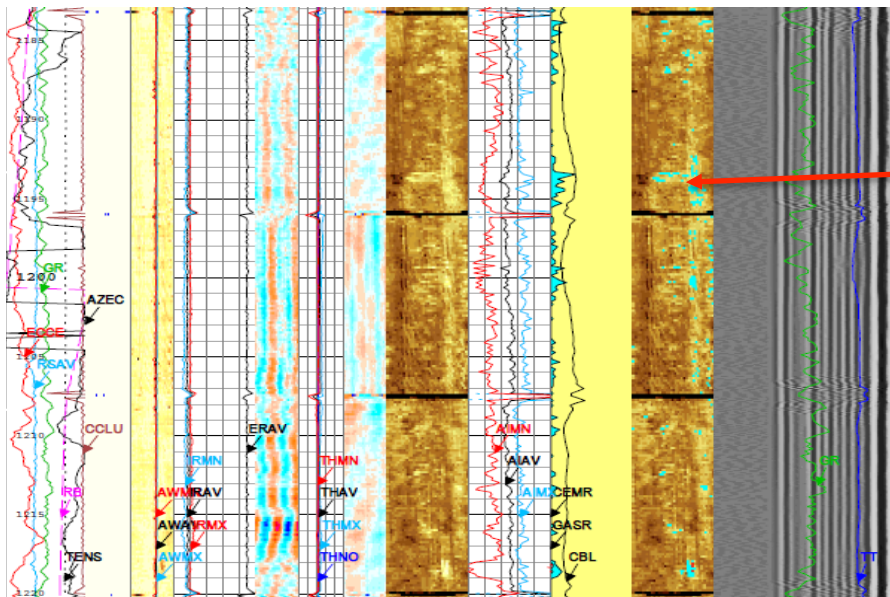


Figure A-20-4: Example Log showing intervals with well bonded formation material above and below a free pipe interval (where the geology is such that it has not crept into the formation) there are also some characteristic 'sinusoidal' bedding patterns at the bottom of the log related to thin "stiffer" beds that have also not crept in to fill the annulus and bond with the casing



Medium ultrasonic impedance indicating medium sealing potential, indication of some mud/ water presence in annulus

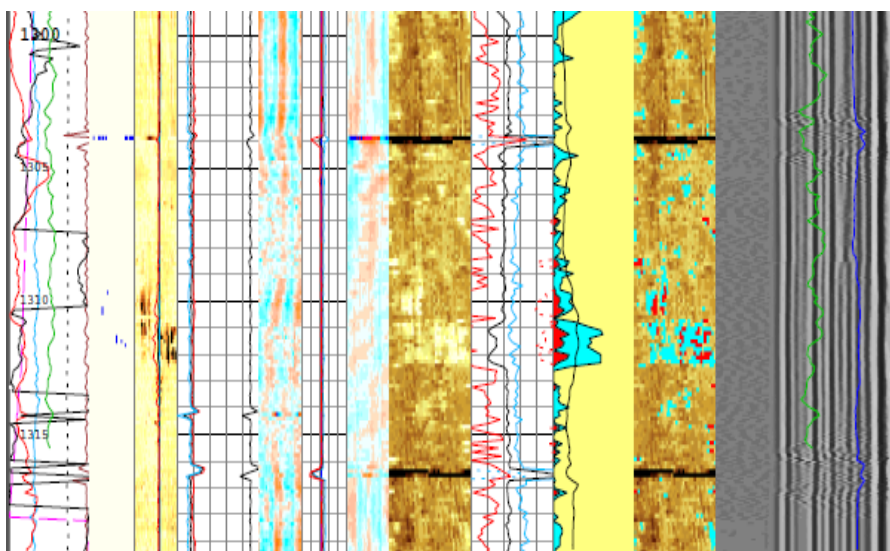
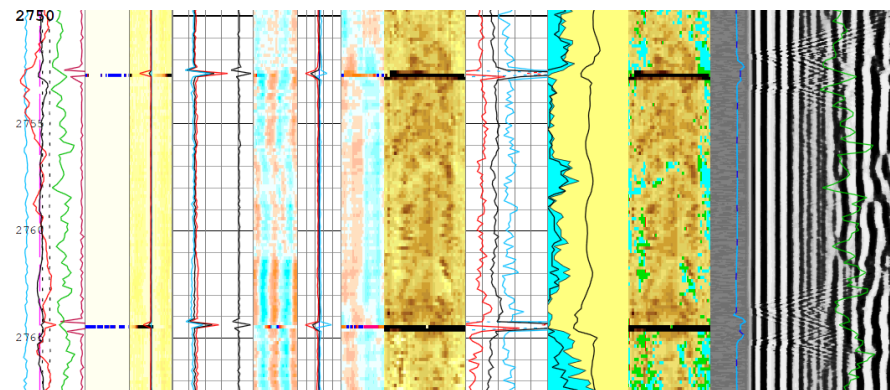
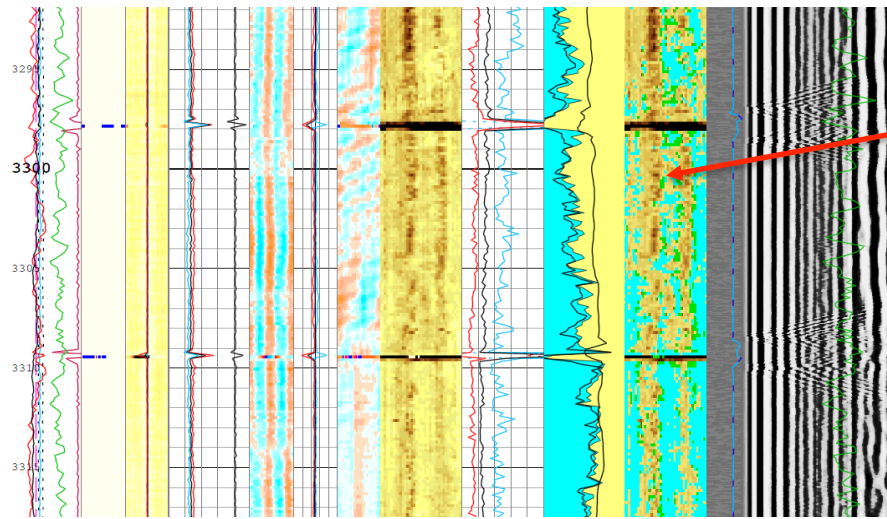


Figure A-20-5: Three example log sections showing bonded formation material that would be classified as having medium sealing potential



Low ultrasonic impedance indicating poor sealing potential, indicates mud/water presence in the annulus

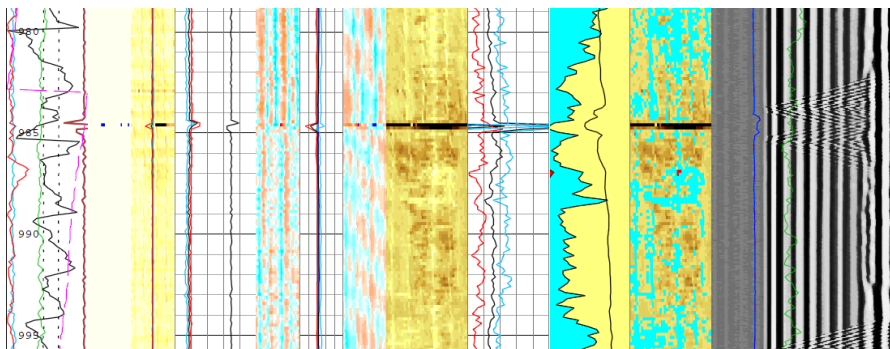
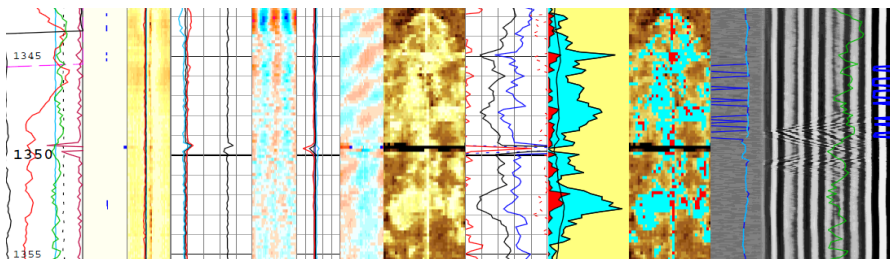
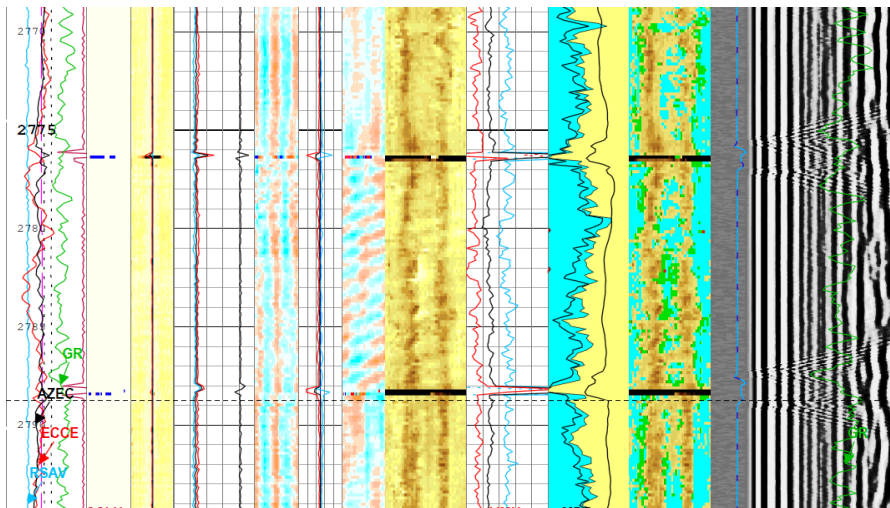


Figure A-20-6: Four example log sections showing of bonded formation material that would be classified as having low sealing potential

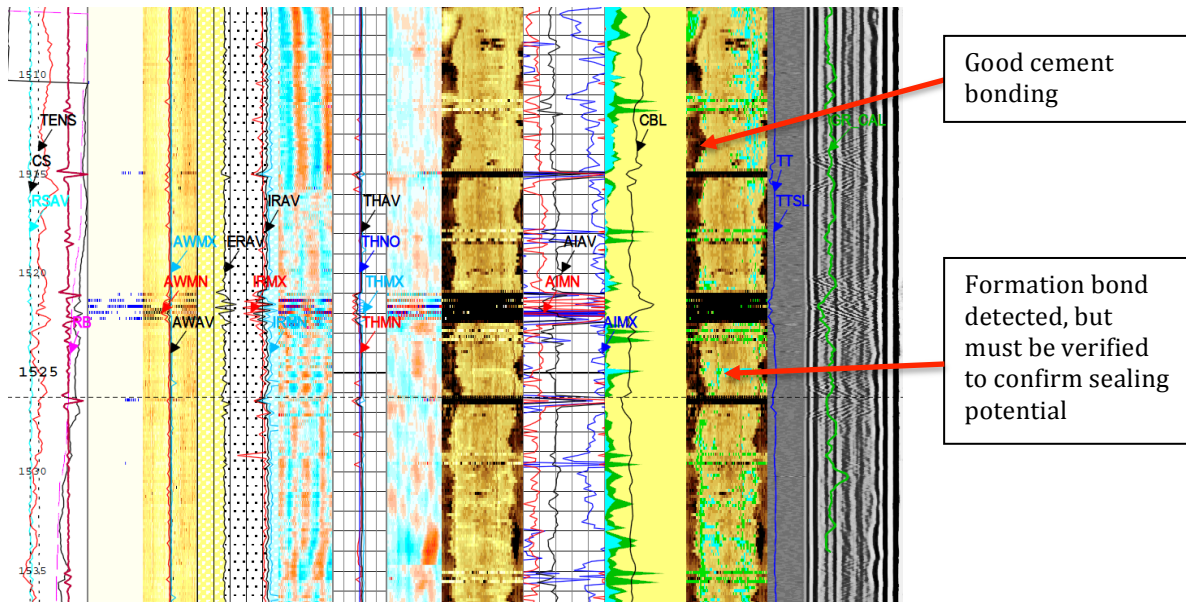


Figure A-20-7: Log example showing a combination of formation and cement material. Cement channelling results in low side liquid filled channels which, over time, are ‘filled’ with formation material. In this case it is not possible to confirm the sealing potential and each individual case will need to be tested.

21 References

1. Carlsen, T. Specialist Drill Tech Wellbore stab. Statoil
2. Williams, S., Carlsen, T., Constable, K., et al. 2009. Identification and Qualification of Shale Annular Barriers Using Wireline Logs During Plug and Abandonment Operations. SPE/IADC Drilling Conference and Exhibition, Amsterdam, The Netherlands, 17–19 March. SPE-119321-MS. <https://doi.org/10.2118/119321-MS>.
3. Offshore. 2011. P&A innovations increase efficiency, safety. 02.01.11, <http://www.offshore-mag.com/articles/print/volume-71/issue-2/production-operations/pa-innovations-increase-efficiency-safety.html> (Accessed 29 December 2016)
4. Technology Subgroup of the Operations & Environment Task Group. 2011. Plugging and abandonment of oil and gas wells. 15.09.11, https://www.npc.org/Prudent_Development-Topic_Papers/2-25_Well_Plugging_and_Abandonment_Paper.pdf, Page 16 (Accessed 29 December 2016)
5. Saasen, A. Fjelde, K. K. Vrålstad, T et al. 2013. Plug and Abandonment of Offshore Exploration Wells. Offshore Technology Conference, Houston, Texas, USA, 6–9 May 2013. <https://doi.org/10.4043/23909-MS>.
6. SSC. 2010. BP Gulf of Mexico disaster. 20.04.10. <http://www.tripodincidentanalyse.com/1486> (Accessed 15 January 2017)
7. NTNU, Norsk Olje&Gass, UIS. 2012. An Introduction to Well Integrity. 04.12.12, <http://www.norskoljeoggass.no/Global/2013%20Dokumenter/Andre%20vedlegg/INTRODUCTION%20TO%20WELL%20INTEGRITY%20-%2004%20December%202012.pdf> (Accessed 15 January 2017)
8. NORSOK Standard D-010 Rev. 4, June 2013. <https://www.standard.no/en/sectors/energi-og-klima/petroleum/norsok-standard-categories/d-drilling/d-0104/> (Accessed 13 December 2017)
9. Norrish, K. 1953. The swelling of montmorillonite. Vol: 18. Page 120. <http://dx.doi.org/10.1039/DF9541800120>.
10. Williams, S.M., Carlsen, T., Constable, K.C. et al. 2009. Identification and Qualification of Shale Annular Barriers Using Wireline Logs During Plug and Abandonment Operations. SPE/IADC Drilling Conference and Exhibition. Amsterdam, 17-19 March. SPE-119321-MS. <https://doi.org/10.2118/119321-MS>.
11. Kwamboka, M.B. 2016. Soil Liquefaction. Bachelor Thesis, University of Nairobi. http://civil.uonbi.ac.ke/sites/default/files/cae/engineering/civil/MONGARE%20BRENDA%20KWAMBOKA_1.pdf

12. Huotari, T. Kukkonen, I. 2004. Thermal Expansion Properties of Rocks. http://www.posiva.fi/files/2259/POSIVA-2004-04_Working-report_web.pdf
13. Khalifeh, M., Saasen, A., Hodne, H. et al. 2013. Techniques and Materials for North Sea Plug and Abandonment Operations. Offshore Technology Conference, Houston, Texas, USA, 6–9 May. OTC-23915-MS. <https://doi.org/10.4043/23915-MS>.
14. Al-Bazali, T.M., Zhang, J. and Chenevert, M.E. 2005. Measurement of the Sealing Capacity of Shale Caprocks. SPE Annual Technical Conference and Exhibition, Dallas, Texas, 9-12 October. SPE-96100-MS. <https://doi.org/10.2118/96100-MS>.
15. Hobart, K. Shale. Geology.com. <http://geology.com/rocks/shale.shtml> (Accessed 05 January 2017)
16. Lal, M. 1999. Shale Stability: Drilling Fluid Interaction and Shale Strength. SPE Asia Pacific Oil and Gas Conference and Exhibition, Jakarta, Indonesia, 20-22 April. SPE-54356-MS. <https://doi.org/10.2118/54356-MS>.
17. M. J. Wilson, L. Wilson. 2014. Clay mineralogy and shale instability: an alternative conceptual analysis. 49: 127-145. <https://doi.org/10.1180/claymin.2014.049.2.01>.
18. Zhang, Q., Jia, W., Fan, X., et al. 2015. A review of the shale wellbore stability mechanism based on mechanical–chemical coupling theories. 1 (2): 91-96
19. William K. T. 2000. Introduction to Clay Minerals & Soils. Oakton Community College. <http://www.oakton.edu/user/4/billtong/eas100/clays.htm> (Accessed 15 May 2017)
20. UCL. Clays and Clay Minerals. <https://www.ucl.ac.uk/earth-sciences/impact/geology/london/ucl/materials/clay> (Accessed 01 February 20)
21. Ketterings, Q. Reid, S. Rao, R. 2007. Cation Exchange Capacity (CEC). College of Agriculture and Life Sciences. <http://nmsp.cals.cornell.edu/publications/factsheets/factsheet22.pdf>
22. Leung, P.K. and Steig, R.P. 1992. Dielectric Constant Measurements: A New, Rapid Method To Characterize Shale at the Wellsite. SPE/IADC Drilling Conference, New Orleans, Louisiana, 18-21 February. SPE-23887-MS. <https://doi.org/10.2118/23887-MS>.
23. Deng, J.G., Cheng, Y.F., Chen, M., et al. 2008. Wellbore stability evaluation technique. Petroleum industry press, Beijing.
24. Mojid, A. 2014. Diffuse Double Layer (DDL). Springer, 28 August, https://link.springer.com/referenceworkentry/10.1007%2F978-90-481-3585-1_41 (Accessed 02 February 2017)

25. Asef, M. and Farrokhrouz, M. 2013. Shale Engineering: Mechanics and Mechanisms. CRC Press
26. Oort, E. V. 2003. On the physical and chemical stability of shales. *Journal of Petroleum Science and Engineering*. **38** (3–4): 213-235.
[https://doi.org/10.1016/S0920-4105\(03\)00034-2](https://doi.org/10.1016/S0920-4105(03)00034-2).
27. Elert, G. 2017. Thermal Expansion. *The Physics Hypertextbook*.
<http://physics.info/expansion/summary.shtml> (Accessed 17 April 2017)
28. Schlumberger. Salt creep.
http://www.slb.com/services/technical_challenges/geomechanics/drilling_management/salt_creep.aspx (Accessed 18 February 2017)
29. Orlic, B. and Buijze, L. 2014. Numerical modeling of wellbore closure by the creep of rock salt caprocks. *US Rock Mechanics / Geomechanics Symposium*, 1-4 June, Minneapolis, USA. ARMA 14-7499.
30. Nelson, E.B. and Guillot, D. 2006. Well cementing. 2nd edition. Texas. Schlumberger
31. Salt Domes of South Louisiana. 1960. **1** : 4-12.
<http://archives.datapages.com/data/nogs/data/003/003001/0004.htm>
32. Jones, I. F. and Davison, I. 2014. Seismic imaging in and around salt bodies. *Interpretation*, **2** (4). <http://dx.doi.org/10.1190/INT-2014-0033.1>.
33. Baar, C.A. 1977. *Applied Salt-Rock Mechanics 1st Edition: The in-situ behavior of salt rocks*. Elsevier
34. SSC. 2000. Ch.1 Soil Physical Properties.
<http://lawr.ucdavis.edu/classes/ssc107/SSC107Syllabus/chapter1-00.pdf>. (Accessed 18 February 2017)
35. Chang, C. and Zoback, M. D. 2009. Viscous creep in room-dried unconsolidated Gulf of Mexico shale (I): Experimental results. *Journal of Petroleum Science and Engineering*. **69**: 239–246. <https://doi.org/10.1016/j.petrol.2009.08.018>.
36. Olsen, J.R. 2015. Investigation of Creep Characteristics for Stresses close to Failure. MS thesis. Norwegian University of Science and Technology, Trondheim, June 15.
37. NDT Resource Center. Creep and Stress Rupture Properties. <https://www.nde-ed.org/EducationResources/CommunityCollege/Materials/Mechanical/Creep.htm> (Accessed 01 January 2017)

38. Lavrov, A. 2012. Evaluation of possible mechanisms responsible for annular sealing observed in shale. Report SINTEF – 7020045/04/12. Report IRIS – 2012/441.
39. Fjær, E., Holt, R.M., Raaen, A. M. et al. 2008. Petroleum Related Rock Mechanics 2nd ed. Elsevier Science.
40. University of Minnesota
<http://www.me.umn.edu/labs/composites/Projects/Polymer%20Heat%20Exchanger/Creep%20description.pdf> (Accessed 02 January 2017)
41. NDT Resource Center. Strengthening/Hardening Mechanisms. <https://www.nde-ed.org/EducationResources/CommunityCollege/Materials/Structure/strengthening.htm> (Accessed 10 March 2017)
42. O'Brien, D. E. and Chenevert, M. E. 1973. Stabilizing sensitive shales with inhibited potassium-based drilling fluids. **25** (9). SPE-4232-PA. <https://doi.org/10.2118/4232-PA>.
43. Lyu, Q., Ranjith, P. G., Long, X. et al. 2015. A review of shale swelling by water adsorption. *Journal of Natural Gas Science and Engineering* **27** (3): 1421–1431. <https://doi.org/10.1016/j.jngse.2015.10.004>.
44. Petrowiki. 2016. Formation damage from swelling clays. Petrowiki, 09 December. http://petrowiki.org/Formation_damage_from_swelling_clays (Accessed 03 March 2017)
45. Grim, R.E. 1939. Relation of the composition to the properties of clays. **22** (1-12): 141–151. <http://dx.doi.org/10.1111/j.1151-2916.1939.tb19440.x>.
46. Mooney, R.W., Keenan, A.G. and Wood, L.A. 1952. Adsorption of Water Vapor by Montmorillonite. II. Effect of Exchangeable Ions and Lattice Swelling as Measured by X-Ray Diffraction. <http://dx.doi.org/10.1021/ja01126a002>.
47. Skempton AW, 1953. The Colloidal Activity of Clays. 3rd International Conference Soil Mech found Eng. Switzerland. **1**; 57-61. <https://doi.org/10.1680/sposm.02050.0009>.
48. Norrish, K. 1953. The swelling of montmorillonite. Vol: 18. Page 120. <https://doi.org/10.1039/DF9541800120>.
49. Foster, W. R., Savins, J.G. and Waite, J.M. Lattice expansion and theological behavior relationships in water- montmorillonite systems: in *Clays and Clay Minerals*. <http://dx.doi.org/10.1346/CCMN.1954.0030124>
50. Madsen, F, T. and Vanmoos, M. M. 1989. The swelling behaviour of clays **4** (2): 143-156. [https://doi.org/10.1016/0169-1317\(89\)90005-7](https://doi.org/10.1016/0169-1317(89)90005-7).

51. Fink, J. 2015. Petroleum Engineer's Guide to Oil Field Chemicals and Fluids. 2nd Edition. Elsevier
52. Ezzat, A. M. 1990. Completion Fluids Design Criteria and Current Technology Weaknesses. SPE Formation Damage Control Symposium, Lafayette, Louisiana, 22-23 February. SPE-19434-MS. <https://doi.org/10.2118/19434-MS>.
53. Karaborni, S., Smit, B., Heidug, W., et al., 1996. The swelling of clays: Molecular Simulations of Hydration of Montmorillite. Vol. 271.
54. Chenevert, M. E. 1970. Shale Alteration by Water Adsorption **22** (9). SPE-2401-PA. <https://doi.org/10.2118/2401-PA>.
55. O'Brien, D. E. and Chenevert, M. E. 1973. Stabilizing sensitive shales with inhibited, potassium-based drilling fluids **25**: 1089-1100. <https://doi.org/10.2118/4232-PA>.
56. Wang, Y. Roman, R. Lidofsky, S.D., et al. 1996. Autocrine signaling through ATP release represents a novel mechanism for cell volume regulation. Proceedings of the National Academy of Sciences of the USA. **93** (21): 12020–12025. <https://doi.org/10.1073/pnas.93.21.12020>.
57. Holsrud, P., Bostrøm, B., Sønstebø, E.F. et al. 1998. Interaction between shale and water-based drilling fluids: Laboratory exposure test give new insight into mechanisms and field consequences of KCl contents. SPE annual technical conference and exhibition, New Orleans, Louisiana, USA, 27-30 September
58. Schlemmer, R. 2003. Progression of Water-Based Fluids Based on Amine Chemistry – Can the Road Lead to True Oil Mud Replacements? AADE 2003 National Technology Conference “Practical Solutions for Drilling Challenges”, Houston, Texas, April 1 – 3. AADE-03-NTCE-36
59. Sabtan, A. A. 2005. Geotechnical properties of expansive clay shale in Tabuk, Saudi Arabia. Journal of Asian Earth Sciences. **25** (5): 747-757. <https://doi.org/10.1016/j.jseaes.2004.07.003>.
60. Ewy, T. R. and Morton, K. 2009. Wellbore-Stability Performance of Water-Based Mud Additives **24** (3). SPE-116139-PA. <https://doi.org/10.2118/116139-PA>.
61. Gomez-Gutierrez, I. C. Bryson, L. S. and Hopkins, T. C. 2011. Correlations between Geotechnical Properties and the Swell Behavior of Compacted Shales. [https://doi.org/10.1061/41165\(397\)421](https://doi.org/10.1061/41165(397)421).
62. Zhao, H. Liu, J. Guo, J., et al. 2014, 'Reexamination of Lime Stabilization Mechanisms of Expansive Clay', Journal of Materials in Civil Engineering **27** (1). [https://doi.org/10.1061/\(ASCE\)MT.1943-5533.0001040#sthash.r4LONdZG.dpuf](https://doi.org/10.1061/(ASCE)MT.1943-5533.0001040#sthash.r4LONdZG.dpuf).

63. Wikipedia. 2017. Self-Healing material. (02 June 2017 revision),
http://en.wikipedia.org/wiki/Self-healing_material (Accessed 03 January 2017)
64. Vibeke Henriksen. 2013. Plug and Abandonment on the Norwegian Continental Shelf. MS thesis. University of Stavanger, Stavanger.
65. Allerstorfer, C. 2011. Investigation of the “Plastic- Behavior” Region in Leak-Off Tests. MS thesis. Montanuniversitat Leoben.
66. Godwin Nwafor. 2014. Formation Strength Tests. LinkedIn. 14 June,
<https://www.linkedin.com/pulse/20140614143802-128515676-formation-strength-tests>. [Accessed 05.05.17]
67. Engineering Archives. Creep.
http://www.engineeringarchives.com/les_matsci_creep.html (Accessed 15 January 2017)
68. Bauer, A., Stenebråten, J.F., Li, L., and Fjær, E. 2017. Can heating-induced creep result in shale barriers for P&A applications? US Rock Mechanics / Geomechanics Symposium, San Francisco, California, USA, 25- 28 June.
69. Kristiansen, T. G. 2017. Creating Barriers with Natural Materials. Sintef Conference: Experimental P&A Research for the North Sea, Trondheim, 20-21 March.
70. Zhang, Q., Jia, W., Fan, X. et al. 2015. A review of the shale wellbore stability mechanism based on mechanical–chemical coupling theories **1** (2): 91-96
<https://doi.org/10.1016/j.petlm.2015.06.005>.
71. Sønstebø, E. F. and Holt, R. M. 2001. Brine Exposure Effects on a Tertiary North Sea Shale. US. Symposium on Rock Mechanics, Washington D.C., 7-10 July. ARMA-01-1375
72. Al-Bazali, T. M., Al-Mudh’hi, S. and Chenevert, M. E. 2012. An Experimental Investigation of the Impact of Diffusion Osmosis and Chemical Osmosis on the Stability of Shales. 2012 **29** (3): 312-323.
<http://dx.doi.org/10.1080/10916460903393989>.
73. Ewy, R.T. and Stankovic, R.J. 2000. Pore pressure change due to shale-fluid interactions: Measurements under simulated wellbore conditions. 4th North American Rock Mechanics Symposium, Seattle, Washington, 31 July-3 August. ARMA-2000-0147
74. Noble Research Institute. 2004. Don't Overlook Role of Potassium.
<https://www.noble.org/news/publications/ag-news-and-views/2004/february/dont-overlook-role-of-potassium/> (Accessed 20 May 2017)
75. OOrt, E.V. 2017. Shale Stabilization by High-Salinity Formate Drilling Fluids. AADE National Technical Conference and Exhibition, Houston, Texas, April 11-12.

76. Carrier, B., Vandamme, M., Bornet, M. et al. 2016. Effect of Water on Elastic and Creep Properties of Self-Standing Clay Films.
<http://dx.doi.org/10.1021/acs.langmuir.5b03431>.
77. Xie, X., Fjær, E. and Pradhan, S. 2017. Long-term creep prediction with a modified power law model. 51st US Rock Mechanics / Geomechanics Symposium, San Francisco, California, USA, 25- 28 June.
78. Hansen, A., Hemmer, P. C. And Pradhan, S. 2015. The Fiber Bundle Model: Modeling Failure in Materials. Wiley-VCH
79. Weibull, W. 1951. A statistical distribution function of wide applicability. Journal of Applied Mechanics **18**: 293-297.
80. Fjær, E., Larse, I., Holt, R.M., et al. 2014. A creep model for creep. 48th US Rock Mechanics / Geomechanics Symposium, Minneapolis, MN, USA, 1-4 June. ARMA-2014-7398.
81. Fjær, E. 1999. Static and dynamic moduli for weak sandstones. Rock Mechanics for Industry, The 37th U.S. Symposium on Rock Mechanics (USRMS), Vail, Colorado USA, 7-9 June. ARMA-99-0675.
82. Briggs, B.N. and Forbes, M. H. 2011. Viscoelasticity. Teachengineering.
https://www.teachengineering.org/lessons/view/cub_surg_lesson04 (Accessed 15 May 2017)
83. Murata, H. 2012. Rheology – Theory and Application to Biomaterials. Intech.
<http://dx.doi.org/10.5772/48393>.
84. Scheiner, S.,and Helmich, C. 2009. Continuum Microviscoelasticity Model for Aging Basic Creep of Early-Age Concrete . Journal of engineering mechanics **135** (4)
[https://doi.org/10.1061/\(ASCE\)0733-9399\(2009\)135:4\(307\)#sthash.H37TUQv2.dpuf](https://doi.org/10.1061/(ASCE)0733-9399(2009)135:4(307)#sthash.H37TUQv2.dpuf).
85. Fjær, E., Folstad, J.S. and Li, L. 2016. How creeping shale may form a sealing barrier around a well. 50th US Rock Mechanics / Geomechanics Symposium, Houston, Texas, USA, 26-29 June. ARMA-2016-482
86. Fjær, E. and Stenebråten, J.F. How shale may form a sealing barrier around a well. Fifth eage shale workshop, Catania, Italia 2-4 May.
87. Fjær, E. PhD, SINTEF, Chief Scientist, Formation Physics